Departamento de Física
Faculdade de Ciências da Universidade do Porto

String and Brane Networks in Higher Dimensions

Author: Lara Rodrigues da Costa Gomes de Sousa
Supervisor: Prof. Pedro Pina Avelino
Co-Supervisor: Carlos J. A. P. Martins

Outubro de 2011

Departamento de Física
Faculdade de Ciências da Universidade do Porto

String and Brane Networks in Higher Dimensions

TESE SUBMETIDA À FACULDADE DE CIÊNCIAS DA UNIVERSIDADE DO PORTO
PARA A OBTENÇÃO DO GRAU DE DOUTOR EM FÍSICA

Outubro de 2011

Acknowledgements

First and foremost, I would like to thank my supervisor, Pedro Avelino, and my co-supervisor, Carlos Martins, for the shared knowledge and the support. Without their insights and patience this work surely would not be possible. I would also like to acknowledge the valuable collaboration of Roberto Menezes in this work. Moreover, I would like to thank everybody that contributed to this work directly or indirectly in any way — even those who helped me maintain my sanity by doing anything else. I know I'm bound to forget someone, so I mention no one.

I would also like to thank CFP and the Physics Department of the Faculty of Science of the University of Porto for the support, and the hospitality of everybody at the Physics Department of Federal University of Paraíba, during my visits to João Pessoa. Finally, I would like to acknowledge the financial support of Fundação para a Ciência e Tecnologia through the doctoral grant SFRH/BD/41657/2007 and research projects.

Resumo

A Teoria de Cordas — a uma das teorias candidatas à unificação da gravitação com as restantes forças fundamentais —é geralmente formulada em 9 dimensões espaciais. Segundo o modelo mundo-brana, o universo é uma brana de Dirichlet com 3 dimensões espaciais, que se pode mover num espaço-tempo 9+1-dimensional. Neste contexto, se existisse um par de branas adicional no espaço-tempo, as interacções entre estas poderiam provocar uma aceleração da expansão do universo. Esta concretização natural do paradigma da inflação em teoria de cordas — a Inflação de Branas [1] — tem a interessante propriedade de terminar tipicamente com uma transição de fase, levando à produção de p-branas de menor dimensionalidade [2, 3]. Assim, espera-se que a inflação de branas leve à formação de redes de p-branas evoluindo em universos com dimensões extra.

Nesta tese, estudamos a evolução cosmológica de redes de p-branas em universos de Friedmann-Robertson-Walker (FRW) com $N + 1$ dimensões. Neste contexto, começamos por deduzir a equação do movimento para p-branas infinitamente finas em espaços-tempo homogéneos e isotrópicos. Este resultado serve-nos de ponto de partida para derivar as equações que descrevem a evolução cosmológica do comprimento característico e da velocidade quadrática média de uma rede de p-branas. Estas equações permitem-nos generalizar o modelo VOS para cordas [4] para o caso de p-branas de dimensionalidade arbitrária em espaços-tempo $N+1$-dimensionais. Este modelo VOS generalizado permite-nos, então, descrever quantitativamente a evolução de redes de p-branas e estudar os diferentes regimes que emergem durante a sua evolução em universos em expansão ou em colapso. Em particular, estudos da dinâmica de p-branas fechadas maximamente simétricas permitem-nos limitar os valores possíveis para a velocidade quadrática média de redes de p-branas e determinar as condições que devem ser satisfeitas para estas possam atingir um regime invariante de escala.

Estudamos ainda as conexões possíveis entre redes de paredes de domínio e

a energia escura. As redes de paredes, se congeladas em coordenadas comóveis ou frustradas, podem provocar a aceleração da expansão do universo. Por esta razão, este tipo de redes foram sugeridas como candidatas a energia escura [5]. Estudos anteriores [6, 7, 8], baseados em modelos analíticos e simulações de teoria de campo de alta resolução, revelaram que a frustração de redes de paredes de domínio não resulta naturalmente da sua evolução cosmológica. Nesta tese, consideramos o efeito de junções massivas tipo-corda e tipo-monopólo em redes de paredes de domínio, desenvolvendo para isso um modelo VOS semi-analítico que incorpora esses efeitos. Chegamos à conclusão que, apesar de a presença de junções massivas poder levar à frustração de redes de paredes, a sua contribuição para a densidade de energia do universo não pode ser reconciliada com os resultados observacionais. Analisamos ainda o efeito de um mecanismo alternativo genérico para a frustração de redes de p-branas e verificamos que só poderá frustrar efectivamente a rede de branas se for a componente dominate da densidade de energia. Por esta razão, as redes frustradas de paredes de domínio não poderão contribuir para a energia escura: se a frustração ocorresse efectivamente, a sua contribuição para a densidade de energia seria subdominante.

A constante cosmológica seria a explicação mais simples para a aceleração actual do universo. Contudo, as previsões teóricas e o valor observado da constante cosmológica são dramaticamente discrepantes. Em [9], os autores propõe uma solução dinâmica para este problema — que denominam Devaluação —, que tem como base a dinâmica de redes de paredes de domínio viciadas. Este tipo de rede é originado, na sua concretização mais simples, se existir uma ligeira diferença de energia de vácuo nos domínios. Esta diferença de energia provoca o aparecimento de um pressão de volume que "empurra" a parede em direcção ao domínio com maior densidade de energia, provocando o seu colapso. Para estudar o efeito desta diferença de energia entre domínios na dinâmica de paredes, desenvolvemos um modelo analítico que o incorpora. Este modelo é, então, usado para analisar o mecanismo da devaluação: se o universo for composto por vários domínios com densidades de energia de vácuo ligeiramente diferentes, separados por paredes de domínio, as regiões com maior densidade de energia seriam progressivamente suprimidas. Consequentemente, o universo evoluiria naturalmente para valores baixos da densidade de energia de vácuo. A nossa análise, contudo, revela que este mecanismo necessitaria de um ajuste preciso dos parâmetros do potencial para reproduzir o valor observacional da constante cosmológica e, por essa razão, não pode ser considerado uma solução satisfatória para o problema da constante cosmológica.

Abstract

String Theory — one of the candidates for the unification of gravitation with the other fundamental forces — is generally formulated in ten spacetime dimensions, instead of the usual four. In the brane-world realization, the visible universe is a Dirichlet brane with 3 spatial dimensions, moving within the higher dimensional space. In this context, if the spacetime contains an additional pair of branes, their interactions could accelerate the expansion of the universe and, thus, drive an inflationary epoch. This natural realization of inflation in the framework of string theory — know as brane inflation [1] — has the compelling property that it ends with a phase transition, in which the production of p-branes of lower dimensionality is expected to occurs [2, 3]. Therefore, brane inflation is expected to lead to the formation of p-brane networks, that appear as topological defects, evolving in higher dimensional cosmologies.

In this thesis, we study the cosmological evolution of p-brane networks in $N+1$-dimensional Friedmann-Robertson-Walker (FRW) universes. In order to do so, we derive the equations of motion for infinitely thin and featureless p-branes in higher dimensional homogeneous and isotropic backgrounds. These results are, then, used as a stepping-stone to derive the cosmological evolution equations for the characteristic lengthscale and root-mean-square (RMS) velocity of a p-brane network. These equations constitute a generalized version of the Velocity-Dependent One-Scale (VOS) Model for cosmic strings [4] to branes of arbitrary dimensionality in $N+1$-dimensional backgrounds. This VOS model then allow us to describe quantitatively the evolution of p-brane networks, and to study the different scaling regimes that arise in expanding and collapsing universes. In particular, studies of the dynamics of maximally symmetric closed p-branes solutions allow us to obtain constraints on the RMS velocity of brane networks, that are then used find the conditions that the networks need to satisfy in order to attain linear scaling regimes.

We also study the possible connections between domain wall networks and dark energy. Domain wall networks, if frozen in comoving coordinates or frustrated, can drive a phase of accelerated expansion. For that reason, they were proposed as dark energy candidates [5]. Previous studies [6, 7, 8], resorting to analytical tools and high-resolution field-theory simulations, revealed that frustration does not arise naturally as the result of cosmological evolution. In this thesis, we consider the effect of massive string and monopole-type junctions on domain wall networks, by developing a semi-analytical VOS model that incorporates their dynamical effects. We find that, although the presence of massive junctions can lead to the frustration of domain wall networks, their contribution to the energy density of the universe cannot be reconciled with the observational results. We also analyse the effect of an alternative mechanism for the frustration of p-brane networks and verify that it cannot decelerate the branes effectively unless it is the dominant energy component. For this reason, frustrated domain wall networks cannot contribute to dark energy: if frustration occurred effectively, their contribution to the energy density would be subdominant.

The cosmological constant would be the simplest explanation for the current acceleration of the universe. However, there is a dramatic difference between the theoretical predictions and the observed values of the cosmological constant that is yet to be explained. In Ref. [9], the authors proposed a dynamical solution — dubbed Devaluation — to this cosmological constant problem, that relies on the dynamics of biased domain wall networks. These domain wall networks originate, in the simplest realization, if there is a slight energy difference between the vacuum energy density of the domains. This energy difference causes a volume pressure that pushes the wall towards the higher vacuum density domain, leading to its collapse. We develop a analytic model for the effect of bias on domain wall dynamics, and use the results to analyse the devaluation scenario. According to this scenario, if the universe was composed of several domains with slightly different vacuum energy densities, separated by biased domain walls, the regions with higher energy densities would be progressively suppressed. Consequently, the universe would naturally evolve towards low values of vacuum energy density. Our analysis, however, reveals that, in order to obtain the observed value of the cosmological constant, this scenario would require a fine-tuning of the parameters of the potential, and, for that reason, cannot be considered a satisfactory solution to the cosmological constant problem.

Declaration

The work in this thesis, except where reference is made to the work of others, is my own and to the best of my knowledge original. This work was carried out in collaboration with Pedro Avelino. Roberto Menezes also collaborated in the work presented in Subsec. 2.3, and the work in Sec. 4.3 was carried out in collaboration with Carlos Martins.

Parts of this thesis appeared in various papers [10, 11, 12, 13, 14, 15, 16], however the complete set of results has never been submitted for any other degree, diploma or qualification.

Notation and Units

Throughout this work natural units are used, and a $(+,-,-,-)$ metric signature is employed. Unmarked greek and latin indices run over spacetime and space coordinates, respectively; while, greek and latin indices marked with a tilde take the values $0,\cdots,p$ and $1,\cdots,p$, respectively (except in Subsec. 2.2.1). Italic type is used to represent $N+1$-vectors, while bold type denotes N-vectors — so that $x^\mu = (x^0, \mathbf{x})$. We also use Einstein summation convention whereby when indices appear twice in a single term, once in an upper and once in a lower position, they are implicitly summed over. Moreover, commas denote, in general, partial derivatives — so that $A_{,B} \equiv \partial A/\partial B$ and $A_{,\mu} \equiv \partial A/\partial x^\mu$ — and dots represent derivatives with respect to the conformal time, η.

Contents

List of Figures

1

Introduction

There is overwhelming evidence that the universe has been expanding throughout its evolution, ever since its extremely dense and hot outset. The early universe was much denser and hotter than in the present, and therefore cosmology and particle physics should merge in any rigorous attempt to study this period.

Some important recent developments in cosmology stem particularly from the application of particle physics theoretical frameworks to the early universe. For instance, the quantum theoretical description of the contents of the universe lead to the suggestion that the universe should have underwent, in its early history, a series of phase transitions and that, and as a consequence, networks of topological defects might have been formed. These defect networks, although formed in the early universe, might have important cosmological consequences for the late-time evolution of the universe. In particular, it has been suggested that domain wall networks might be related to the puzzling recent acceleration of expansion: they could contribute to the dark energy budget or, if the network is rendered unstable, help to explain the small observed value of the vacuum energy density.

String theory emerged in the endeavour to construct a quantum theory of gravity, in order to provide a unified description of the fundamental particles and the four fundamental interactions. Such a theory would be necessary to describe the very early universe (until $10^{-43}\,s$ after the big bang). Recent developments in string theory suggest that its fundamental objects — p-dimensional Dirichlet branes and fundamental strings — might play a cosmological role, and even be

detectable in upcoming observational probes.

In this chapter, we start by reviewing the Standard Cosmological Model — that successfully describes the evolution of the universe since, at least, $10^{-2}\,s$ after the big bang — and by discussing its successes and shortcomings. We also discuss the observational evidence for the existence of an exotic energy component that accounts for more than two thirds of the total energy density of the universe which is causing the expansion of the universe to accelerate. We discuss the properties of this component and review briefly the dark energy candidates suggested in the literature. Moreover, we review the concept of spontaneous symmetry breaking in the early universe and the consequent formation of topological defects. Finally, we briefly discuss superstring theory and brane inflationary scenarios, and the recent studies that indicate that brane inflation might lead to the formation of cosmic superstring and p-brane networks that might play important cosmological roles.

1.1 STANDARD COSMOLOGICAL MODEL

The Standard Cosmological Model is the prevailing physical description of the evolution of the universe. This model rests upon the *Cosmological Principle*, whereby the properties of the universe are identical everywhere in space — the universe is homogeneous — and in every direction — it is also isotropic. Under this assumption, there are no preferred points or directions in the universe, and thus the same laws of physics apply throughout space. Clearly, the universe is not homogeneous nor isotropic on small scales, since matter clusters to form stars, galaxies, and other cosmic structures. However, in cosmology, homogeneity and isotropy are defined in a statistical sense and on sufficiently large scales (larger than the size of the large-scale structure of the universe).

Another cornerstone of this model is the realization that *the universe is expanding* over time. In 1929, Edwin Hubble published the measurements of the shifts of spectral lines of 18 nearby galaxies (at a fairly known distance), and found that all these galaxies were receding from Earth in all directions. Moreover, he found that the recessional velocities appear to increase proportionally with the distance. If the universe was not expanding (or collapsing), one would expect the galaxies to move in random directions, with no clear correlation between velocity and distance. Although the expanding-universe solution to Einsteins's equations was found in 1922 by Alexander Friedmann, the expanding universe paradigm only gained general acceptance when Hubble's observational

evidence for expansion was published.

In the framework of General Relativity, cosmological expansion is regarded as an intrinsic expansion: it is the spacetime itself that expands, leading to an increase of the (proper) physical distance between any two well-separated comoving observers. The physical distance between these observers scales as:

$$d_{\rm ph}(t) = a(t) d_{\rm ph}(t_0)\,, \tag{1.1}$$

where we took $a(t_0) = 1$. Note that, if the observers do not have any peculiar dynamics (*id est*, if they are comoving with the Hubble expansion), the variations of $d_{\rm ph}(t)$ consist merely of changes on the scale of physical distances due to cosmological expansion, $a(t)$. $a(t)$, then, encodes the dynamics of the universe's expansion, and, for this reason, it is generally denominated cosmic scale factor. The Hubble velocity is, then, given by

$$v = \frac{d(d_{\rm ph}(t))}{dt} = H(t) d_{\rm ph}\,, \tag{1.2}$$

where the rate of change of the scale factor, usually denominated Hubble Parameter, defined as

$$H = \frac{1}{a}\frac{da}{dt}\,, \tag{1.3}$$

was introduced. Eq. (1.2) is known as the Hubble law, and it is the empirical relation found by Hubble between the recessional velocity of galaxies and their distance from Earth

$$v \propto d_{\rm ph}. \tag{1.4}$$

The assumption that the universe is homogeneous and isotropic is sufficient to determine the spacetime metric of an expanding universe: the Friedmann-Robertson-Walker (FRW) metric, whose line element is

$$ds^2 = dt^2 - a^2(t)\left[\frac{dr^2}{1-Kr^2} + r^2\left(d\theta^2 + \sin^2\theta d\phi^2\right)\right] \tag{1.5}$$

where r, θ and ϕ are comoving coordinates (since a particle at rest in these coordinates will remain at rest). Here, K is the spatial curvature of the 3-dimensional space. An homogeneous and isotropic spacetime has three possible geometries: if $K < 0$, the universe is open with an hyperbolic topology; if $K = 0$ the spacetime is flat; and, if $K > 0$, the universe is closed, with a spherical topology.

1.1.1 Friedmann Equations

The dynamics of the expansion of the universe is generally assumed to be governed by General Relativity. According to Einstein's equation

$$G_{\mu\nu} \equiv R_{\mu\nu} - \frac{1}{2} g_{\mu\nu}\mathcal{R} = 8\pi G T_{\mu\nu} + \Lambda g_{\mu\nu}\,, \tag{1.6}$$

where

$$R_{\mu\nu} = \Gamma^{\alpha}_{\mu\nu;\alpha} - \Gamma^{\alpha}_{\mu\alpha;\nu} + \Gamma^{\alpha}_{\beta\alpha}\Gamma^{\beta}_{\mu\nu} - \Gamma^{\alpha}_{\beta\nu}\Gamma^{\beta}_{\mu\alpha} \tag{1.7}$$

is the Ricci tensor, $\mathcal{R} = R^{\mu}_{\mu}$ the is Ricci Scalar, and

$$\Gamma^{\mu}_{\alpha\beta} = \frac{g^{\mu\nu}}{2}\left(g_{\alpha\nu,\beta} + g_{\beta\nu,\alpha} - g_{\alpha\beta,\nu}\right) \tag{1.8}$$

are the Christoffel symbols. Λ is a constant, dubbed, for historical reasons, Cosmological Constant, that accounts for the intrinsic energy of vacuum, describing the energy of empty space. $T^{\mu\nu}$ is the Stress-Energy tensor, describing the energy and pressure of the background universe. Note that if the universe is assumed to be homogeneous and isotropic, the energy density and pressure of the universe only depend on t. Moreover, isotropy implies the absence of heat conduction (so that any changes occurring in the fluid are adiabatic), and the absence of viscosity or shear forces. Therefore, we assume that the *background behaves as a perfect fluid*, and thus it can be described by a stress-energy tensor of the form

$$T_{\mu\nu} = (\mathcal{P}_b + \rho_b)U_\mu U_\nu - \mathcal{P}_b g_{\mu\nu}\,, \tag{1.9}$$

where ρ_b and $\mathcal{P}_b$ are, respectively, the energy density and the pressure of the background fluid, U^μ represents its 4-velocity defined as $U^\mu = dX^\mu/d\tau$, and τ represents the proper time. In the comoving frame, the fluid is at rest with respect to expansion, so that U^μ is such that form $U^0 = 1$ and $U^i = 0$.

Assuming an energy-momentum tensor of this form, Eq. (1.6) allows us to write two independent equations:

$$H^2 = \frac{8}{3}\pi G\rho_b - \frac{K}{a^2} + \frac{\Lambda}{3}\,, \tag{1.10}$$

$$\frac{dH}{dt} = -4\pi G\left(\rho_b + \mathcal{P}_b\right) + \frac{K}{a^2}\,, \tag{1.11}$$

generally called Friedmann equations. These two equations may be equated to eliminate K/a^2, in order to obtain the Raychaudhuri equation:

$$\frac{1}{a}\frac{d^2a}{dt^2} = -\frac{4}{3}\pi G\left(\rho_b + 3\mathcal{P}_b\right) + \frac{\Lambda}{3}\,. \tag{1.12}$$

Moreover, energy-momentum conservation,

$$T^{\mu\nu}{}_{;\nu} = 0\,, \tag{1.13}$$

allows us to obtain a continuity equation for the energy density

$$\frac{d\rho}{dt} + 3H\left(\rho_b + \mathcal{P}_b\right) = 0\,. \tag{1.14}$$

Note that in many situations of interest, the pressure of a fluid is a linear function of its energy density:

$$\mathcal{P} = w\rho\,, \tag{1.15}$$

where w is the equation-of-state parameter. By introducing Eq. (1.15) in Eq. (1.14), it is easy to see that in this case the energy density of the fluid should scale as

$$\rho \propto a^{-3(1+w)}\,, \tag{1.16}$$

for a constant equation-of-state parameter. Eqs (1.10), (1.12), and (1.14) then allow us to describe the dynamics of expansion, as a function of its contents or *vice-versa*[1].

1.1.2 Cosmological horizons

In this subsection, we will present some concepts which are important in a cosmological model. Let us start by defining more precisely the (proper) physical distance, at a time t, from an arbitrary origin to a comoving object at a radial coordinate r:

$$d_{\rm ph}(r,t) = a(t)\int_0^r \frac{dr}{\sqrt{1-Kr^2}} = a(t)f(r)\,, \tag{1.17}$$

where

$$|K|^{1/2} f(r) = \begin{cases} \sinh^{-1}(|K|^{1/2}\, r) & , \quad \text{for} \quad K<0 \\ |K|^{1/2}\, r & , \quad \text{for} \quad K=0 \\ \sin^{-1}(|K|^{1/2}\, r) & , \quad \text{for} \quad K>0 \end{cases}\,. \tag{1.18}$$

[1] Note that only two of these equations are independent

Since the time dependence stems only from the scale factor, it is easy to see that the rate of change of $d_{\rm ph}(r,t)$ satisfies the Hubble law (Eq. (1.2)).

Consider now a photon propagating throughout the universe. Photons travel along null geodesics, with $ds^2 = 0$. For simplicity, let us choose a coordinate system such that ϕ and θ remain constant. Therefore, along the photon path, we have that

$$ds^2 = dt^2 - a^2(t)\frac{dr^2}{1-Kr^2} = a^2(\eta)\left(d\eta^2 - \frac{dr^2}{1-Kr^2}\right) = 0\,. \tag{1.19}$$

Here, we introduced the conformal time,

$$\eta = \int_0^t \frac{dt}{a(t)}\,, \tag{1.20}$$

that measures the comoving distance travelled by a photon since the big-bang (which we assumed to take place at $t = \eta = 0$). Since the universe has a finite age, photons could only have travelled a finite physical distance until the present time. This distance is commonly named *particle horizon*, and it is given by:

$$d_p(\eta) = a(\eta)f(r) = a(\eta)\int_0^t \frac{dt}{a} = a(\eta)\eta\,. \tag{1.21}$$

An observer is, then, unable to receive signals from a distance larger than the particle horizon[2].

The event horizon measures the distance a photon can travel, since a time t, until a maximum time in the future, $t_{\rm max}$

$$d_e(t) = a(t)\int_t^{t_{\rm max}} \frac{dt}{a}\,, \tag{1.23}$$

where $t_{\rm max}$ is either the time of the big-crunch, for closed models, or $t_{\rm max} \to +\infty$, for flat and open models. This distance defines the boundary of the region for which observers in the future are able to receive signals emitted at time t. This boundary is only relevant for models for which Eq. (1.23) is finite. Otherwise, if $d_e \to \infty$, the event horizon does not exist.

[2]In practise, since before recombination photons were tightly coupled with the baryons, the observable universe is delimited by a smaller horizon

$$d_{\rm opt} = a(\eta)(\eta - \eta_r)\,, \tag{1.22}$$

where η_r is the conformal time at recombination, and $d_{\rm opt}$ is denominated optical horizon.

The *Hubble radius*, R_H, is defined as the distance at which the Hubble velocity equals the velocity of the light,

$$R_H = H^{-1}\,. \tag{1.24}$$

This distance delimits a region, denominated Hubble sphere or volume, for which the recessional velocities are smaller than the velocity of light. Although outside the Hubble sphere the velocities are superluminal, and seem, at first glance, to violate special relativity, that is not the case. Hubble velocities are not physical velocities: they measure the rate of expansion of spacetime itself. In fact, the physical velocity of any object outside the Hubble sphere, if measured in its local inertial frame, is smaller than the speed of light and is, thus, in agreement with special relativity. The Hubble radius is, roughly, the physical distance travelled by a photon in the characteristic expansion time (or Hubble Time), $t_H = H^{-1}$.

As a consequence of the expansion of spacetime, the wavelength of radiation is stretched, increasing proportionally to the scale factor — the light suffers a redshift. In a collapsing universe the radiation would be blueshifted as it traveled through spacetime. If λ_e and λ_0 are, respectively, the wavelength of the emitted radiation and the wavelength measured by a distant observer, then

$$\frac{\lambda_0}{\lambda_e} = \frac{a(\eta_0)}{a(\eta_e)}\,. \tag{1.25}$$

The cosmological redshift, z, is defined as

$$z = \frac{\lambda_0}{\lambda_e} - 1 = \frac{a(\eta_0)}{a(\eta_e)} - 1\,. \tag{1.26}$$

1.1.3 The contents of the Universe and Universe Evolution

In order to describe the dynamics of the universe, it is necessary to know its ernegetic contents. Frequently, one assumes that there are three main contributions to the energy density of the background: matter (ρ_m), radiation (ρ_r), and the vacuum energy density[3] ($\rho_\Lambda = \frac{\Lambda}{8\pi}$). Therefore, we can write

$$\rho_b = \rho_m + \rho_r + \rho_\Lambda\,. \tag{1.27}$$

Each of these components, if minimimally coupled to the others, satisfies the continuity equation in Eq. (1.14). However, each has a different equation

[3]Note that, from now on, we include the effects of the Cosmological Constant in the background energy density, so that the $\frac{\Lambda}{3}$ term in Eqs. (1.10) is absorbed by the definition of the background density.

of state. For a fluid of relativistic particles (radiation), $w = 1/3$, so that

$$\rho_r \propto a^{-4} . \tag{1.28}$$

The pressure of matter (constituted by non-relativistic particles) is negligible compared to its energy density. Thus, in this case, $w = 0$ and

$$\rho_m \propto a^{-3} . \tag{1.29}$$

By definition, Λ remains constant, and, consequently, so does the vacuum energy density.

The critical density, ρ_c, is defined as the energy density of a flat universe (with $K = 0$). Using Eq. (1.10), we find that

$$\rho_c = \frac{3H^2}{8\pi G} . \tag{1.30}$$

The energy density of the universe determines the geometry of spacetime: if $\rho_b > \rho_c$, the universe is closed ($K > 0$), while for $\rho_b < \rho_c$ one has that $K < 0$ and thus the universe is open.

One may define a (dimensionless) density parameter,

$$\Omega_i = \frac{\rho_i}{\rho_c} , \tag{1.31}$$

for each of the species that contribute to the total energy density. It is also common to define a curvature parameter

$$\Omega_K \equiv -\frac{K}{a^2 H^2} , \tag{1.32}$$

so that

$$\Omega_m + \Omega_r + \Omega_\Lambda + \Omega_K = 1 . \tag{1.33}$$

In this case, the geometry of the universe is determined by the value of Ω_K:

$$\begin{aligned} \Omega_K &< 0 \quad \Rightarrow \quad K > 0 , \\ \Omega_K &= 0 \quad \Rightarrow \quad K = 0 , \\ \Omega_K &> 0 \quad \Rightarrow \quad K < 0 . \end{aligned} \tag{1.34}$$

Introducing these density parameters into Eq. (1.10), we obtain

$$H^2 = H_0^2 \left[\Omega_{m0} a^{-3} + \Omega_{r0} a^{-4} + \Omega_{\Lambda 0} + \Omega_{K0} a^{-2} \right] , \tag{1.35}$$

where parameters with the subscript 0 correspond to their values at the present time.

1.1.4 Observational Results: Successes and Shortcomings of the Standard Cosmological Model

The standard cosmological model describes the evolution of an expanding universe from a state of extreme density and temperature until the final stages of its evolution. As we travel backwards in time, towards higher and higher temperatures, the amount of energy available for particle interaction increases: as a consequence, first the atoms are ionized (at $T \sim 0.3\,\mathrm{eV}$); at even earlier times, the nuclei decompose into nucleons (for $T \sim 0.1 - 1\,\mathrm{MeV}$); and these baryons in turn eventually decompose into quarks (for $T \sim 10^2\,\mathrm{MeV}$). Therefore, as we travel backwards in time, the universe enters the realm of particle physics. The perfect relativistic fluid description of the universe may not remain valid for arbitrarily high temperature: its validity before $t \sim 10^{-10}s$ depends on the assumed framework of particle physics [17, 18]. Note however that this description could hold up from times as early as $t_{\mathrm{pl}} = 10^{-43}s$, if the quantum field theoretical description of particle physics remains valid up to such high energy scales $(10^{18}\ \mathrm{GeV})$[4].

Nevertheless, there is a steady observational basis that supports the validity of the Standard Cosmological Model from about $10^{-2}s$ after the big bang. In this section, we present some significant observational results, highlighting the successes of the Standard Cosmological Model, and pointing out some of its shortcomings.

One of the turning points in the Standard Model's history was the discovery of the Cosmic Microwave Background radiation (CMB). This relic radiation, was predicted in 1946 by Gamow [19]. At high temperatures, the universe was opaque (optically thick) to photons, because they were in kinetic equilibrium with the electrons of the plasma via Thompson Scattering. However, as the temperature dropped to $T \sim 0.3$ eV, the formation of neutral hydrogen and helium atoms from the ions of the plasma became energetically favourable, and the nuclei captured the free electrons (in a process known as Recombination). Consequently Thompson scattering ceased and the photons decoupled from matter. After decoupling, most of these photons have been propagating freely through

[4]This energy scale is far beyond the reach of the present day particle accelerators.

spacetime ever since, permeating the whole sky. Given the fact that, before decoupling, the photons were in thermal equilibrium with the surrounding plasma, this radiation is expected to have a blackbody spectrum.

In 1965, Penzias and Wilson [20] discovered a background radiation, which appeared to fill the sky uniformly, in the microwave frequency range, and that could not be explained by any astronomical source or by experimental noise. This radiation was later identified as the Cosmic Microwave Background [21], thus confirming Gamow's prediction, and gaining general acceptance for the standard cosmological model. Several years later, in 1992, the Far Infrared Absolute Spectrophotometer (FIRAS) of the Cosmic Background Explorer (COBE) satellite demonstrated that the CMB has the most perfect blackbody spectrum ever observed in nature [22], characterized by a temperature of $T = 2.725\text{K}$. Moreover, there is direct evidence that the CMB temperature was hotter in the past, scaling as: $T \propto a^{-1}$ (e.g. from the study of absorption lines in the spectra of distant quasars [23]).

The CMB also offers the best evidence for the isotropy of the observed universe: aside from dipole fluctuations that result from the motion of the Earth relative to the CMB's rest frame, temperature fluctuations are very small:

$$\frac{\Delta T}{T} \lesssim 10^{-5}\,. \tag{1.36}$$

The remarkable uniformity of the CMB temperature indicates that the universe was fairly isotropic and homogeneous at the time of Decoupling. This extreme homogeneity and isotropy, however, also highlights one of the shortcomings of the Standard Cosmological Model: the *Horizon Problem*. According to Standard Cosmology, the Last Scattering Surface spans a large number of regions that were causally disconnected at recombination, and therefore it is unable to explain the observed homogeneity and isotropy of the universe.

The Standard Cosmological Model also withstood another important observational test: the primordial abundances of light elements (inferred from observations) seem to be in agreement with the predictions from Big Bang Nucleosynthesis (BBN). BBN theory provides a detailed description of the production of light elements (^4He, D, ^3He and ^7Li), through nuclear fusion, when the universe was between $T \simeq 10$ MeV and $T \sim 0.1$ MeV. This theory predicts precise values for the primordial abundances of these light elements (for a given number

of relativistic particle species), as a function of the baryon-to-photon ratio, η_B. These predictions are consistent with the measured primordial abundances if the a baryon-to-photon ration is within the range [24][5]

$$\eta_B = 6.1^{+0.67}_{-0.52}\,, \tag{1.37}$$

or equivalently,

$$\Omega_{B0}h^2 = 0.022^{+0.003}_{-0.002}\,, \tag{1.38}$$

where Ω_B is the density parameter of baryonic matter. The measurement of CMB anisotropies also allows us to constrain the values of Ω_B and η_B. The 7 year results of the Wilkinson Microwave Anisotropy Prove (WMAP7) [26], combined with the Baryon Acoustic Oscillations (BAO) data from the Sloan Digital Sky Survey (SDSS) [27], and the estimates of the Hubble constant with the Hubble Space Telescope [28], indicate that

$$100\Omega_{B0}h^2 = 2.255 \pm 0.054\,, \tag{1.39}$$

which is in good agreement with the range of values that are consistent with the BBN theory (in Eq. (1.38)).

Remarkably, classical astronomical observations, as well as the measurement of CMB's anisotropies, agree as to the geometry, composition and present day expansion rate of the universe (see Fig. 1.1). According to the combined results of WMAP7, BAO, and the Type Ia Supernova data from Union2 [29], we have that

$$\Omega_{K0} = -0.006^{+0.008}_{-0.007}\,. \tag{1.40}$$

Therefore, observations indicate that, currently, the universe is extraordinarilly flat. Recall that,

$$|\Omega_K| \propto \left(\frac{da}{dt}\right)^{-2}\,. \tag{1.41}$$

Hence, in an universe undergoing decelerated expansion (for which $\dot{a}$ is expected to decrease over time), if $|\Omega_K|$ is non-zero, it is expected to grow over time. This means that the universe should have been even flatter in the past. If we assume

[5]There seems to be a significant discrepancy in the abundance of ^7Li that is yet to be explained [25].

that the initial conditions were set at Planck time, we should have that

$$\Omega_{K0} < 0.02 \quad \Rightarrow \quad \Omega_K(t_{\rm pl}) < 10^{-61} \tag{1.42}$$

Therefore, the observed geometry of the universe in the present requires fine tuning of the initial conditions. This is known as the *Flatness Problem*.

The baryonic matter can only account for a small fraction of the present energy density. As a matter of fact, most of the matter contained in the universe is non-ordinary matter: the cold dark matter. The nature of dark matter is still unknown, however its existence has been inferred several years ago from galaxy rotation curves. According to Refs. [26, 29], one has

$$\Omega_{m0} = 0.281^{+0.018}_{-0.016} \quad \text{and} \quad \Omega_{B0} = 0.0450 \pm 0.0016\,. \tag{1.43}$$

The main contribution to the energy density of the universe seems to come from a Cosmological Constant. In fact, according to [26]:

$$\Omega_{\Lambda 0} = 0.7250 \pm 0.0036\,. \tag{1.44}$$

Note, however, that although observations indicate that this dominant energy component behaves similarly to Λ, observational results allow for other exotic energy component with a time dependent equation of state. In Ref. [30] the observational results from Union2, WMAP, BAO and from the measurement of distances to Cepheids [31] are used to constrain various cosmological models. The results indicate that the energy density of the dominant component of the energy density, if not constant, should be, at the present time, slowly varying. The nature of this energy component is still a matter of speculation, and for that reason it is commonly referred to as *Dark Energy*.

1.1.5 Dark Energy

The first evidence for the existence of dark energy came from observations of Type Ia Supernovae (SNIa). SNIa are ephemeral events that result from the nuclear explosion of certain white dwarfs in binary systems. The luminosity curve of SNIa has a characteristic shape and its peak is well correlated to the duration of the event. Moreover, these supernovae seem to occur both in young and old stellar populations, and they may be observed at high redshift since they are very bright. For these reasons, SNIa can be used as *Standard Candles* to measure the distance to the galaxies that host them [32].

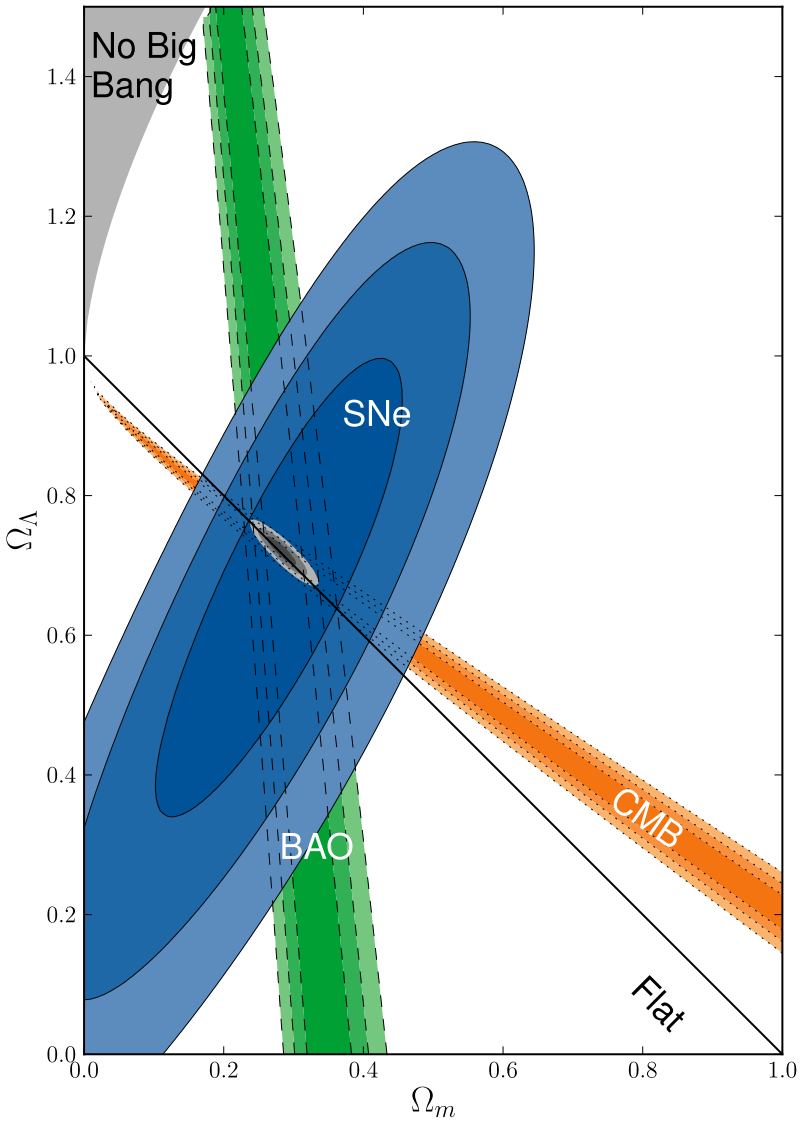

Figure 1.1: $68,3\%$, $95,4\%$ and $99,7\%$ confidence regions of the $(\Omega_\Lambda, \Omega_m)$ plane for Union2 SNIa data, combined with WMAP7 and BAO results. This picture was taken from Ref. [30]

Let L be the absolute luminosity of a light source and f the light flux received from it. Assuming that this source emits photons isotropically, the *Luminosity Distance* to this object is defined as

$$d_L^2 \equiv \frac{L}{4\pi f} \,. \tag{1.45}$$

This luminosity distance is by no means the physical distance to that object: the universe expansion not only redshifts the photons, but also reduces their arrival rate. Therefore,

$$d_L(z) = (1+z) r_s = (1+z) f^{-1}\left(\int_0^z \frac{dz}{H(z)}\right) , \tag{1.46}$$

where r_s is the comoving distance to the source and f^{-1} is defined in Eq. (1.18). For small z, we can write the luminosity distance as

$$d_L \simeq H_0^{-1}\left[z + \frac{1}{2}(1-q_0)z^2\right] + \mathcal{O}(z^3) \,, \tag{1.47}$$

where q_0 is the value of the deceleration parameter, defined as

$$q \equiv -a\frac{\frac{d^2a}{dt^2}}{\left(\frac{da}{dt}\right)^2} \,, \tag{1.48}$$

in the present. Therefore, the measurement of the luminosity distance to Type Ia Supernovae (or any other standard candles) allows us to characterize the expansion of the universe in the present, by determining H_0 and q_0. In 1998, the use of SNIa as standard candles by two independent groups [33, 34, 35] led to the startling discovery that, contrary to what was expected, q_0 is negative, and that the expansion of the universe is then accelerating.

Using Eq. (1.12), we may write the deceleration parameter as

$$q = \frac{1}{2}\left(1 + 3w_{\rm DE}\Omega_{\rm DE}\right) \,, \tag{1.49}$$

where we have assumed that $\Omega_K = 0$ (which is motivated by the observational results presented in the previous section), and that the universe contains only matter and an unknown component which is responsible for the acceleration. This component is commonly denominated Dark Energy and we use $\Omega_{\rm DE} = 1 - \Omega_m$ and $w_{\rm DE}$ to denote, respectively, its density parameter and equation-of-state parameter. The expansion of the universe is accelerated if $q < 0$, or equivalently,

$$w_{\rm DE} < -\frac{1}{3(1-\Omega_m)}. \tag{1.50}$$

Therefore, in order to accelerate the universe, dark energy should be such that $w_{\rm DE} < -1/3$, if $\Omega_m = 0$. This limit is somewhat lowered if we consider the existence of matter: $w_{\rm DE} < -1/2$, for $\Omega_m \approx 1/3$.

The cosmological constant, Λ, was the first dark energy candidate. It is characterized by a constant energy density, and hence Eq. (1.14) yields

$$\mathcal{P}_\Lambda = -\rho_\Lambda, \qquad \text{so that} \quad w = -1\,. \tag{1.51}$$

This value of w seems to be in remarkable agreement with combined observational results from WMAP7, BAO and UNION2 [29]:

$$w = -1.035^{+0.093}_{-0.097}\,. \tag{1.52}$$

However, there are serious problems concerning the physical interpretation of Λ. The zero-point vacuum fluctuations must respect Lorentz invariance, and therefore the vacuum energy would behave like a cosmological constant [36]. This interpretation of Λ as vacuum energy comes with a serious flaw: the energy density generated by vacuum fluctuations is ultraviolet divergent. It is natural, however, to impose a cut-off at the Planck scale (because General Relativity is expected to break down above this scale), and in this case the vacuum energy density would be expected to be of the order of $m_{\rm pl}^4$. The observed cosmological constant energy density,

$$\rho_\Lambda \approx \left(10^{-3}\ \text{eV}\right)^4\,, \tag{1.53}$$

is more than 120 orders of magnitude smaller than the theoretical predictions [37]. This catastrophic discrepancy is still unexplained, and it is known as *Cosmological Constant Problem*.

The Cosmological Constant is even more problematic if we realize that the universe as we know it can only exist for a small range of values of Λ. A larger value of Λ would make the universe accelerate earlier, while large negative values would cause the universe to recollapse in its early history. This is a severe fine-tuning problem: in order to ensure that, in the present, ρ_Λ and ρ_m are of the same order — so that the acceleration of the universe is a recent phenomenon (as the observational results indicate [38]) —, the initial energy density should be very precisely tuned at Planck time: $\rho_\Lambda/\rho_r \simeq 10^{-123}$ [18]. Recall that, as

the universe expands, the matter energy density decreases with a^{-3}, while the vacuum energy density remains constant. Therefore, we are living in a very special epoch in the history of the universe: a transitional period between matter- and cosmological-constant-domination, which is expected to be brief. This approximate coincidence of the values of ρ_m and ρ_Λ at the present time is another puzzling feature of Λ, know as the *Coincidence Problem*.

These difficulties lead to the search of alternative origins for Dark Energy. As previously mentioned, dark energy resembles a cosmological constant, but it is not necessarily so. Observational results allow for a dynamical form of dark energy with a slowly varying equation of state. In this context, scalar field models are natural candidates: they seem to be ubiquitous in particle physics and, consequently, in cosmology. These models — generally dubbed Quintessence — may be realised with a variety of different potentials [39, 40, 41]. Some of these models even alleviate a little the fine-tuning problem by having a cosmological scaling solution [42] or by tracking the background matter field [43]. In any case, fine-tuning of the parameters of the potential is necessary to obtain the adequate acceleration (that fits the observations). Moreover, most of the potentials used in the literature lack a strong theoretical inspiration and are, thus, mainly designed to obtain the correct evolution for $a(t)$. A plethora of alternatives has also been proposed in the literature: scalar fields with non-canonical kinetic terms (the k-essence models) [44]; models based on the Chaplygin gas [45, 46], a fluid which behaves like Λ at late-times; phantom (or ghost) fields [47] — just to name a few. Another class of models, based on modified gravity, does not require the existence of this mysterious energy component. There are several realisations of such models ($F(R)$ gravity, scalar-tensor theories, brane world models, ...[6]) that introduce large-distance corrections to general relativity, which are undetectable at small scales. These modifications would alter the late-time evolution of the universe, and therefore might be designed to cause the cosmic acceleration.

None of the aforementioned models can be considered fully satisfactory. Note, however, that even if an exotic time-dependent form for dark energy is found, the cosmological constant problem will still plague modern physics: we would still need to explain why the vacuum energy vanishes.

In the context of this thesis, we will explore another possible origin for dark energy: frustrated domain wall networks. It has been suggested in Refs. [5, 49]

[6] For a recent review, see [48]

that a domain wall network frozen in comoving coordinates could provide a negative pressure, and, consequently contribute to dark energy. However, it has been shown in Refs. [6, 7, 8], using both analytical models and field theory simulations, that frustrated domain wall networks do not arise in realistic cosmological scenarios. In chapter 4, we study the role of massive string and monopole-like junctions in the frustration of domain wall networks, and investigate if these networks could be suitable dark energy candidates. Moreover, we study the Devaluation Mechanism [9], a dynamical solution to the cosmological constant problem, based on the idea that, after inflation, a biased domain network separating regions with different vacuum energy densities could have been formed. When a domain wall separates two regions with different energy densities, it feels a pressure towards the region with the highest vacuum energy. The regions with higher energy density are suppressed, and therefore this mechanism is expected to lead to lower and lower vacuum energy.

1.2 COSMOLOGICAL PHASE TRANSITIONS AND TOPOLOGICAL DEFECTS

The early stages of the universe are sensitive to the framework of particle physics. The standard model of particle physics describes three of the fundamental interactions between particles — electromagnetic, weak and strong forces— in a quantum theoretical approach. This model is based on the premise of symmetry restoration at high temperatures, according to which the observed symmetries of elementary particles resulted from the breaking of a larger symmetry group.

In this context, spontaneous symmetry breaking is described in terms of a scalar Higgs field. The early universe was, to a good approximation, in thermodynamic equilibrium, so that the equilibrium value of the scalar field is determined by the minimization of the thermodynamic free energy, F

$$F = E - TS\,, \tag{1.54}$$

where E is the internal energy, T is the absolute temperature and S is the entropy. At low enough temperatures, the entropy term in Eq. (1.54) is unimportant, and hence the energy is minimized by one of the vacuum states of the potential. This vacuum state might not be invariant under all the elements of the symmetry group of the lagrangian density, and, in that case, the symmetry is said to be broken. However, at larger temperatures, high-entropy states are energetically favorable. As a matter of fact, the expectation value of ϕ is ex-

pected to vanish above a critical temperature, T_c. At that point, the universe undergoes a phase transition. Typically, this high-temperature phase exhibits the full symmetry of the lagrangian density.

According to the Electroweak Theory, developed by Glashow, Salam and Weinberg in the 70's, the electromagnetic and weak interactions, may be regarded as different aspects of the same force — the electroweak force. In the early universe, at high temperatures, this force was described by a lagrangian density which is invariant under gauge $SU(2) \times U(1)$ transformations. This symmetry, however, was broken as the universe cooled down and, thus, electromagnetic and weak interactions seem independent in the present. This unification of electromagnetic and weak interactions lead to the development of Grand Unified Theories (GUT's) that attempt to unify the electroweak and strong interactions. These theories are based on the same premise as electroweak theory: the lagrangian that describes this single interaction was invariant under a gauge symmetry group but this symmetry is now broken.

The universe is, then, expected to have experienced a series of phase transitions in its early stages:

- At $T_{GUT} \simeq 10^{15}$ GeV, there is a spontaneous breaking of GUT symmetry. In the simplest version of GUT,

$$SU(5) \to SU(3) \times SU(2) \times U(1)\,. \tag{1.55}$$

  After this phase transition, the strong interaction and electroweak interaction become independent.

- At $T_{EW} \simeq 10^2$ GeV, the breaking of electroweak symmetry,

$$SU(3) \times SU(2) \times U(1) \to SU(3) \times U(1)\,, \tag{1.56}$$

  occurs and, therefore, electromagnetic and weak interactions separate.

- At $T_{QH} \simeq 200 - 300$ MeV, another phase transition is expected to occur (or, perhaps several): the quark-hadron phase transition. During this transition, quark confinement into hadrons takes place. This phase transition is characterized by the symmetry breaking:

$$SU(3) \times U(1) \to U(1)\,. \tag{1.57}$$

These cosmological phase transitions may have important cosmological con-

sequences. Recall that, Spontaneous Symmetry Breaking occurs as, at a temperature T_c, the scalar field acquires a vacuum expectation value (VEV). Since the universe is composed, at a given time, of several causally disconnected regions, the VEV of ϕ cannot be expected to be correlated on scales larger than the particle horizon. Therefore, given that all the vacua are equivalent, different patches of the universe — characterized by a correlation length $\zeta < d_p$ — are expected to have different vacuum expectation values. In order for ϕ to be continuous, there must be regions where the underlying field cannot relax into any vacuum state, giving rise to topological defects. This mechanism for the formation of topological defects in cosmological phase transitions is known as *Kibble mechanism* [50, 51].

1.2.1 The ϕ^4-kink

To illustrate the process of symmetry breaking and the formation of topological defects, let us consider the simplest model that admits a topological defect: the Goldstone model [52] with a single scalar field, ϕ. For this model, the lagrangian density is given by

$$\mathcal{L} = \frac{1}{2}\phi_{,\mu}\phi^{,\mu} - V(\phi) \tag{1.58}$$

with a potential of the form

$$V(\phi) = \frac{\lambda}{4}\left(\phi^2 - \eta^2\right)^2 , \tag{1.59}$$

where λ is a coupling constant. The equations of motion for the scalar field, ϕ, may be obtained by varying the action,

$$S = \int d^{N+1}x\sqrt{-g}\mathcal{L} , \tag{1.60}$$

with respect to ϕ:

$$\frac{1}{\sqrt{-g}}\left(\sqrt{-g}\phi^{,\mu}\right)_{,\mu} = -\frac{dV}{d\phi} , \tag{1.61}$$

where N is the number of spatial dimensions, $g_{\mu\nu}$ is the metric tensor and $g = det(g_{\mu\nu})$.

In a $1+1$ dimensional Minkowski spacetime, for which $g = -1$, the static solutions should satisfy the following equation of motion

$$\frac{\partial^2\phi}{\partial x^2} = \frac{dV(\phi)}{d\phi} . \tag{1.62}$$

The lagrangian density in Eq. (1.58), with the potential in Eq. (1.59), is invariant under transformations $\phi \to -\phi$, and thus has a Z_2 symmetry. Moreover, $V(\phi)$ has two degenerate minima at $\phi = -\eta$ and $\phi = \eta$. Now suppose that ϕ acquires an expectation value

$$\phi_\pm = \langle 0 | \, \phi \, | 0 \rangle = \pm\eta \,, \tag{1.63}$$

where $|0\rangle$ is the ground state of the model. Although all transformations of, say, ϕ_+ by elements of Z_2 yield legitimate VEVs of ϕ, not all elements of Z_2 have a non-trivial effect on ϕ_+. As matter of fact, only the identity of the group does so. Therefore, once the scalar field acquires a VEV, the Z_2 symmetry is broken.

Eq. (1.62) has the following static solution [53]

$$\phi(x) = \eta \tanh\left[\eta \lambda^{1/2} 2^{-1/2} \, (x - x_0)\right] \,, \tag{1.64}$$

that corresponds to a kink centered at $x = x_0$ which takes ϕ from $-\eta$ as $x \to -\infty$ to η as $x \to +\infty$. Since $\phi(x)$ passes through $\phi = 0$ at $x = x_0$ (that does not correspond to a minima of the potential), this configuration has non-vanishing energy. Moreover, this solution is stable: one would need an infinite amount of energy in order to relax the field configuration to only one of the vacua. As a matter of fact, this is a consequence of the presence of a conserved topological current,

$$j^\mu = \epsilon^{\mu\nu} \phi_{,\nu} \,, \tag{1.65}$$

where $\epsilon^{\mu\nu}$ is the two-dimensional antisymmetric symbol. This configuration, then, has a non-vanishing conserved charge

$$Q = \int dx j^0 = \phi(+\infty) - \phi(-\infty) \,. \tag{1.66}$$

Since the vacuum state would have $Q = 0$, the kink configuration is unable to relax into the vacuum while conserving the topological charge.

Note that, far from $x = x_0$, the potential lies on one of the minima in one side of the kink and on the opposite minimum on the other. So the kink is, actually, a boundary where the field interpolates between $-\eta$ and η. The energy of this configuration is localized in the region were ϕ is not in the vacuum. This region is centered at x_0 and its thickness is proportional to the mass scale of the model

$$\delta \sim m_\phi^{-1} \sim \frac{1}{\eta} \sqrt{\frac{2}{\lambda}} \,. \tag{1.67}$$

According to *Derrick's Theorem* [54], scalar field theories of the form of Eq.

(1.58) do not admit stable time-independent solitons with a finite energy in more than one spatial dimensions. There is however the possibility of evading this difficulty by not being to selective about the solitons: for instance, by allowing for time-dependence, or by admitting static solutions with an infinite energy. The kink solution may be trivially embedded in higher dimensional backgrounds. In a $3+1$ (or $N+1$) dimensional theory, the static solution Eq. (1.64) remains valid and it represents a 2 (or $N-1$) dimensional planar surface, that depends only on one of the spatial coordinates. This surface separates two domains with different vacuum expectation values and, for that reason, it is commonly denominated a *Domain Wall*. These domain wall solutions have infinite energy (because they have an infinite extension), however their energy per unit area is finite.

1.2.2 The Topology of the Vacuum Manifold and the Production of Topological Defects

Let us now consider a general field theory model, whose action is invariant under a symmetry group G. If the field acquires a VEV, ϕ_0 (and, thus, the symmetry breaks), some of the elements of G will have non-trivial effects on ϕ_0, transforming it into another vacuum state ϕ_1. However, there exists a subgroup of G, the unbroken group H, whose elements will leave ϕ_0 unchanged. The coset space, G/H — the space of all non-trivial transformations of ϕ_0 — contains all the vacuum states. This space is the vacuum manifold of the theory, $\mathcal{M}$, and its topological properties signal the possible existence of defects and the type of defects that might appear.

Topological defects appear if the vacuum has a non-trivial topology. Let us now return to the case of a Z_2-domain wall. In this case, $G = Z_2$ and $H = \mathbb{1}$ (where $\mathbb{1}$ is the identity), and therefore the vacuum manifold consists merely of two points. These points cannot be continuously deformed into one another. This fact signals the possible occurence of domain walls: these defects can only arise if the vacuum manifold is disconnected, due to the breaking of a discrete symmetry.

Other types of defects may arise if $\mathcal{M}$ has different topological properties. Let us consider the Goldstone model with a complex scalar field:

$$\mathcal{L} = \frac{1}{2}\phi_{,\mu}\bar{\phi}^{,\mu} - \frac{\lambda}{4}\left(\phi\bar{\phi} - \eta^2\right)^2 . \tag{1.68}$$

In this case, the potential has a continuous (global) $U(1)$ symmetry and it is invariant under transformations of the form

$$\phi \to e^{i\alpha}\phi\,. \tag{1.69}$$

The minima of the potential lie in the circle $|\phi| = \eta$. Now let us suppose that ϕ acquires a VEV

$$\phi_0 = \langle 0|\,\phi\,|0\rangle = \eta e^{i\theta}\,. \tag{1.70}$$

A transformation of the form of Eq. (1.69) will transform ϕ_0 into $\phi_1 = \eta e^{i(\theta+\alpha)}$, which, in general, does not correspond to the same vacuum state — the symmetry is broken.

Points in physical space are mapped non-trivially into the circle of minima, so ϕ might span the whole manifold as we travel around a circle in physical space. Along one such path, ϕ has a non-trivial winding: the phase of ϕ varies by 2π. By continuity, ϕ must vanish in a point inside this closed circle, and therefore there must be a non-vanishing energy density at this point. This indicates the presence of a line-like topological defect, usually named *Cosmic String*. The number of times ϕ winds around $\mathcal{M}$ as a circle is spun around the string — the winding number — is a topological conserved charge. The energy of these global $U(1)$ strings is, unfortunately, not localized to a small region around the core of the defect. Consequently, the energy per unit length of this configuration is divergent. However, string originated in the spontaneous symmetry breaking of gauge symmetries do not suffer from the same problem.

Cosmic strings can arise whenever the vacuum manifold is not simply connected, or equivalently, if it contains unshrinkable loops. This type of manifolds result, in general, from the breaking of an axial symmetry.

Moreover, if the vacuum manifold contains unshrinkable surfaces, the field might develop non-trivial configurations corresponding to point-like defects, generally dubbed monopoles. The breaking of GUT symmetry is expected to lead to the copious production of magnetic monopoles, which would overclose the universe. However objects of this kind were never observed. This discrepancy between theory and observation is known as *Monopole Problem*. In $3+1$-dimensions, another type of defect may also arise if the vacuum manifold has unshrinkable 3-spheres. These defects, usually denominated textures, are space-time defects and are, in general, unstable to collapse.

These results may be summarized in terms of homotopy theory (which is

used to characterize the topological properties of a topological space). Roughly speaking, the n^{th} homotopy group of a topological space, X, is the set of all the mappings from the n-dimensional sphere into X, and it is denoted by $\pi_n(X)$. The types of defects that can be formed in a symmetry breaking are determined by the non-trivial homotopy groups of $\mathcal{M}$ [50]: in $3+1$-dimensions, a p-dimensional defect can be formed if

$$\pi_{3-(p+1)}(\mathcal{M}) \neq \mathbb{1}\,. \tag{1.71}$$

This condition is necessary for the formation of defects, but it is not sufficient: the topology of $\mathcal{M}$ only indicates which type of defects *can* be formed.

1.2.3 The inflationary paradigm

As we pointed out in Sec. 1.1, the extreme flatness and homogeneity of the observed universe cannot be explained by the Standard Cosmology model. However, Guth [55] realised that both these problems may be resolved if the universe underwent a period of accelerated expansion. The essential feature of inflation is that the scale factor, $a(t)$, grows faster than the Hubble radius, so that the comoving Hubble radius decreases with time

$$\frac{d}{dt}\left(\frac{H^{-1}}{a}\right) < 0\,. \tag{1.72}$$

Therefore, if the expansion is fast enough, the size of the comoving Hubble radius decreases drastically during inflation. In this case, the observed universe — which appears to be composed of several causally disconnected regions — might have been within a causal horizon in the early stages of inflation and the observed homogeneity might be justifiable on physical grounds. Moreover, since the final stages of the inflationary epoch are expected to occur after the GUT phase transition, the density of magnetic monopoles — which are expected to be copiously produced during this phase transition — is expected to decrease steeply during this period. This solves the magnetic monopole problem: magnetic monopoles are expected to have been diluted by inflation to undetectable levels. This phase of accelerated expansion would also lead to the flattening of the universe. One sees that, during an inflationary period, Ω_K will gradually decrease towards zero, and, consequently, the universe becomes locally flat.

Inflation also seems to explain the origin of the large-scale structure in the universe. During an inflationary epoch, small-scale inhomogeneities (due to quantum fluctuations of scalar or gravitational fields) are stretched to large

scales. Therefore, these quantum fluctuations might have been the source of the primordial fluctuation spectrum that seeded structure formation.

The original implementation of inflation, suggested by Guth, was abandoned due to some inherent flaws. However, the basic idea remained due to the potential to solve some of the most pressing problems of Standard Cosmology. It has been replaced by a new inflationary scenario [56, 57], in which inflation is driven by a very weakly coupled scalar field (the inflaton). In this scenario, accelerated expansion occurs as the inflaton, which is initially displaced from the minimum of the inflaton potential, slowly rolls towards it. As in the case of dark energy, several models of inflation have been suggested in the literature, but none of them is particularly compelling or considered definitive. However, the graceful solutions provided for the shortcomings of the Standard Cosmological Model, make inflation a generally accepted paradigm.

1.3 DEFECT PRODUCTION IN BRANE INFLATION

Fundamental string theory originated in the search for the unification of gravity with the other fundamental forces. In quantum field theory, when treating spacetime as a continuum, several infinite results appear in measurable quantities. As a consequence, a set of techniques was developed, known as renormalization, to deal with these divergences by absorbing them into the definition of measurable quantities. However, many efforts to construct a renormalizable quantum theory of gravity have been thwarted. Most of the infinities in these theories appear when treating the elementary particles as point-particles. This realization lead to the development of String Theory, in which elementary particles are represented by extended 1+1-dimensional objects: the particles are regarded as different modes of oscillation of a Fundamental String. Although by incorporating supersymmetry, it is possible to construct a theory — Superstring Theory— that appears to be free of the undesirable infinities, this theory is only consistent in 10 (9+1) dimensions. As a consequence, the suggestion emerged that our universe is in fact 9+1-dimensional, but 6 of the spatial dimensions are compactified, so that they are very small and undetectable from our macroscopic perspective.

Initially, cosmic strings and fundamental superstrings were thought to be unrelated. In Ref. [58], Witten investigated whether or not superstrings could grow to macroscopic scales and play the role of cosmic strings. However, in his work several incompatibilities were brought to light. First of all, the tension of superstrings appeared to be too high: superstring energy scale is close to the

Planck scale, so that

$$G\mu \gtrsim 10^{-3}\,. \tag{1.73}$$

If superstrings were to play the role of cosmic strings, they should be such that [59, 60]

$$G\mu \lesssim 10^{-6.5}\,, \tag{1.74}$$

in order to agree with the observed power spectrum of CMB[7]. Witten also noted, in the same article, that macroscopic superstrings would be unstable, due to fragmentation into microscopic strings (corresponding to light particle excitations), and to confinement by axion domain walls. Moreover, the production of superstrings after inflation seemed unlikely, due to the string's energy scale. As a consequence, any existing superstring would have been diluted to undetectable values during the inflationary epoch.

This article seemed to settle the matters for a decade, however the picture has changed due to the introduction of the brane-world scenario. This scenario was proposed as an alternative way to recover the observed 3+1 dimensions, in a 9+1-dimensional universe. In this scenario there are two types of objects: Dirichlet Branes (or Dp-branes), which are p-dimensional surfaces embedded in the larger space, and Fundamental strings (or F-strings), that may be open-ended or form closed loops. Open F-strings can end on Dp-branes, with Dirichlet boundary conditions. In this scenario, the visible universe is, in fact, a very large D3-brane, that can move within the 9+1-dimensional space. The constituents of the universe consist of segments of fundamental strings with their ends attached to our brane and are, thus, bound to it. Gravitons, on the other hand, correspond to vibrational states of closed F-string loops that are not bound to our brane. Consequently, gravitational effects may depend upon the extra-dimensions.

1.3.1 Brane Inflation and Defect Production

In the braneworld context, a natural model for inflation, based on the interaction between branes, emerged: the brane inflation scenario. Although this scenario may be realized in a variety of other different ways (see for example [61, 62, 63]), brane-antibrane (D-$\overline{\text{D}}$) inflation [1, 64, 65] is particularly interesting in what regards to cosmic superstrings. Suppose the universe has an extra

[7] At the time, before COBE and WMAP probes, the constraint was looser, but nonetheless incompatible with superstring tension.

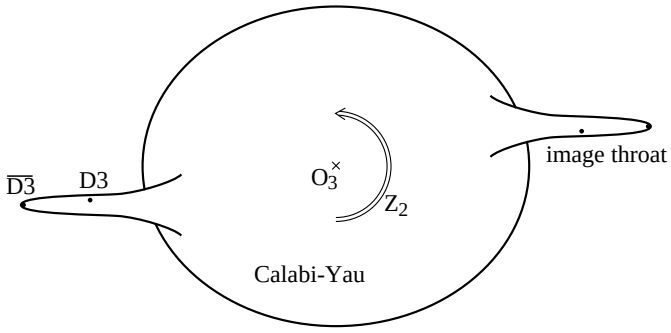

Figure 1.2: Schematic representation of the KLMT geometry: a warped Calabi-Yau Manifold with throats. This picture was taken from Ref. [70].

D-$\overline{\text{D}}$ pair separated in the compact dimensions. In this case, inflation occurs as the branes move towards each other, and it ceases as they collide and annihilate. The role of the inflaton is played by the inter-brane distance and the inflaton potential is originated by the interactions between branes. An interesting feature of this model is that the annihilation of the branes is expected to provide a mechanism for converting the energy of the relative brane motion into reheating the universe. Even more compelling is the fact that, during a D-$\overline{\text{D}}$ collision, a significant portion of this energy may be trapped and lead to the production of daughter branes.

As a matter of fact, there is a tachyon field living on the worldvolume of the D-$\overline{\text{D}}$ pair (an open string mode stretching between the two branes). As the inter-brane distance falls bellow a critical value, the tachyon develops an instability and triggers a spontaneous symmetry breaking. This, not only leads to the decay of the original branes, but also leads to the formation of defects via Kibble Mechanism [66, 67]. In Refs. [2, 68, 69, 3], it has been shown that the production of branes with lower dimensionality is expected in a large variety of brane inflation models, and that these defects appear as topological defects to the 4-dimensional observer. The production of 1+1-dimensional D-branes (or D-strings) is favoured over the production of branes with higher dimensionality. Note however that other defects may be produced at a detectable level. Brane inflation may, therefore, provide a natural mechanism for the formation of cosmic strings and p-brane networks evolving in a higher dimensional space. Note also that, since this production occurs in the final stages of inflation, this defects are not expected to be dispersed by the accelerated expansion.

Brane inflation also found ways off tackling the superstring tension problem, by recurring to different compactifications of the extra-dimensions. For instance,

a particularly interesting way of realising brane inflation is the KLMT model [71]. In this model, spacetime is compactified on a Calabi-Yau manifold (see Fig. 1.2):

$$ds^2 = e^{2A(x_\perp)}\eta_{\mu\nu}dx^\mu dx^\nu + ds_\perp^2\,, \tag{1.75}$$

where $x_\perp$ denotes the coordinates in the compact space. The metric of the physical 4-dimensional spacetime is scaled by a factor $e^{A(x_\perp)}$— a gravitational redshift— that varies strongly as function of the compact dimensions. In most of the compact space, $e^{A(x_\perp)}$ is approximately 1, however it may be much smaller in some regions, the so-called 'throats'. In the KLMT model, inflation occurs as a D3-$\overline{\text{D}}$3 pair moves towards each other down one of this throats, and the consequent string formation occurs in the bottom of the throat. In this case, the effective string tension measured by a 4-dimensional physicist is, then, suppressed by gravitational redshift

$$\mu = e^{A(2x_\perp)}\mu_0\,, \quad \text{with} \quad e^{A(x_\perp)} \ll 1, \tag{1.76}$$

while a 10-dimensional observer measures a string tension μ_0 (which corresponds to a string energy scale similar to the 4-dimensional Planck scale). Another possibility would be the existence of large compact dimensions. In this case the 4-dimensional Planck length can be much smaller than the string length, and, consequently, the strings appear to the 4-dimensional observer to have smaller tensions.

Finally, F- and D-strings can only play the a cosmological role of cosmic strings if there is a way to suppress their natural decay mechanisms (the detais depend on the particular model considered [70, 72]). However, in Refs. [73, 68, 2], the authors found that D-$\overline{\text{D}}$ inflation naturally leads to the formation of stable cosmic superstrings with tensions within the range

$$10^{-12} \leqslant G\mu \leqslant 10^{-6}, \tag{1.77}$$

but mainly concentrated along $G\mu \simeq 10^{-7}$. This range is compatible with the bound set by the observational CMB data (in Eq. (1.74)).

1.3.2 Cosmic Superstring Properties

Cosmic superstrings have distinct properties that demarcate them from ordinary cosmic strings. First of all, there are two types of cosmic superstrings, F- and D-strings, that have similar properties but have different tensions

$$\mu_D = \frac{\mu_F}{g_s}\,, \tag{1.78}$$

where μ_D and μ_F are, respectively, the tensions of D- and F-strings and g_s is the dimensionless string coupling. Also, superstrings might have a smaller reconnection probability. It has been shown in Ref. [74] that in the case of F-strings, the reconnection probability is of the order of g_s^2, and, consequently, it can be significantly smaller than unity. More recently, it was shown in Ref. [75] that the reconnection probability, P, is within the range $0.1 \lesssim P \lesssim 1$ for D-D collisions, and $10^{-3} \lesssim P \lesssim 1$ for the case of F-F string crossings.

These distinctive features of cosmic superstrings are expected to have some influence on the evolution of cosmic superstring networks. Ordinary cosmic string networks evolve towards a linear scaling regime, during which its energy density remains constant relative to the (matter) background density. The attainment of this regime guarantees that cosmic strings do not become pathological: their energy density never overcomes the background density and, thus, they cannot dominate the universe. Note that, as a result of cosmic string interactions, the network loses energy due to the formation of cosmic string loops, and this energy loss is beneficial for the attainment of the linear scaling regime. In the case of cosmic superstring networks, given that the reconnection probability might be smaller than unity, this energy loss mechanism is expected to be less efficient. Consequently, the density of (long) strings is expected to increase. As a matter of fact, it has been shown in Ref. [76], using numerical simulations of Nambu-Goto string networks, that if $P \leqslant 0.1$, then $\rho_{\rm st} \propto P^{-\alpha}$, with $\alpha \sim 0.6$ (whereas for $P \geqslant 0.1$ little enhancement of cosmic string density was observed).

The most significant difference between superstrings and ordinary strings, however, is a consequence of the crossings of superstrings of different types. In this case, strings are unable to intercommute or pass through each other. Instead, if a pF-string and a qD-string collide, they bind together, giving rise to a new type of string, usually denoted as (p, q)-string. The tension of this bound state is different, in general, from that of the colliding strings, and it is given by

$$\mu(p, q) = \mu_F \sqrt{p^2 + \frac{q^2}{g_s^2}}\,. \tag{1.79}$$

Cosmic superstring crossings may result then in the formation of a trilinear vertices (or Y-type junctions) where 3 different types of strings meet. This process, occurring recursively, may lead to the formation of several types of cosmic superstrings with different tensions. As a matter of fact, when a (p, q)-string meets a (p', q') string, there are two possible outcomes: either a $(p+p', q+$

q')-string or a $(p-p', q-q)$-string is formed. The outcome of the intersection is determined by the angle between the strings at the moment of collision [70, 75]. Another important point is that these bound states are only stable if q and p are co-prime. If they have a common factor, so that $p = np''$ and $q = nq''$ (for any natural number n), the resulting (p, q)-string will rapidly decay into n (p'', q'')-strings[8].

Therefore, the creation of (p, q) bound states is expected to lead to the formation of entangled networks with multi-tension spectra, where different types of strings meets at Y-type junctions. Whether or not the presence of junctions prevents string networks from attaining a scaling regime is still an open question. However, both analytical models [77, 78, 79], and numerical simulations of non-abelian field-theory networks [80, 81, 82, 83] seem to indicate that F-, D- and (p, q)-strings reach a linear scaling regime.

The realization that inflation might lead to the formation of cosmic string and p-brane networks evolving in higher dimensional spacetime, triggered a revival of the interest in topological defects in cosmology. This interest was enhanced due to the possibility of detecting the signatures of cosmic strings and/or cosmic superstrings on the B-mode polarization [84, 85] and on the small scale anisotropies [86, 87, 88] of the Cosmic Microwave background with the Planck mission, and the possibility of detecting their gravitational waves in LIGO2 and LISA missions (depending on their tension) [89].

In this thesis we study the cosmological evolution of p-brane networks in $N + 1$-dimensional FRW universes. In order to so, we start by deriving, in Chapter 2, a equation of motion for thin curved domain walls in higher dimensional backgrounds, which is independent of the underlying field theory model. This result is then generalized to the case of infinitely-thin p-branes of arbitrary dimensionality. We also study in detail maximally symmetric p-brane solutions in collapsing and expanding backgrounds, by determining the microscopic evolution equations for their velocity and physical radius.

In Chapter 3, we develop an analytical model that describes the cosmological evolution of the root-mean-square velocity and the characteristic length of a p-brane network. This model describes the whole cosmological evolution of p-brane networks in expanding and collapsing models, and allows us to study the different scaling regimes that arise in their evolution. In particular, we will study the conditions under which p-brane networks evolve towards a linear scaling regime, with or without energy-loss mechanisms.

[8]The reconnection probability for collisions of two (p, q)-strings of the same kind might also be significantly smaller than unity [75].

2

p-brane Equation of Motion

The inflationary paradigm [55, 56], based on the idea that the universe underwent a period of accelerated expansion in its early history, provides the most plausible solution to the main shortcomings of the Standard Cosmological Model — the flatness, horizon and magnetic monopole problems — and explains the origin of the large-scale structure of the universe. In the context of the brane-world realization of string theory, cosmological inflation could be driven by the interaction between p-dimensional D-branes, which are (along with superstrings) the fundamental objects of this theory [61]-[65]. These brane inflationary scenarios typically end with a symmetry breaking phase transition, triggering the production of daughter branes with lower dimensionality, that appear as topological defects to the 4-dimensional observer. Despite the fact that, in this process, the production of 1-branes (cosmic strings) is strongly favoured, higher-dimensional p-branes may also be generated at a detectable level [69, 2]. Therefore, inflation may offer a natural mechanism for the formation of p-brane networks evolving in a higher-dimensional spacetime.

In this chapter, we will study the dynamics of p-branes of arbitrary dimensionality in $N+1$-dimensional FRW universes. We will start by deriving, in Sec. 2.1, the equations of motion for $N-1$-branes (or domain walls) in $N+1$-dimensional backgrounds. In Sec. 2.2, we will generalize this result for p-branes with $p \neq N-1$. Finally, in Sec. 2.3, we will study in detail the evolution of maximally symmetric closed p-branes, in $N+1$-dimensional expanding and

collapsing FRW universes.

2.1 DOMAIN WALL DYNAMICS

In this section, we will derive the evolution equation for the velocity of domain walls in homogeneous and isotropic universes of arbitrary dimensionality, and we will demonstrate that this equation is independent of the underlying field theory model. This work was published in Ref. [13].

Consider the Goldstone model with a single real scalar field, ϕ, described by the lagrangian density

$$\mathcal{L} = \frac{1}{2}\phi_{,\mu}\phi^{,\mu} - V(\phi)\,, \tag{2.1}$$

where $V(\phi)$ is the potential. Domain walls are expected to arise in models with spontaneously broken discrete symmetries. Therefore, in order for this theory to admit domain wall solutions, the potential must have a discrete set of degenerate minima. The dynamics of these domain walls is determined by the underlying field theory. By varying the action,

$$S = \int d^N x \sqrt{-g}\mathcal{L}\,, \tag{2.2}$$

with respect to the scalar field ϕ, we obtain the following equation of motion:

$$\frac{1}{\sqrt{-g}}\left(\sqrt{-g}\ \phi^{,\mu}\right)_{,\mu} = -\frac{dV}{d\phi}\,, \tag{2.3}$$

where $g = \det(g_{\mu\nu})$ and $g_{\mu\nu}$ is the metric tensor. In a $N+1$-dimensional flat Friedmann-Robertson-Walker universe (FRW), whose line element is

$$ds^2 = -dt^2 + a^2(t)\, d\mathbf{x}\cdot d\mathbf{x}\,, \tag{2.4}$$

we find that

$$\frac{\partial^2\phi}{\partial t^2} + NH\frac{\partial\phi}{\partial t} - \nabla_c^2\phi = -\frac{dV}{d\phi}\,, \tag{2.5}$$

where $\nabla_c^2\phi = a^{-2}\nabla^2\phi$ is the comoving laplacian.

In a 3+1-dimensional Minkowski spacetime (with $a = 1$), a planar domain wall static solution oriented along the x-direction is described by $\phi = \phi_s(l)$, with

$$\frac{d^2\phi_s}{dl^2} = \frac{dV}{d\phi}\,, \tag{2.6}$$

where $l = x$ and we took $\mathbf{x} = (x_1, x_2, x_3)$ and $x = x_1$. By Lorentz invariance, this static solution may be boosted up to arbitrary velocities along the (positive) x-direction. In this case, the planar domain wall solution to Eq. (2.5) is still given by $\phi_s(l)$ and satisfies Eq.(2.6), but now

$$l = \gamma\,(x - vt)\ , \tag{2.7}$$

where v is the domain wall velocity and $\gamma = (1 - v^2)^{-1/2}$ is the Lorentz factor. In this case, $\partial l/\partial t = -\gamma v$ and $\partial l/\partial x = \gamma$.

Consider the more general case of a curved domain wall in a flat FRW Universe. Let us assume that the curvature radii of the domain wall are much larger than its thickness. As a consequence, we expect the scalar field ϕ to vary quickly in directions orthogonal to the wall and to vary slowly in the tangential directions [90]. It is convenient to choose a coordinate system (u_1, u_2, u_3) such that the wall is, at a given point, a coordinate surface satisfying the condition $u_1 =$ constant. The coordinate u_1 is then chosen to be a length parameter along the unit (geodesic) normal to the surface at that particular point, $\hat{\mathbf{u}}_1$ (which is then normal to all u_1 coordinate surfaces). The domain wall is then locally parametrized by the coordinates u_2 and u_3, and it moves along the u_1-direction. Moreover, it is also useful to choose an orthogonal coordinate system in which the coordinate lines $u_2 =$ constant and $u_3 =$ constant are lines of curvature. In this case, the principal directions of curvature — along which the normal curvature of the surface takes its extremal values — coincide with the u_2 and u_3-directions and the normal curvatures along these directions are the principal curvatures of the surface. It is always possible to construct such a coordinate system in the vicinity of any non-umbilic point — in which the two principal curvatures exist and are not equal — of a coordinate surface embedded in a flat space (see e. g. [91, 92]). Note that this set of coordinates is defined locally in the vicinity of the core of the domain wall. According to Refs. [93, 94], the range of validity of u_1 is, roughly speaking, constrained by the smaller curvature radius of the domain wall in its local rest frame.

Let v be the velocity of the domain wall segment at the chosen point. The domain wall solution is still given by $\phi_s(l)$, but in this case l is such that

$$\frac{\partial l}{\partial t} = -\gamma v, \quad \frac{\partial l}{\partial s_1} = \gamma\,, \quad \text{and} \quad \frac{\partial l}{\partial s_2} = \frac{\partial l}{\partial s_3} = 0\,, \tag{2.8}$$

where $ds_i = |d\mathbf{x}_i|$ is the arc length along direction u_i, $d\mathbf{x}_i = h_i du_i \hat{\mathbf{u}}_i$, $\hat{\mathbf{u}}_i$ is the unit vector along the direction u_i, and h_i are the scale factor (or Lamé coefficients) of the coordinate system. We shall use the gauge freedom to choose the coordinate u_1 in such a way that measures the arclength along the direction perpendicular to the domain wall, so that $h_1 = 1$ and $ds_1 = du_1$.

Therefore, we have that

$$\frac{\partial\phi}{\partial t} = -\frac{d\phi_s}{dl}\gamma v, \qquad \frac{\partial\phi}{\partial s_1} = \frac{d\phi_s}{dl}\gamma\,, \qquad \frac{\partial^2\phi}{\partial s_1^2} = \gamma^2\frac{d^2\phi_s}{dl^2} \tag{2.9}$$

$$\frac{\partial^2\phi}{\partial t^2} = (\gamma v)^2\frac{d^2\phi_s}{dl^2} - \frac{\partial}{\partial t}(\gamma v)\frac{d\phi_s}{dl} \tag{2.10}$$

Taking into account that, in the thin-wall approximation, $\phi = \phi(t, u_1)$, the laplacian is given by

$$\nabla^2\phi = \frac{1}{h_1h_2h_3}\left[\frac{\partial}{\partial u_1}\left(\frac{h_2h_3}{h_1}\frac{\partial\phi}{\partial u_1}\right)\right] = \left[\left(\frac{1}{h_2}\frac{\partial h_2}{\partial u_1} + \frac{1}{h_3}\frac{\partial h_3}{\partial u_1}\right)\frac{\partial\phi}{\partial u_1} + \frac{\partial^2\phi}{\partial u_1^2}\right]. \tag{2.11}$$

The first term in the Laplacian is a curvature term. The curvature vector of a curve parameterized by p is given by:

$$\mathbf{k_p} = \frac{d\hat{\mathbf{e}}_p}{ds_p}\,, \tag{2.12}$$

where $\hat{\mathbf{e}}_p$ is the unitary vector tangent to the curve and ds_p is the arclength.

The principal curvatures of the surface are, at any point, given by the normal curvature along its lines of curvature. The principal curvatures are then given by

$$k_2 = \mathbf{k}_2 \cdot \hat{\mathbf{u}}_1\,, \qquad \text{and} \qquad k_3 = \mathbf{k}_3 \cdot \hat{\mathbf{u}}_1\,, \tag{2.13}$$

where

$$\mathbf{k_2} = \frac{1}{h_2}\left[\frac{\partial\hat{\mathbf{u}}_2}{\partial u_2}\right]_{u_3=u_3^0}, \tag{2.14}$$

$$\mathbf{k_3} = \frac{1}{h_3}\left[\frac{\partial\hat{\mathbf{u}}_3}{\partial u_3}\right]_{u_2=u_2^0}, \tag{2.15}$$

and u_3^0 and u_2^0 are constants.

The vectors $\hat{\mathbf{u}}_1$, $\hat{\mathbf{u}}_2$ and $\hat{\mathbf{u}}_3$ form an orthonormal but, in general, a non-coordinate basis. Their derivatives can be calculated using the relation

$$\frac{\partial \hat{\mathbf{u}}_i}{\partial u_j} = \frac{1}{h_i}\frac{\partial h_j}{\partial u_i}\hat{\mathbf{u}}_j - \sum_k \frac{1}{h_k}\frac{\partial h_i}{\partial u_k}\hat{\mathbf{u}}_k\,, \tag{2.16}$$

and, hence

$$k_2 = -\frac{1}{h_2}\frac{\partial h_2}{\partial u_1}, \qquad k_3 = -\frac{1}{h_3}\frac{\partial h_3}{\partial u_1}\,. \tag{2.17}$$

The relevant curvature for domain wall dynamics is the extrinsic curvature: the "bending" of the wall in relation to the flat embedding universe. Mathematically this is measured the curvature parameter

$$\kappa = \mathbf{k}_2 \cdot \hat{\mathbf{u}}_1 + \mathbf{k}_3 \cdot \hat{\mathbf{u}}_1 = -\left(\frac{1}{h_2}\frac{\partial h_2}{\partial u_1} + \frac{1}{h_3}\frac{\partial h_3}{\partial u_1}\right)\,. \tag{2.18}$$

Therefore, Eq. (2.11) can be written as[1]

$$\nabla^2\phi = -\kappa\frac{\partial \phi}{\partial u_1} + \frac{\partial^2 \phi}{\partial u_1^2}\,, \tag{2.19}$$

which inserted into Eq. (2.5) (and taking into account Eqs. (2.9-2.10)) yields

$$-\frac{d^2\phi_s}{dl^2} + \mathcal{F}\frac{d\phi_s}{dl} = -\frac{dV}{d\phi_s}\,, \tag{2.20}$$

where

$$\mathcal{F} = -\frac{\partial}{\partial t}\left(\gamma v\right) - 3H\gamma v + \kappa\gamma\,. \tag{2.21}$$

However, given that ϕ_s is a solution to Eq. (2.6), we should have that $\mathcal{F} = 0$. Therefore, we find that the evolution equation for the velocity of a domain wall in a $(3+1)$-dimensional background is given by

$$\frac{\partial v}{\partial t} + (1-v^2)\left[3Hv - \kappa\right] = 0\,. \tag{2.22}$$

It is straightforward to generalize this procedure to the case of $N+1$-dimensional FRW Universes. In this case, domain walls are defects with $N-1$ spatial dimensions whose dynamics is described by

$$\frac{\partial v}{\partial t} + (1-v^2)\left[NHv - \kappa\right] = 0\,, \tag{2.23}$$

where

[1] In Refs. [95, 90, 96, 93, 94], higher order thickness and curvature corrections to this expression are obtained.

$$\kappa = \hat{\mathbf{u}}_1 \cdot \sum_{i=2}^{N} \mathbf{k}_i \,, \tag{2.24}$$

and

$$\mathbf{k}_i = -\sum_{j \neq i} \frac{1}{h_i} \frac{\partial h_i}{\partial u_j} \hat{\mathbf{u}}_j \,, \tag{2.25}$$

are, respectively, the curvature parameter and the curvature vectors associated with the $N-1$ coordinate curves of the domain. Here, we chose an auxiliary coordinate system $(u_1, \cdots, u_N)$ such that the brane moves in the u_1 direction and $u_2, \cdots, u_N$ are parameters whose coordinate curves coincide with the lines of curvature. Note that, in general, the extrinsic curvature and velocity vary along the domain wall, and, therefore, Eq. (2.23) is valid at each point on the surface.

2.1.1 Generic Domain Wall Models

In this subsection, we show that Eq. (2.23) describes the dynamics of generic thin domain walls independently of the lagrangian density, $\mathcal{L}(\phi, X)$, of the model (where X represents the kinetic term). We will follow closely the derivation presented in Ref. [8], where the validity of Eq. (2.23) has been demonstrated for planar domain walls. Varying the action in Eq. (2.2) with respect to ϕ, one obtains

$$\frac{1}{\sqrt{-g}} \left(\sqrt{-g}\mathcal{L}_{,X}\ \phi^{,\mu}\right)_{,\mu} = \mathcal{L}_{,\phi} \,, \tag{2.26}$$

where $\mathcal{L}_{,X} = \frac{\partial \mathcal{L}}{\partial X}$ and $\mathcal{L}_{,\phi} = \frac{\partial \mathcal{L}}{\partial \phi}$.

Assuming a $N+1$-dimensional FRW metric, this equation yields

$$\frac{\partial}{\partial t}\left(\mathcal{L}_{,X}\frac{\partial \phi}{\partial t}\right) + NH\mathcal{L}_{,X}\frac{\partial \phi}{\partial t} - \nabla \mathcal{L}_{,X} \cdot \nabla \phi - \mathcal{L}_{,X}\nabla^2 \phi = \mathcal{L}_{,\phi} \,. \tag{2.27}$$

In Minkowski spacetime, a planar static domain wall solution oriented along the x direction will be given by $\phi = \phi_s(l)$ with

$$-\frac{d}{dl}\left(\mathcal{L}_{,X}\frac{d\phi_s}{dl}\right) = \mathcal{L}_{,\phi} \,. \tag{2.28}$$

with $l = x$.

Now, consider the coordinate system $(u_1, \cdots, u_N)$ (as described in Sec. 2.1)

and suppose that the domain wall is moving along the direction u_1 with velocity v. Taking into account that

$$\nabla\mathcal{L}_{,X}\cdot\nabla\phi = \frac{\partial\mathcal{L}}{\partial u_1}\frac{\partial\phi}{\partial u_1}\,, \tag{2.29}$$

as well as Eqs. (2.8)-(2.10) and (2.19), the equation of motion yields

$$-\frac{d}{dl}\left(\mathcal{L}_{,X}\frac{d\phi_s}{dl}\right) + \mathcal{F}\mathcal{L}_{,X}\frac{d\phi_s}{dl} = \mathcal{L}_{,\phi}\,. \tag{2.30}$$

Again, since $\phi_s(l)$ must be a solution Eq. (2.28), we should have $\mathcal{F}=0$ and, consequently, Eq. (2.23) remains valid, independently of the form of the kinetic term. Furthermore, although we only considered models with a single real scalar field, it is straightforward to verify that Eq. (2.23) describes the correct thin domain wall dynamics in the context of generic models with various scalar fields. In this case, we would have an expression of the same for as Eq. (2.27) for each of the scalar fields and, consequently, we would still recover the same equation of motion for the domain walls.

2.1.2 Application: The PRS algorithm

By changing the time coordinate in Eq. (2.5) to the conformal time we find

$$\ddot{\phi} + (N-1)\mathcal{H}\dot{\phi} - \nabla^2\phi = -a^2\frac{dV}{d\phi}\,, \tag{2.31}$$

where dots represent partial derivatives with respect to conformal time, η.

Domain walls have a constant physical thickness, and consequently their comoving thickness decreases as a^{-1}. In cosmological numerical studies of domain walls, this rapid decrease poses a serious problem: the comoving thickness becomes rapidly smaller than the grid-size resolution of the simulations, and therefore it is only possible to resolve the walls during a small fraction of the dynamical range.

In Ref. [97], it is argued that the dynamics of domain walls is unaffected by its thickness, in $3+1$-dimensional universes. The authors then proposed the following modification to Eq. (2.31):

$$\ddot{\phi} + \alpha\mathcal{H}\dot{\phi} - \nabla^2\phi = -a^\beta\frac{dV}{d\phi}\,, \tag{2.32}$$

where α and β are constant parameters. They also argue that this modification preserves the dynamics of domain walls as long as the parameters satisfy

$$\alpha + \frac{\beta}{2} = 3\,. \tag{2.33}$$

If one sets $\beta = 0$ (and thus $\alpha = 3$), the comoving thickness is set to a constant by fiat, and therefore the difficulty in resolving the domain walls throughout the full dynamical range is overcome. This modification, implemented in most field-theory simulations of cosmological domain wall evolution, is known as Press-Ryden-Spergel (PRS) algorithm. Although the claim that the dynamics of domain walls is unaffected if the parameters of the algorithm satisfy Eq. (2.33) is strongly supported by numerical tests, it has never been demonstrated that the same dynamics is recovered from both Eq. (2.31) and Eq. (2.32). The procedure described in Sec. 2.1 can be used to prove the validity of the PRS algorithm. Changing the spacetime coordinates in Eq. (2.32) to a new set of coordinates $(\xi, \mathbf{y})$, defined as

$$\frac{\partial}{\partial \xi} = \frac{1}{a^{\beta/2}} \frac{\partial}{\partial \eta}\,, \tag{2.34}$$

$$\mathbf{y} = a^{\beta/2}\mathbf{x}\,, \tag{2.35}$$

one obtains

$$\frac{\partial^2 \phi}{\partial \xi^2} + \left(\alpha + \frac{\beta}{2}\right) \mathbf{H} \frac{\partial \phi}{\partial \xi} - \nabla^2_{\mathbf{y}} \phi = \frac{dV}{d\phi}\,, \tag{2.36}$$

where $\nabla^2_{\mathbf{y}} = a^{-\beta} \nabla^2_{\mathbf{x}}$ and $\mathbf{H} = a^{-\beta/2} \mathcal{H}$.

In Minkowski space, a static domain wall solutiondescribed by Eq. (2.36) is given by $\phi = \phi_s(l)$ and satisfies Eq. (2.6), but in this case $l = y$ (we take $\mathbf{y} = (y_1, ..., y_N)$ and $y_1 = y$). If we now consider the case of a curved domain wall in a $N+1$-dimensional Universe, it is useful to choose a set of spatial coordinates $(u_1, \cdots, u_N)$ as described in Sec. 2.1: the wall is given by $u_1 =$ constant, and the coordinate lines on the surface coincide with the principal directions of curvature (note that, in this case, the coordinates are scaled by a factor of $a^{\beta/2}$). In this case, the domain wall solution will still be of the form $\phi = \phi_s(l)$, but now $l = \gamma(u_1 - v\xi)$.

If we proceed as described in Sec. 2.1, Eq. (2.36) may be written in the form of Eq. (2.20), but in this case we have that

$$\mathcal{F} = -\frac{\partial}{\partial \xi}(\gamma v) - \left(\alpha + \frac{\beta}{2}\right) \mathbf{H} \gamma v + \kappa^c \gamma\,, \tag{2.37}$$

where κ^c is the comoving extrinsic curvature of the domain wall, defined as

$$\kappa^c = a^{\beta/2}\hat{\mathbf{u}}_1 \cdot \sum_{i=2}^{N} \mathbf{k}_i \,, \tag{2.38}$$

and $\mathbf{k}_i$ is given by Eq. (2.25). The factor $a^{\beta/2}$ in this definition stems from the fact that, in this case, ds_i is not comoving length along the direction u_i since the space coordinates have been scaled by a factor of $a^{-\beta/2}$.

Again, taking into account Eq. (2.6), we should have that $\mathcal{F} = 0$. If we change back to the physical coordinates, we finally find that

$$\frac{\partial v}{\partial t} + (1 - v^2)\left[\left(\alpha + \frac{\beta}{2}\right) Hv - \kappa\right] = 0 \,. \tag{2.39}$$

Hence, if the modified equations are to yield the correct domain wall dynamics, Eqs. (2.23) and (2.39) should be identical, or equivalently, we should have that

$$\alpha + \frac{\beta}{2} = N \,, \tag{2.40}$$

which proves the claim (2.33), and generalizes it to FRW backgrounds with an arbitrary number of spatial dimensions. One may then conclude that the dynamics of thin domain walls is unaffected by the implementation of the PRS algorithm.

2.2 P-BRANE DYNAMICS

The equation of a p-brane may be derived from the underlying field theory, and it is then determined by an action of the form of Eq. (2.2). However, in most situations of interest in cosmology, the thickness of p-branes is negligible when compared to its curvature radii. Assuming that the p-branes are featureless, their properties do not change along their surface. In this case, the velocity of the brane is purely orthogonal to it. A infinitely thin and featureless p-brane sweeps, while moving in spacetime, an effectively $p+1$-dimensional surface (the worldsheet). The world history of the p-brane may then be represent by

$$x^\mu = x^\mu(u_{\tilde{\nu}}) \,, \tag{2.41}$$

where $u_{\tilde{\nu}}$ with $\tilde{\nu} = 0, 1, \cdots, p$ are the parameters of the surface, u_0 is a timelike parameter, and $u_{\tilde{i}}$ are spacelike parameters. These parameters may be regarded, at least locally, as coordinates on the worldsheet. The spacetime interval between two events on the worldsheet is

$$ds^2 = g_{\alpha\beta} x^\alpha_{,\tilde{\mu}} x^\beta_{,\tilde{\nu}} du^{\tilde{\mu}} du^{\tilde{\nu}} \,, \tag{2.42}$$

and, therefore, the induced metric of the $p+1$-dimensional worldsheet (or pull-back metric) is given by

$$\tilde{g}_{\tilde{\mu}\tilde{\nu}} = g_{\alpha\beta} x^{\alpha}_{,\tilde{\mu}} x^{\beta}_{,\tilde{\nu}} \,. \tag{2.43}$$

In analogy to the case of a point-particle, the action of an infinitely thin and featureless p-brane should be a functional of the worldvolume. In the case of a particle, which sweeps a 2-dimensional worldline in spacetime, the action is proportional to the proper length along the worldline. It is then natural to expect the action of an infinitely thin and featureless p-brane to be proportional to the "proper" p-dimensional area of the worldvolume:

$$S = -\sigma_p \int d^{p+1}u \sqrt{-\tilde{g}} \,, \tag{2.44}$$

where σ_p is the p-brane mass per unit p-dimensional area. This action is invariant under reparametrizations of the worldsheet and it is a generalization of the Nambu-Goto action for cosmic strings to p-branes of arbitrary dimensionality.

As a matter of fact, in the vicinity of an infinitely thin p-brane, the line element can be written as [98]

$$ds^2 = \tilde{g}_{\tilde{\mu}\tilde{\nu}} dx^{\tilde{\mu}} dx^{\tilde{\nu}} + d\mathbf{r} \cdot d\mathbf{r} \,, \tag{2.45}$$

where $(d\mathbf{r} \cdot d\mathbf{r})^{1/2}$ is the infinitesimal distance to the brane's (p-dimensional) core. Therefore, the volume element is given by

$$d^{N+1}x = \sqrt{|\tilde{g}|} d^{p+1}u d^{N-p}x \,. \tag{2.46}$$

Since we are assuming that the p-brane is thin and featureless, the lagrangian density may only vary along the perpendicular directions and, as consequence, it depends only on the $x^{p+1}, \cdots, x^N$ coordinates. Integrating the action in Eq. (2.2) with respect to these coordinates, one obtains the Nambu-Goto action for infinitely thin p-branes in Eq. (2.44), with

$$\sigma_p = -\int d^{N-p}x \mathcal{L} \,. \tag{2.47}$$

2.2.1 Equation of motion p-Branes

In this section, we will use the procedure described in Sec. 2.1 to derive the equations of motion for p-branes of arbitrary dimensionality in $N+1$-dimensional FRW universes. This work has been published in [15]. If we have prior knowl-

edge of the motion described by the brane during its evolution — or equivalently if the shape of the worldsheet is known — we can, in principle, define a real scalar field multiplet, ϕ^e, in the worldvolume. These fields have some interesting properties:

- The initial conditions may be set up in such a way that these scalar fields define a new p-brane whose velocity coincides with the velocity of the original brane. The dynamics of this new p-brane is then described by the same equation of motion.

- Since the fields ϕ^e were defined on the world-volume of the original p-brane, the energy of the new p-brane is localized.

- This p-brane might be treated as a $n-1$ brane (a domain wall) in the $n+1$ dimensional space swept by the p-brane throughout its motion (with $n = p+1$), since the brane divides this space in two domains.

The dynamics of the scalar field multiplet, ϕ^e, is defined by the lagrangian density

$$\mathcal{L} = X - V(\phi^e)\,, \tag{2.48}$$

where $X = -\phi^e{}_{,\tilde{\mu}}\,\phi^{e,\tilde{\mu}}/2$, and $V(\phi^e)$ is the potential (on the remainder of this subsection we shall omit the index e). The potential, V, needs to have, at least, two degenerate minima in order to admit p-brane solutions, and they can be made arbitrarily thin by appropriate tuning. Note that the dynamics of the p-brane is independent of the specific model we choose to describe it, as discussed in Sec. 2.1.1.

By varying the action

$$S = \int \mathcal{L}\sqrt{-\tilde{g}}d^{n+1}u, \tag{2.49}$$

with respect to ϕ, one finds the equation of motion

$$\frac{1}{\sqrt{-\tilde{g}}}\left(\sqrt{|\tilde{g}|}\phi^{,\tilde{\mu}}\right)_{,\tilde{\mu}} = -V_{,\phi}\,. \tag{2.50}$$

Notice that in Eqs. (2.49) and (2.50) (and on the remainder of this section), $\tilde{g}$ refers to the induced metric of the $n+1$ dimensional space in which the brane lives. In this case, it is still given by Eq. (2.43) but now $\tilde{\mu} = 0, \cdots, p+1$[2].

[2]In this subsection, greek and latin indices marked with a tilde take the values $0, \cdots, p+1$ and $1, \cdots, p+1$ respectively

Note that this new p-brane is a planar wall in an intrinsically curved $n+1$ dimensional space. So, in order to write down the equation of motion for ϕ, we need to start by determining the metric induced by the $N+1$ dimensional FRW background on this $n+1$-dimensional space. One may identify the timelike coordinate with the conformal time ($u_0 = \eta$), so that $\tilde{g}_{00} = -a^2(\eta)$. Moreover, the velocity of the brane may be taken to be orthogonal to the brane itself and, therefore, perpendicular to all spatial directions along the brane:

$$\tilde{g}_{0\tilde{i}} = \tilde{g}_{\tilde{i}0} = 0, \quad \text{with} \qquad \tilde{i} = 1, ..., p+1\,. \tag{2.51}$$

Consider a set of local spatial coordinates $(u_1, ..., u_p, u_{p+1})$ such that the brane is locally a coordinate surface for which u_{p+1} is constant and it moves along this direction. The spatial coordinates $(u_1, ..., u_p)$ may be chosen in such a way that they form an orthogonal set which parametrizes the brane locally and, for simplicity, whose coordinate lines coincide with the principal directions of curvature of the surface.

In this coordinate system, the metric elements may be written as

$$\tilde{g}_{\tilde{i}\tilde{j}} = \begin{cases} \sum_{k=1}^{n} a^2 \left(x^k_{,\tilde{i}}\right)^2 = a^2 h^2_{\tilde{i}}\,, & \text{if } \tilde{i} = \tilde{j}\,, \\ 0\,, & \text{if } \tilde{j} \neq \tilde{i}\,, \end{cases} \tag{2.52}$$

so that

$$\tilde{g} = -a^{2(p+2)} h_1^2 ... h_{p+1}^2\,, \tag{2.53}$$

where the scale factors of the coordinate system, $h_{\tilde{i}} = \left|\mathbf{x}_{,\tilde{i}}\right|$ were introduced.

Eq. (2.50) then becomes

$$\ddot{\phi} + p\mathcal{H}\dot{\phi} - \nabla^2_{\mathbf{u}}\phi = -a^2 \frac{dV}{d\phi}\,, \tag{2.54}$$

with $\mathcal{H} = \dot{a}/a$ and where

$$\nabla^2_{\mathbf{u}}\phi = \left(\prod_{j=1}^{p} h_j\right)^{-1} \left(\frac{\partial}{\partial u_{p+1}} \left(\frac{\partial \phi}{\partial u_{p+1}} \prod_{j=1}^{p} h_j\right)\right)\,, \tag{2.55}$$

is the laplacian for this set of coordinates. Here, we considered the zero-thickness limit, neglecting the variation of the scalar field ϕ on the directions tangent to the brane [90] ($\partial\phi/\partial u_i = 0$, for $i = 1, ..., p$). We have also taken $h_{p+1} = 1$, so that du_{p+1} is the infinitesimal arc-length along the u_{p+1} direction.

It is now possible to follow closely the procedure described in Sec. 2.1. The only point that needs special attention is the laplacian. Note that there are

$N-p$ directions perpendicular to the brane, and there is no reason why the velocity's direction should coincide with the curvature normals. Therefore, when we defined ϕ^e, we necessarily lost information about the normal acceleration of the p-brane. Nevertheless, in order to write the equation of motion for the evolution of v, one only needs the tangential acceleration of the p-brane.

If we apply directly the procedure in Sec. 2.1, we find

$$\nabla^2\phi = \frac{\partial^2\phi}{\partial u_{p+1}^2} - \frac{\partial\phi}{\partial u_{p+1}}\left(\sum_{i=1}^{p}\mathbf{k}_i\cdot\hat{\mathbf{v}}\right), \tag{2.56}$$

where $\mathbf{k}_i$ is the curvature vector of the curve u_i (defined as u_j = constant, for $i\neq j$ and $i,j=1,\cdots,p$), and $\hat{\mathbf{v}}$ is the unitary vector along the velocity direction. Since $\mathbf{k}_i$ and $\hat{\mathbf{v}}$ are not necessarily parallel, we find that

$$k_{i\parallel} = \mathbf{k}_i\cdot\hat{\mathbf{v}} \tag{2.57}$$

is the tangential component of the principal curvature along the direction u_i, and we can define the total tangential curvature as

$$\kappa_\parallel = \sum_{i=1}^{p} k_{i\parallel}\,, \tag{2.58}$$

Given Eqs. (2.54) and (2.56-2.58), and using the method described in detail in Sec. 2.1, one obtains the equation of motion for the velocity of a p-brane in $N+1$-dimensional FRW universes

$$\dot{v} + \left(1-v^2\right)\left[(p+1)\,\mathcal{H}v - \kappa_\parallel\right] = 0\,. \tag{2.59}$$

2.2.2 A simple test: Cosmic Strings

The world-history of an infinitely thin cosmic string in a flat FRW universe can be represent by a two dimensional worldsheet, $x^\mu(u_0,u_1)$, obeying the usual Nambu-Goto action

$$S = -\mu\int\sqrt{-\tilde{g}}\;d^2u\,. \tag{2.60}$$

By varying the action in Eq. (2.60) with respect to x^μ, and using the Jacobi identity,

$$d\tilde{g} = \tilde{g}\tilde{g}^{\tilde{\mu}\tilde{\nu}}d\tilde{g}_{\tilde{\mu}\tilde{\nu}}\,, \tag{2.61}$$

we obtain the following equation of motion

$$x^{\mu}_{,\tilde{\nu}}{}^{;\tilde{\nu}} + \Gamma^{\mu}_{\beta\lambda}\tilde{g}^{\tilde{\mu}\tilde{\nu}}x^{\beta}_{,\tilde{\nu}}x^{\lambda}_{,\tilde{\nu}} = 0\,, \tag{2.62}$$

with

$$x^{\mu}_{,\tilde{\nu}}{}^{;\tilde{\nu}} = \frac{1}{\sqrt{-\tilde{g}}}\left(\sqrt{-\tilde{g}}\tilde{g}^{\tilde{\mu}\tilde{\nu}}x^{\mu}{}_{,\tilde{\nu}}\right)_{,\tilde{\mu}}\,. \tag{2.63}$$

Since the action in Eq. (2.60) is invariant under worldsheet reparametrizations, we have gauge freedom to impose some gauge conditions. In a flat FRW background, it is common to choose the temporal-transverse gauge conditions

$$u_0 \equiv \eta \qquad \text{and} \qquad \dot{\mathbf{x}}\cdot\mathbf{x}' = 0\,, \tag{2.64}$$

where $\mathbf{x}(\eta, u)$ is the 3-vector representing the string trajectory, $u = u_1$ and where dots and primes are the derivatives with respect to η and u, respectively. In this gauge, $\dot{\mathbf{x}}$ is perpendicular to the string's tangent, and it represents the observable velocity. We can thus, define, at any given point,

$$\dot{\mathbf{x}} = v\hat{\mathbf{v}}\,, \qquad \text{and} \qquad \mathbf{x}' = \left|\mathbf{x}'\right|\hat{\mathbf{u}}\,, \tag{2.65}$$

where $|\dot{\mathbf{x}}| = v(\eta, u)$ is the velocity of the string and $\hat{\mathbf{v}}$ and $\hat{\mathbf{u}}$ are local unitary vectors with the direction of the velocity and the string tangent at that particular point, respectively.

In this gauge, the equations of motion in Eq. (2.62) may be written as [99]:

$$\ddot{\mathbf{x}} + 2\mathcal{H}\left(1-\dot{\mathbf{x}}^2\right)\dot{\mathbf{x}} = \epsilon^{-1}\left(\epsilon^{-1}\,\mathbf{x}'\right)' \tag{2.66}$$

$$\dot{\epsilon} = -2\mathcal{H}\epsilon\dot{\mathbf{x}}^2\,, \tag{2.67}$$

with

$$\epsilon = \left(\frac{\mathbf{x}'^2}{1-\dot{\mathbf{x}}^2}\right)^{\frac{1}{2}}\,. \tag{2.68}$$

Using the definitions in Eq. (2.65), the left-hand side of Eq. (2.66) yields

$$\ddot{\mathbf{x}} + 2\mathcal{H}\left(1-\dot{\mathbf{x}}^2\right)\dot{\mathbf{x}} = \dot{v}\hat{\mathbf{v}} + v\dot{\hat{\mathbf{v}}} + 2\mathcal{H}\left(1-v^2\right)v\hat{\mathbf{v}}\,. \tag{2.69}$$

Notice that $\dot{\hat{\mathbf{v}}}$ must necessarily be perpendicular to $\hat{\mathbf{v}}$. Moreover, the right-hand side yields of Eq. (2.66)

$$\epsilon^{-1}\left(\epsilon^{-1}\mathbf{x}'\right)' = \frac{1}{\gamma}\frac{\partial}{\partial l}\left(\frac{\hat{\mathbf{u}}}{\gamma}\right) = \left(\frac{1}{\gamma^2}\mathbf{k} - v\frac{\partial v}{\partial l}\hat{\mathbf{u}}\right), \tag{2.70}$$

where we have taken into account that $\epsilon = \gamma\,|\mathbf{x}'|$, with $\gamma = (1-v^2)^{-1/2}$. Moreover, we have used the definition of curvature vector,

$$\mathbf{k} = \frac{\partial\hat{\mathbf{u}}}{\partial s}, \tag{2.71}$$

where $ds = |d\mathbf{x}| = |\mathbf{x}'|\,du$ is the physical length along the string. Note that $\mathbf{k}$ is perpendicular to $\hat{\mathbf{u}}$, and that $\hat{\mathbf{v}}$ does not necessarily coincide with the principal curvature normal. Consequently, one may define the tangential curvature component as

$$\kappa_{\parallel} = \mathbf{k}\cdot\hat{\mathbf{v}}\,. \tag{2.72}$$

The component of Eq. (2.66) parallel to $\hat{\mathbf{v}}$, then yields

$$\dot{v} + (1-v^2)\left(2\mathcal{H}v - \kappa_{\parallel}\right) = 0\,, \tag{2.73}$$

which is equivalent to Eq. (2.23) in the particular case $p = 1$.

2.2.3 Tangential and Normal Acceleration of Nambu-Goto p-Branes

In this section, we derive the evolution equation for the velocity of featureless infinitely-thin p-branes directly from the Nambu-Goto action. This computation fully validates the results obtained using field theory equations in the thin-brane limit (Subsec. 2.2.1), and allows us to obtain the normal acceleration of the p-brane. This work was published in Ref. [16].

By varying the Nambu-goto action in Eq. (2.44) with respect to x^μ, one obtains an equation of motion of the same form of Eq. (2.62). Let us choose a local set of orthogonal coordinate system $(u_1,\cdots,u_N)$, at a given point on the brane's surface, such that $u_{\tilde{i}}$ parameterize the p-brane locally and $u_{p+1},\cdots,u_N$ are perpendicular to it. For simplicity, we shall also assume the $u_{\tilde{i}}$ coordinate lines are lines of curvature. As in the case of cosmic strings, in a flat $N+1$-dimensional FRW universe, it is convenient to impose temporal-tranverse gauge conditions

$$u^0 = \eta\,, \quad \text{and} \qquad \dot{\mathbf{x}}\cdot\mathbf{x}_{,\tilde{i}} = 0\,, \tag{2.74}$$

where $\mathbf{x}$ represents the spatial profile of the p-branes in cartesian coordinates, and we defined $_{,\tilde{i}} \equiv \partial/\partial u_{\tilde{i}}$.

Given this choice of gauge, $\dot{\mathbf{x}}$ represents the physical velocity, which is perpendicular to the p-brane itself. In a FRW background, Eq. (2.62) then yields

$$\ddot{\mathbf{x}} + (p+1)\,\mathcal{H}(1-\dot{\mathbf{x}}^2)\dot{\mathbf{x}} = {\epsilon_p}^{-1}\sum_{i=1}^{p}\left[\frac{\mathbf{x}_{,\tilde{i}}}{\epsilon_p}\Pi_{\tilde{j}\neq\tilde{i}}(\mathbf{x}_{,\tilde{j}})^2\right]_{,\tilde{i}}\,, \tag{2.75}$$

$$\dot{\epsilon_p} = -(p+1)\,\mathcal{H}\epsilon_p\dot{\mathbf{x}}^2\,, \tag{2.76}$$

where

$$\epsilon_p = \left(\frac{(\mathbf{x}_{,1})^2\cdots(\mathbf{x}_{,p})^2}{1-\dot{\mathbf{x}}^2}\right)^{\frac{1}{2}}\,. \tag{2.77}$$

Let $\hat{\mathbf{e}}_i$ be a set of unitary vectors with the directions of the axis of the $(u_1,\cdots,u_N)$ coordinate system. These vectors form an orthonormal basis, and their derivatives satisfy Eq. (2.16). Note that, for $i=1,\cdots,p$:

$$\hat{\mathbf{e}}_{\tilde{i}} = \frac{\mathbf{x}_{,\tilde{i}}}{\left|\mathbf{x}_{,\tilde{i}}\right|}\,. \tag{2.78}$$

Note also that, $\left|\mathbf{x}_{,\tilde{i}}\right|$ coincide with the scale factors of the coordinate system, $h_{\tilde{i}}$. Moreover, given the choice of gauge, we can define a unitary vector with the direction of the p-brane's velocity:

$$\hat{\mathbf{v}} = \frac{\dot{\mathbf{x}}}{v}\,. \tag{2.79}$$

This vector is perpendicular to all $\hat{\mathbf{e}}_{\tilde{i}}$, however it is a linear combination of the $\hat{\mathbf{e}}_{p+1},\cdots,\hat{\mathbf{e}}_N$ vector.

By differentiating Eq. (2.75) with respect to conformal time, we find

$$\mathbf{a}_{\tilde{i}} \equiv (\ddot{\mathbf{x}}\cdot\hat{\mathbf{e}}_{\tilde{i}})\,\hat{\mathbf{e}}_{\tilde{i}} = -\frac{v}{\left|\mathbf{x}_{,\tilde{i}}\right|}v_{,\tilde{i}}\hat{\mathbf{e}}_{\tilde{i}}\,, \tag{2.80}$$

and, consequently, there is a component of the acceleration parallel to the p-brane given by

$$\ddot{\mathbf{x}}_{=} = \sum_{i=1}^{p}\mathbf{a}_{\tilde{i}}\,. \tag{2.81}$$

The right-hand side of Eq. (2.75) yields

$$\epsilon_p{}^{-1}\sum_{\tilde{i}=1}^{p}\left[\frac{\mathbf{x}_{,\tilde{i}}}{\epsilon_p}\Pi_{\tilde{j}\neq\tilde{j}}(\mathbf{x}_{,\tilde{j}})^2\right]_{,\tilde{i}}=\frac{1}{\gamma^2}\sum_{\tilde{i}=1}^{p}\left[\sum_{\tilde{j}\neq\tilde{i}}\frac{\left|\mathbf{x}_{,\tilde{j}}\right|_{,\tilde{i}}}{\left|\mathbf{x}_{,\tilde{i}}\right|\left|\mathbf{x}_{,\tilde{j}}\right|}\hat{\mathbf{e}}_{\tilde{i}}+\frac{\partial\hat{\mathbf{e}}_{\tilde{i}}}{\partial s_{\tilde{i}}}+\gamma\frac{\partial}{\partial s_{\tilde{i}}}\left(\frac{1}{\gamma}\right)\hat{\mathbf{e}}_{\tilde{i}}\right], \tag{2.82}$$

where we introduced the physical length along the $\tilde{i}$ direction, $ds_{\tilde{i}}=\left|\mathbf{x}_{,\tilde{i}}\right|du_{\tilde{i}}$. Note the curvature vector along the direction $\tilde{i}$,

$$\mathbf{k}_{\tilde{i}}=\frac{\partial\hat{\mathbf{e}}_{\tilde{i}}}{\partial s_{\tilde{i}}}\,, \tag{2.83}$$

may be written as

$$\frac{\partial\hat{\mathbf{e}}_{\tilde{i}}}{\partial s_{\tilde{i}}}=-\sum_{\tilde{j}\neq\tilde{i}}\frac{\left|\mathbf{x}_{,\tilde{i}}\right|_{,\tilde{j}}}{\left|\mathbf{x}_{,\tilde{i}}\right|\left|\mathbf{x}_{,\tilde{j}}\right|}\hat{\mathbf{e}}_{\tilde{j}}+\mathbf{k}_{\tilde{i}}^{N}\,, \tag{2.84}$$

where we have separated the geodesic curvature (the components of the curvature which are parallel to the brane) from the normal curvature along $\tilde{i}$ direction, $\mathbf{k}_{\tilde{i}}^{N}$. Eq. (2.82) may then be written as

$$\frac{1}{\gamma^2}\sum_{\tilde{i}=1}^{p}\left[\sum_{\tilde{j}\neq\tilde{i}}\left(\frac{\left|\mathbf{x}_{,\tilde{j}}\right|_{,\tilde{i}}}{\left|\mathbf{x}_{,\tilde{i}}\right|\left|\mathbf{x}_{,\tilde{j}}\right|}\hat{\mathbf{e}}_{\tilde{i}}-\sum_{\tilde{j}\neq\tilde{i}}\frac{\left|\mathbf{x}_{,\tilde{i}}\right|_{,\tilde{j}}}{\left|\mathbf{x}_{,\tilde{i}}\right|\left|\mathbf{x}_{,\tilde{j}}\right|}\hat{\mathbf{e}}_{\tilde{j}}\right)+\mathbf{k}_{\tilde{i}}^{N}+\gamma\frac{\partial}{\partial s_{\tilde{i}}}\left(\frac{1}{\gamma}\right)\hat{\mathbf{e}}_{\tilde{i}}\right]. \tag{2.85}$$

Note that the first term in Eq. (2.85) is anti-symmetric with respect to changes of the form $\tilde{i}\leftrightarrow\tilde{j}$. Therefore, when considering all possible values of these indices, this sum cancels out.

Therefore, using Eq. (2.75) one finds that

$$\ddot{\mathbf{x}}-\ddot{\mathbf{x}}_{=}=-(p+1)\mathcal{H}(1-v^2)v\hat{\mathbf{v}}+\frac{1}{\gamma^2}\sum_{\tilde{i}=1}^{p}\mathbf{k}_{\tilde{i}}^{N}\,, \tag{2.86}$$

where we used the fact that

$$\frac{1}{\gamma^2}\frac{\partial}{\partial s_{\tilde{i}}}\left(\frac{1}{\gamma}\right)\hat{\mathbf{e}}_{\tilde{i}}=\mathbf{a}_{\tilde{i}}\,. \tag{2.87}$$

Using Eq. (2.86), taking into account that $\ddot{\mathbf{x}}=\dot{v}\hat{\mathbf{v}}+v\dot{\hat{\mathbf{v}}}$ and that $\dot{\hat{\mathbf{v}}}$ is perpendicular to $\hat{\mathbf{v}}$, one finds that the tangential acceleration (parallel to the velocity) is given by

$$\mathbf{a}_T \equiv \ddot{\mathbf{x}}_\parallel = (\ddot{\mathbf{x}}\cdot\hat{\mathbf{v}})\,\hat{\mathbf{v}} = \hat{\mathbf{v}}(1-v^2)\left[\sum_{\tilde{i}=1}^{p} k_{\tilde{i}\parallel} - (p+1)\mathcal{H}v\right], \tag{2.88}$$

where we defined the tangential curvature as the projection of the comoving curvature vectors along the velocity direction

$$k_{\tilde{i}\parallel} = \mathbf{k}^N_{\tilde{i}}\cdot\hat{\mathbf{v}}\,. \tag{2.89}$$

This tangential acceleration allows us to obtain an evolution equation for the velocity of the p-brane:

$$\dot{v} + \left(1-v^2\right)\left[(p+1)\mathcal{H}v - \kappa_\parallel\right] = 0\,, \tag{2.90}$$

where the total tangential curvature,

$$\kappa_\parallel = \sum_{\tilde{i}=1}^{p} k_{\tilde{i}\parallel}\,, \tag{2.91}$$

was introduced. This equation is identical to that obtained from field theory equations in Sec. 2.2.1 .

The acceleration along the perpendicular direction $\hat{\mathbf{e}}_l$ is given by

$$\mathbf{a}_l \equiv (\ddot{\mathbf{x}}\cdot\hat{\mathbf{e}}_l)\,\hat{\mathbf{e}}_l = \hat{\mathbf{e}}_l(1-v^2)\sum_{\tilde{i}=1}^{p}\mathbf{k}^N_{\tilde{i}}\cdot\hat{\mathbf{e}}_l = \hat{\mathbf{e}}_l(1-v^2)\kappa_{\perp l}\,, \tag{2.92}$$

for $l = p+1,\cdots,N$. Here we have introduced the total comoving curvature along the perpendicular direction l,

$$\kappa_{\perp l} = \sum_{\tilde{i}}\mathbf{k}^N_{\tilde{i}}\cdot\hat{\mathbf{e}}_l\,. \tag{2.93}$$

Therefore, the total perpendicular acceleration —which is simultaneously perpendicular to the velocity of the brane and the brane itself — is given by

$$\ddot{\mathbf{x}}_\perp = (1-v^2)\sum_{l=p+2}^{N}\hat{\mathbf{e}}_l\kappa_{\perp l} - \ddot{\mathbf{x}}_\parallel\,, \tag{2.94}$$

with $\ddot{\mathbf{x}} = \ddot{\mathbf{x}}_= + \ddot{\mathbf{x}}_\parallel + \ddot{\mathbf{x}}_\perp$. The total normal acceleration of the brane is, then, given by

$$\mathbf{a}_N = \ddot{\mathbf{x}}_\perp + \ddot{\mathbf{x}}_=\,. \tag{2.95}$$

2.3 P-BRANE LOOP SOLUTIONS

In this section we study the dynamics of closed maximally symmetric p-brane solutions — which, for simplicity, we will denominate p-brane loops (in analogy to the case of cosmic strings). The formation of p-brane loops may, as in the case of cosmic strings, result from brane interaction during the cosmological evolution of a p-brane network. The evolution of circular cosmic string loops and spherical domain walls in a flat FRW universe has previously been studied in [100] (see also [101]), where the existence of periodic solutions in a de Sitter universe has been demonstrated. Cosmic strings and other defects can be formed during an inflationary era or, if various stages of inflation occur, they may be formed in between. It is thus crucial to understand their evolution in these regimes in order to quantify their ability to survive any inflationary period which might occur after they are formed [102, 103]. We will, then, generalize the results in Ref. [100] by explicitly computing the phase space trajectories and determining the critical radius for spherical p-branes in space-times with an arbitrary number of dimensions. We also study in detail the more general evolution of maximally symmetric p-branes with a $S_{p-i}\otimes\mathbb{R}^i$ topology in expanding and collapsing FRW universes. This work was published in [11].

2.3.1 Equations of Motion for Maximally Symmetric p-Branes

In a $N+1$-dimensional Minkowski spacetime, the trajectory of a p-brane with spherical symmetry may be written, in hyperspherical coordinates, as

$$\begin{aligned}\mathbf{x}(t,\theta_1,\cdots,\theta_{p-1}) = q(t)\,(&\cos\theta_1, \sin\theta_1\cos\theta_2, \sin\theta_1\sin\theta_2\cos\theta_3,\cdots\\ &\cdots,\sin\theta_1...\sin\theta_{p-2}\cos\theta_{p-1}, \sin\theta_1...\sin\theta_{p-1}, 0,\cdots,0)\ ,\end{aligned} \tag{2.96}$$

where $\theta_1,\cdots,\theta_{p-2}\in[0,\pi[$ and $\theta_{p-1}\in[0,2\pi[$ and, for simplicity, the coordinate system was chosen in order for the defect to be aligned with the first p-dimensions.

The area of a p-dimensional spherically symmetric p-brane is given by

$$S_p = (p+1)\,C_{p+1}\,|q|^p\ , \tag{2.97}$$

where $|q|$ is the physical radius and

$$C_j = \frac{\pi^{j/2}}{\Gamma\left(\frac{j}{2}+1\right)}\,. \tag{2.98}$$

The energy of the p-brane is, proportional to $S_p\gamma$. It then follows from energy conservation that

$$\frac{dv}{dt} = (1-v^2)\left(\frac{p\gamma^{1/p}s}{R}\right), \tag{2.99}$$

where $s = sign(-q)$, and the invariant radius, proportional to the energy of the p-brane,

$$R = |q|\,\gamma^{1/p}, \tag{2.100}$$

was introduced. Note that, it follows from energy conservation that

$$\frac{dR}{dt} = 0. \tag{2.101}$$

This is no longer the case in FRW Universes, since in this case the energy of the p-brane is no longer conserved: the expansion (or collapse) of the universe decelerates (accelerates) the p-branes. Therefore, we need to include the usual Hubble damping term in the equation of motion for v. Recall that the momentum per comoving p-dimensional area is proportional to a^{-1}, and therefore, in a FRW universe, the velocity of a (planar) p-brane satisfies

$$v\gamma \propto a^{p+1}. \tag{2.102}$$

The complete equation of motion for v is, then

$$\frac{dv}{dt} = (1-v^2)\left[\frac{p\gamma^{1/p}s}{R} - (p+1)Hv\right], \tag{2.103}$$

so that

$$\frac{dR}{dt} = HR\left[1 - \frac{p+1}{p}v^2\right], \tag{2.104}$$

where the invariant radius is now defined as

$$R = \gamma^{1/p}\,|r|, \quad \text{with} \quad r = aq. \tag{2.105}$$

Now let us consider the case p-branes with a $S_{p-i}\otimes\mathbb{R}^i$ topology (where $0 \leqslant i \leqslant p$). In this case, the p-brane has a number i of dimensions with no curvature and $p-i$ directions with spherical symmetry. The area per unit of i-dimensional area of the non curved dimensions of the defect is

$$S_p^i = (p-i+1)C_{p-i+1}\gamma\,|q|^{p-i}, \tag{2.106}$$

and energy-momentum conservation leads to the following equations of motion (which generalize Eqs. (2.103) and (2.104)):

$$\frac{dv}{dt} = (1-v^2)\left[\frac{(p-i)\gamma^{1/(p-i)}s}{R} - (p+1)vH\right], \tag{2.107}$$

$$\frac{dR}{dt} = HR\left[1 - \frac{p+1}{p-i}v^2\right], \tag{2.108}$$

where the invariant radius is now given by

$$R = |q|\,\gamma^{1/p-i}a\,. \tag{2.109}$$

Note that these equations are invariant with respect to the transformation $q \to -q$ and $t \to -t$. This implies that the phase space trajectories in expanding and collapsing universes related by the transformation $H \to -H$ are identical. However, the transformation $t \to -t$ implies that the direction in which the trajectory is travelled is reversed.

2.3.2 p-Brane Dynamics with H =constant

Eq. (2.108) may be rewritten as

$$\frac{dv}{dt} = v + Hr\,. \tag{2.110}$$

Let us consider the case of the de Sitter universe, whose Hubble parameter is time independent. For the case of spherically symmetric p-branes ($i = 0$), it is possible to determine the (r, v) trajectories in phase space. Integrating Eqs. (2.107) and (2.110) we find that the orbits of these p-branes are of the form

$$\gamma r^p(1 + vHr) = \mathcal{C}\,, \tag{2.111}$$

where $\mathcal{C}$ is constant.

The stationary solution of Eqs. (2.107) and (2.110), characterized by fixed critical velocity, v_c, ($dv/dt = 0$), and fixed physical radius, r_c, ($dr/dt = 0$), is given by

$$v_c^2 = H^2 r_c^2 = \frac{p-i}{p+1}\,. \tag{2.112}$$

This solution describes a p-brane standing still against Hubble expansion or collapse. We are then able to find the value of $\mathcal{C}$ corresponding to this stationary solution (denoted by $\mathcal{C}_c$)

$$\mathcal{C}_c = \frac{1}{|H|^p} \frac{p^{p/2}}{(p+1)^{(p+1)/2}} \,. \tag{2.113}$$

Trajectories with $\mathcal{C} > \mathcal{C}_c$ will asymptote the line defined by

$$v = -(Hr)^{-1} \,, \quad \text{when} \quad |r| \to \infty \,, \tag{2.114}$$

and, therefore, in this limit, the p-brane loop freezes in comoving coordinates ($v \to 0$). On the other hand, if $\mathcal{C} < \mathcal{C}_c$, we may have two types of trajectories: if $|r| > r_c$, the trajectories would be of the same form as that with $\mathcal{C} > \mathcal{C}_c$; otherwise, if $|r| < r_c$, the p-branes describe periodic trajectories in phase space. This is clearly illustrated in Fig. 2.1, where the trajectories of a spherically symmetric domain wall in a $3+1$-dimensional universe (with $p = 2$ and $i = 0$) are represented. Trajectories with $\mathcal{C} < \mathcal{C}_c$ are represented by solid lines and the dashed lines represent trajectories with $\mathcal{C} > \mathcal{C}_c$. Note that all the non-periodic trajectories start at a critical point (represented by a yellow dot) defined by the condition

$$v = -Hr = \pm 1 \,, \tag{2.115}$$

and end at $(r = \infty, v = 0)$. In a collapsing universe, the trajectories are travelled in the inverse direction.

Notice also that the periodic trajectories are asymmetric. From Eq. (2.109), we have that

$$v = \pm \sqrt{1 - \left(\frac{r}{R}\right)^{2(p-i)}} \,. \tag{2.116}$$

This expression, combined with Eq. (2.110), shows clearly why this asymmetry between the collapse and the expansion of the p-brane loop occurs. If the universe is expanding then there is a damping term that contributes to decrease $|v|$. On the other hand, the curvature term differentiates expansion and collapse of the loop: curvature accelerates or decelerates the p-brane depending whether it is collapsing or expanding. In the case of a collapsing universe, this asymmetry is also verified: although, in this case, the Hubble term contributes to the increase of $|v|$, the curvature also differentiates expansion, and collapse of the loop.

We may compute a critical (initial) radius, r_c^0, corresponding to an initially static p-brane solution ($v^0 = 0$) with $\mathcal{C} = \mathcal{C}_c$ (in an expanding universe, it will

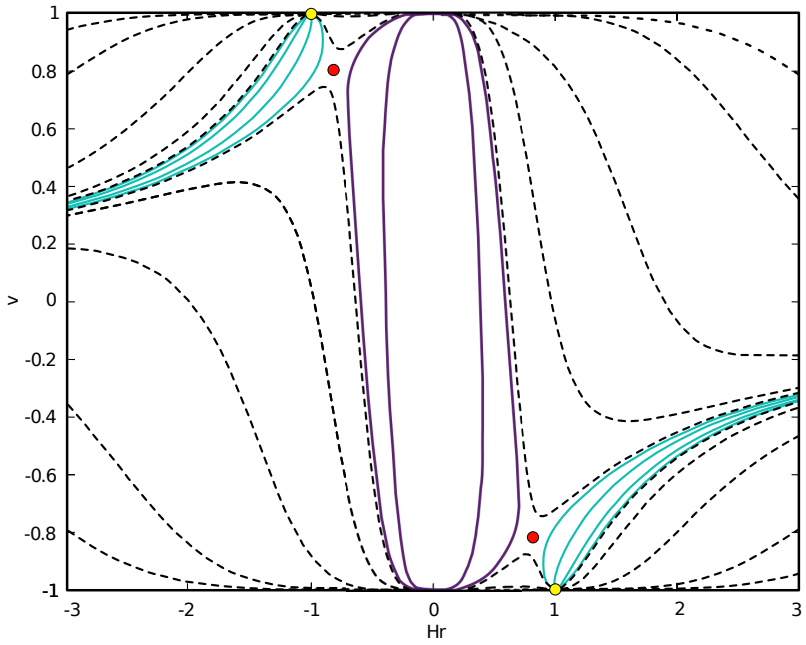

Figure 2.1: Representation of the trajectories in phase space of spherical domain walls in a $3+1$-dimensional universe ($p = 2, i = 0$). The critical points marked with a red dot represent the critical stationary solution defined in Eq. (2.112) and the yellow dots correspond to the critical points defined by $v = -Hr = \pm 1$. The solid lines correspond to trajectories of spherical domain walls with $\mathcal{C} < \mathcal{C}_c$. Those with $|r| < r_c$, which correspond to domain walls with periodic trajectories in phase space, are represented by the purple lines. The blue solid lines correspond to trajectories with $\mathcal{C} < \mathcal{C}_c$ and $|r| > r_c$. The dashed lines correspond to trajectories with $\mathcal{C} > \mathcal{C}_c$ which start at the critical point defined by Eq. (2.115) and end at $(r = \infty, v = 0)$

asymptote to the stationary solution when $t \to \infty$). This critical radius is given by

$$r_c^0 = \frac{1}{|H|} \frac{p^{1/2}}{(p+1)^{(p+1)/(2p)}} \,. \tag{2.117}$$

In the case of circular cosmic string loops ($p = 1$) and spherical domain walls ($p = 2$), we find that the initial critical radii are $r_c^0 = |H|^{-1}/2$ and $r_c^0 = 2^{1/2} 3^{-3/4} |H|^{-1}$ respectively. We recover the initial critical radius for a cosmic string loop found in Ref. [100], however for a spherical domain wall it is slightly smaller (by about 10%) than the approximate solution given therein. For larger initially static spherically symmetric p-branes with an initial physical radius, r^0, such that $|r^0| > r_c^0$, the motion is not periodic and, if $H > 0$, the brane eventually freezes in comoving coordinates. Specifically, the p-brane will asymptotically behave as

$$q = \text{constant}\,, \qquad \text{so that} \qquad R \propto a,\,, \quad \text{and} \quad v \propto a^{-1}\,. \tag{2.118}$$

If $H < 0$, all solutions with $\left|r^0\right| > r_c^0$ will asymptote the critical point defined in Eq. (2.115) when $t \to \infty$.

The periodic solutions, with $\left|r^0\right| < r_c^0$, satisfy

$$\left\langle \frac{d(\ln R)}{dt} \right\rangle = 0\,, \tag{2.119}$$

and, consequently, it follows from Eq. (2.107) (with $i = 0$) that the velocity is such that

$$\left\langle v^2 \right\rangle = \frac{p}{p+1}\,, \tag{2.120}$$

where the brackets denote a time average over one period.

If $i \neq 0$, these periodic solutions no longer exist. This can easily be seen in the $R\left|H\right| \ll 1$ limit. In this limit, the Hubble damping term has a very small impact on the dynamics of the p-brane on timescales of approximately R, and, consequently, the dynamics of the p-brane is quasi periodic. Hence, from Eq. (2.107), we see that the evolution of the velocity is essentially the same for all branes with the same value of $p - i$. As a matter of fact, we find that

$$\left\langle v^2 \right\rangle = \frac{p-i}{p-i+1}\,, \tag{2.121}$$

which depends only on the number of dimensions with spherical symmetry. We may write Eq. (2.108) as

$$\frac{dR}{dt} = HR\left[1 - \frac{p-i+1}{p-i}v^2 - \frac{i}{p-i}v^2\right]. \tag{2.122}$$

Averaging this equation over one quasi period one obtains

$$\frac{d\left\langle R\right\rangle}{dt} = H\left\langle R\right\rangle\left[1 - \frac{p-i+1}{p-i}\left\langle v^2\right\rangle - \frac{i}{p-i}\left\langle v^2\right\rangle\right] = -H\left\langle R\right\rangle\frac{i}{p-i+1}\,, \tag{2.123}$$

so that

$$\left\langle R\right\rangle \;\propto\; \exp\alpha_1 Ht\,, \quad \text{with} \quad \alpha_1 = -\frac{i}{p-i+1}\,. \tag{2.124}$$

Hence, if $i \neq 0$ and the universe is expanding, the invariant radius of the p-brane shrinks over cosmological timescales (the opposite occurs if $H < 0$). In Fig. 2.2 we compare the evolution of the invariant radius, computed numerically using Eqs. (2.107) and (2.108), against the analytical macroscopic solution given by Eq. (2.124), and the results seem to confirm the above results.

2.3.3 p-Brane Dynamics with $H \neq$ Constant

Let us now consider the case of an expanding or collapsing universe, with a time dependent expansion rate. For simplicity we shall assume that the dynamics of the universe is driven by a fluid with $w =$ constant $\neq -1$, so that $a \propto |t|^{\beta}$, with $\beta = 2/(N(w+1))$. We identify $t = 0$ with either the big-bang (for $w > -1$) or with the big-rip (for $w < -1$).

For $-1 < w < w_c$, with $w_c = (2-N)/N$, (or equivalently for $\beta > 1$), the comoving Hubble radius, H^{-1}/a, decreases with time. Consequently, it is still possible to find a critical radius associated with a solution characterized by

$$v \to v_c \neq 0\,, \qquad \text{when} \qquad t \to \infty\,. \tag{2.125}$$

By requiring that the first and second time derivatives of v vanish asymptotically at late times, and using Eq. (2.107), we find that

$$(r_c H)^2 = \frac{p-i}{p+1}\frac{\beta}{\beta-1}\,, \tag{2.126}$$

$$v_c^2 = \frac{\beta-1}{\beta}\frac{p-i}{p+1}\,. \tag{2.127}$$

In the $\beta \to 1$ limit, $v_c \to 0$ and, therefore,

$$r_c H \propto (\beta-1)^{\gamma_c} \propto (w_c - w)^{\gamma_c} \to \infty\,. \tag{2.128}$$

Here, the value of the critical exponent, γ_c, is equal to $-1/2$ and is independent of i, p and N.

The critical radius in Eq. (2.126) no longer exists for $w < -1$ or $w > w_c$. If $w > w_c$, the comoving Hubble radius increases throughout the evolution. This means that all p-branes (even those that are initially very large), will eventually come inside the Hubble sphere. Consequently, at late times the physical radius will be such that $r \ll H^{-1}$, and the p-branes will oscillate quasi-periodically. If $w < -1$, however, the Hubble radius decreases with increasing physical time.

Therefore, any p-brane that initially describes a quasi-periodic trajectory (with $r \ll H^{-1}$) will eventually freeze in comoving coordinates.

The analysis of the collapsing case is trivial and follows directly from the $q \to -q$ and $t \to -t$ duality described in Section 2.3.1. In this case, if $w < w_c$, the comoving Hubble radius, $|H|^{-1}/a$, increases with time. Hence, all p-branes will eventually come inside the horizon, and they will oscillate quasi-periodically when $R|H|$ becomes much smaller than unity. On the other hand, if $w > w_c$, the comoving Hubble radius decreases with time. Therefore, all p-branes will eventually have a physical radius much larger than $|H|^{-1}$, and asymptotically the physical radius behaves as $|r| \propto a$ so that $\gamma v \propto a^{-(p+1)}$. Consequently, as the universe collapses ($a \to 0$), the p-branes become ultra-relativistic while staying effectively frozen in comoving coordinates. This result has been demonstrated in refs. [104, 105] for defect networks in $3+1$ dimensions, and we will discuss this regime in more detail in Sec. 3.82.

2.3.4 The impact of Cosmology on small Cosmic String Loops

In Sec. 2.3.2, we have shown that a spherically symmetric ($i = 0$) p-brane loops with an initial physical radius smaller than the critical radius in Eq. (2.112) oscillate periodically. Therefore, their macroscopic dynamics never become dominated by the background cosmology: its effects average to zero on each period of brane motion. As a matter of fact, if we consider the evolution of p-branes with $R|H| \ll 1$ in a flat FRW universe, Eqs. (2.107) and (2.108) imply that the impact of background cosmology should be very small on timescales $\lesssim R$. In this section we investigate whether or not there are cosmological models, in which the large-scale of the universe can affect the macroscopic dynamics of small spherically symmetric p-brane. Let us assume that H is no now time dependent, but instead it is of the form

$$H(t) = H_0 + \Delta H(t)\,, \tag{2.129}$$

where $H_0 > 0$ is a constant and $|\Delta H| < H_0$. For simplicity, in this section, we consider the case of a circular cosmic string loop in $3+1$ dimensions ($N = 3, p = 1, i = 0$). The generalization of our analysis for arbitrary N and p is straightforward. If we take

$$\Delta H = H_1 \left(1 - 2v^2(t+\theta)\right)\,, \tag{2.130}$$

where v is the microscopic velocity of the loop and θ is a constant phase, Eq. (2.108) becomes

$$\frac{dR}{dt} = R\left(1-2v^2(t)\right)\left[H_0 + H_1\left(1-2v^2(t+\theta)\right)\right] . \tag{2.131}$$

The evolution of the loop during one quasi period is hardly affected by the cosmological expansion and, consequently, the Minkowski space solution — given by

$$r = r_0 \cos\left(\frac{t}{r_0}\right) , \tag{2.132}$$

$$v = -\sin\left(\frac{t}{r^0}\right) , \tag{2.133}$$

— is still a very good approximation, in the $RH \ll 1$ limit and on timescales much smaller than H^{-1}. Taking into account that $1-2v^2(t) = \cos(2t)$, and averaging the right-hand side of Eq. (2.131) over one time period, one obtains the following equation for macroscopic evolution of circular loops

$$\frac{d\langle R\rangle}{dt} = \frac{H_1}{2}\cos(2\theta)\langle R\rangle , \tag{2.134}$$

and, hence, we should have that

$$\langle R\rangle \propto \exp(\alpha_2 H_1 t) , \quad \text{with} \quad \alpha_2 = \frac{1}{2}\cos(2\theta) . \tag{2.135}$$

We clearly see that the evolution of the universe may have an impact on the macroscopic evolution of cosmic string loops over cosmological timescales, even if they are very small. To illustrate this effect, we solved numerically the equations of motion for a cosmic string loop. In Fig. 2.3, we plot the results for the time evolution of the invariant radius of a loop with initial radius $R(t_i)H_0 = 0.002$ and for a Hubble parameter given by $H_0 = 2H_1$ and $\theta = 0$. As expected, this particular cosmology has indeed an impact on the evolution of the invariant radius making its mean value increase, after each period, by the predicted amount. Note, however, that this case serves merely for illustrative purposes, and that these kind of effect is only expected in special cases. Nonetheless, this shows that there are situations in which the evolution of the universe as a whole may affect the microscopic p-brane dynamics over cosmological timescales, even though this effect is expected to be very small.

It is interesting to realize that we may write the Hubble parameter as a function of the loop parameters, R and v, using Eqs. (2.107) and (2.108):

$$H = \frac{d\ln R}{dt}\left(1 - \frac{p+1}{p-i}v^2\right)^{-1} . \tag{2.136}$$

This equation clearly shows that the dynamics of a single p-brane might be used to infer the dynamics of the underground cosmology.

2.4 CONCLUSIONS

In this Chapter, we derived the evolution equation for the velocity of curved thin domain walls in $N+1$-dimensional Friedmann-Robertson-Walker universes. We also demonstrated that this equation of motion is valid independently of the underlying field theory model. Moreover, we used this result to obtain the equation of motion for an infinitely-thin p-brane of aribitrary dimensionality in FRW universes with an arbitrary number of spatial dimensions. Furthermore, we derived the equation of motion for infinitely thin and featureless p-branes, by computing the tangential and normal components of the acceleration directly from the Nambu-Goto action.

We demonstrated explicitly that the Press-Ryden-Spergel algorithm preserves the dynamics of thin domain walls in FRW universes with an arbitrary dimensionality, if its parameters satisfy $\alpha + \beta/2 = N$. This result then validates the use of the PRS algorithm in field theory simulations of domain wall network evolution, independently of the lagrangian density of the model. Notice, however, that the implementation of the PRS algorithm may affect the small-scale dynamics of the networks: an increasing physical thickness may lead to the destruction of its small scale structure, and it necessarily affects the dynamics of small closed loops. The PRS algorithm also increases artificially the impact of junctions on the overall network dynamics, however this effect is expected to be negligible for light junctions.

We have also studied the dynamics of p-branes with a $S_{p-i} \otimes \mathbb{R}^i$ topology in expanding and collapsing homogeneous and isotropic universes, with $N+1$-dimensions. We have demonstrated that, in a FRW universe with a time independent Hubble parameter, the spherically symmetric p-branes may have a periodic motion, provided that their initial radius is small enough compared to the Hubble radius. We have obtained analytically the equations for these trajectories in phase space for spherical branes and the corresponding critical points, and we computed the root-mean-square velocity of the periodic solutions. We have also found that spherically symmetric branes with an initial radius larger than a critical value will eventually freeze in comoving coordinates. Therefore, one would expect realistic small loops to decay, due to the emission of gravi-

tational radiation, while large loops are stretched if the universe is expanding at a constant rate. Despite the fact that these loops are idealistic in the sense that they are maximally symmetric and they do not contain small-scale structure, these results are expected to provide a good insight into the behaviour of realistic loops produced during the evolution of string networks. These results may also be relevant to understand cosmic string network evolution during inflationary stages, as discussed in Ref. [100].

We also studied the case of p-branes with $i \neq 0$, and shown that, in this case, periodic solutions do not exist over cosmological timescales, even if $R\,|H| \ll 1$. Moreover, we investigated the case of collapsing and expanding universes with a time dependent Hubble parameter and we found that, for $\beta > 1$, a critical radius may still be defined. We found that, as $\beta \to 1$, $r_c H \propto (w_c - w)^{\gamma_c}$, with $\gamma_c = -1/2$. Finally, we discussed the impact that the large scale dynamics of the universe can have on the macroscopic evolution of very small loops, showing that there are situations in which the evolution of the universe as a whole may affect the macroscopic p-brane dynamics over cosmological timescales.

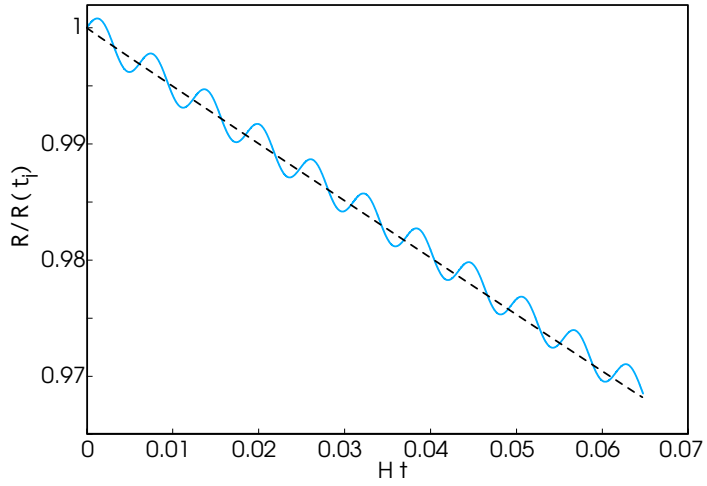

Figure 2.2: Time evolution of the invariant radius, R, of a domain wall with cylindrical symmetry with $R(t_i)H = 0.002$ (solid line) and the evolution of $\langle R \rangle$ as predicted in Eq. (2.124) (dashed line)

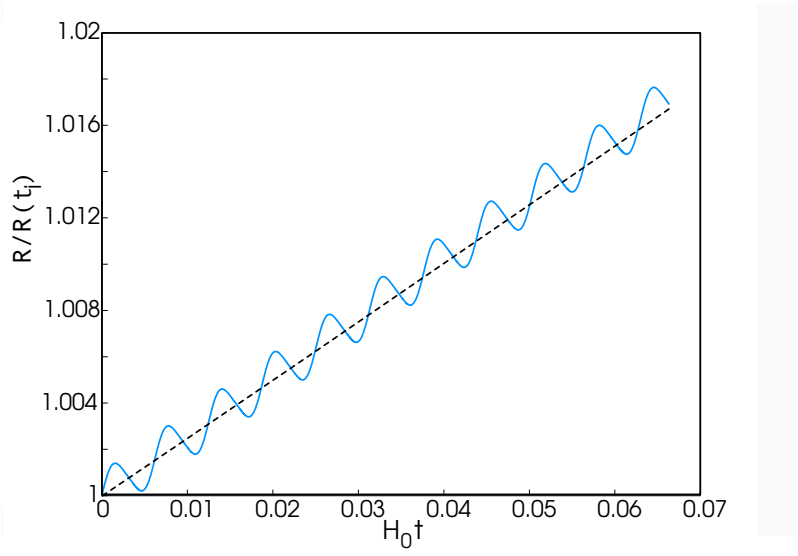

Figure 2.3: Time evolution of the invariant radius, R, of a circular cosmic string loop for $H(t) = H_0 + H_1(1 - 2v^2(t))$ (solid line) and the expected evolution of $\langle R \rangle$ (dashed line). We have taken $H_0 = 2H_1$ and $R(t_i)H_0 = 0.002$.

3

Velocity-Dependent One-Scale Model for p-Branes

In order to understand the cosmological consequences of p-brane networks, it is necessary to understand their cosmological evolution. The main features of the evolution of standard cosmic strings have been extensively studied in the literature, using both analytical and numerical tools. The formation of string networks is expected to occur as a result of symmetry breaking phase transitions in the early universe, which is a very dense environment. Therefore, cosmic string motion is expected to be, right after formation, heavily damped due to interactions with the relativistic particles of the surrounding plasma. The early evolution of string networks is then essentially determined by the frictional forces caused by these interactions, and, for that reason, their dynamics are said to be friction-dominated in this phase. The friction-dominated epoch, however, is transient: as the universe expands and the radiation energy density decreases, the effects of friction become progressively less important and eventually become negligible.

Once friction becomes sub-dominant, the evolution of the network is essentially determined by the interplay between the damping caused by Hubble expansion, and the energy loss provoked by string interactions. This energy loss, caused by the formation of closed loops and subsequent radiative decay, plays a key role in the network's evolution. In the absence of any energy loss mechanisms, the background energy density would decrease faster than the cosmic string energy, and thus cosmic strings would eventually dominate the energy density of the universe. If an energy-loss mechanism exists, however, the net-

work may evolve towards a scale-invariant regime, in which the string energy density remains a constant fraction of the background energy density. In this case, the cosmic string networks do not have pathological cosmological consequences.

The first attempts to describe the large-scale evolution of string networks analytically were based on the assumption that a single lengthscale — the correlation length — is sufficient to describe their dynamics [106, 107, 108]. Using these One-scale models, the authors were able to demonstrate that the linear scaling regime is stable and, therefore, if the networks attain this regime, it will determine their late-time evolution. Moreover, subsequent numerical simulations [109, 110, 111, 112, 113, 114] revealed that these models provide a fairly good description of the large-scale dynamics of string networks, but they are inadequate at small-scales. In particular, these studies revealed that string interactions lead to the production of small cosmic string loops — much smaller than the correlation length — and therefore one-scale models are inadequate to describe the small-scale structure of the strings. On the positive side, in these simulations, the string networks appeared to be evolving towards a linear scaling regime, indeed. Several other analytical models, resorting to the use of more than one lengthscale, were subsequently developed in an attempt to account for the small-scale structure and to provide a more accurate description of loop production and decay [115, 116, 117]. These models, however, have the unattractive feature of having several phenomenological terms.

In Ref. [4], the one-scale model was ameliorated by treating the average root-mean-square velocity of the network as a dynamical variable (in the original one-scale model it was assumed to remain constant). This Velocity-dependent One-scale model provides a quantitative description of the string network throughout its evolution, describing the friction-dominated early-time evolution as well as the natural attainment of a linear scaling regime. We will outline this model in Sec. 3.1.

In Sec. 3.2, we will, then, generalize this model to describe the large-scale evolution of p-brane networks of arbitrary dimensionality, in $N+1$-dimensional Friedmann-Robertson-Walker universes, using the results of the previous chapter. As in the case of cosmic strings, the evolution of p-brane networks may be separated in two different epochs: a friction-dominated era, in which the motion of p-branes is damped due to particle scattering; and a frictionless era, in which the evolution of the network is mainly determined by Hubble expansion (or collapse) and by brane interactions. In Sec. 3.3, we study the different scaling regimes that may arise during the frictionless era, in expanding and collapsing universes. We will focus particularly on the conditions that a p-brane

network must satisfy in order to attain a linear scaling regime. In Sec. 3.4, we will study the scaling regimes that may arise while the p-brane motion is friction-dominated, in collapsing and expanding universes.

3.1 VELOCITY-DEPENDENT ONE-SCALE MODEL FOR COSMIC STRINGS

The Velocity-dependent One-scale (VOS) model, proposed in Ref. [4] and later extended in [118], describes the evolution of the root-mean-square velocity and characteristic lengthscale of cosmic string networks in $3+1$-dimensional FRW universes. This model provides a quantitative description of the large-scale evolution of cosmic string network, both at early and late times. Interestingly, the linear scaling regime is an attractor solution of the VOS equations, and, therefore, in this framework, string domination is naturally avoided.

3.1.1 Lengthscale Evolution

The VOS equations for cosmic strings are obtained by averaging the Nambu-Goto equations of motion in $3+1$-dimensional FRW universes, in Eqs. (2.66) and (2.67).

The total string energy is defined as

$$E = \mu a(\eta) \int \epsilon du \,, \tag{3.1}$$

where ϵ is the coordinate energy per unit length defined in Eq. (2.68), and μ is string energy per unit length. The total string energy density should scale as

$$\rho \propto \frac{E}{a^3} \,, \tag{3.2}$$

and, thus, by differentiating Eq. (3.1), and using Eq. (2.66), we find that

$$\frac{d\rho}{dt} + 2H\rho(1+\bar{v}^2) = 0 \,, \tag{3.3}$$

where the root-mean-square (RMS) string velocity,

$$\bar{v}^2 \equiv \left\langle \dot{\mathbf{x}}^2 \right\rangle = \frac{\int \dot{\mathbf{x}}^2 \epsilon du}{\int \epsilon du} \,, \tag{3.4}$$

was introduced.

The VOS model is based on the assumption that the large-scale evolution of a long-string network may be described by a single lengthscale, the characteristic

length L. This lengthscale can be interpreted both as the typical distance between nearby strings, and the typical radius of curvature of the cosmic strings. In each volume L^3, there is, on average, a string segment of length L, therefore we can define the characteristic length as

$$\rho \equiv \frac{\mu L}{L^3} = \frac{\mu}{L^2} \,. \tag{3.5}$$

Using Eq. (3.3), we obtain

$$\frac{dL}{dt} = HL(1+\bar{v}^2) \,, \tag{3.6}$$

which describes the cosmological evolution of the characteristic length of the string network.

3.1.2 Velocity Evolution

Another key feature of the VOS model is the fact that the RMS velocity is a dynamical variable. Therefore, to complete the description of the network's evolution, we need an equation of motion for its RMS velocity. By differentiating Eq. (3.4), and using Eqs. (2.66) and (2.67), we obtain the evolution equation of motion for $\bar{v}$

$$\frac{d\bar{v}}{dt} = (1-\bar{v}^2)\left[\frac{k}{\bar{R}} - 2Hv\right] , \tag{3.7}$$

which is exact up to second order [4], and was derived under the assumption that

$$\left\langle \dot{\mathbf{x}}^4 \right\rangle = \left\langle \dot{\mathbf{x}}^2 \right\rangle^2 \,. \tag{3.8}$$

Moreover, the average radius of curvature, $\bar{R}$, defined by

$$\frac{a(\eta)}{\bar{R}}\hat{\mathbf{u}} = \frac{d^2\mathbf{x}}{ds^2} \,, \tag{3.9}$$

was introduced. In Eq. (3.9), $\hat{\mathbf{u}}$ represents the unitary curvature vector and ds is the physical length along the string,

$$ds = \left|\mathbf{x}'\right| du = (1-\dot{\mathbf{x}}^2)^{\frac{1}{2}} \epsilon du. \tag{3.10}$$

In Eq. (3.7), a dimensionless curvature parameter k, defined by

$$\left\langle (1-\dot{\mathbf{x}}^2)(\dot{\mathbf{x}}\cdot\hat{\mathbf{u}}) \right\rangle \equiv k\bar{v}(1-\bar{v}^2) \,, \tag{3.11}$$

was also introduced. This momentum parameter measures the angle between the curvature vector and the velocity of the cosmic strings, and, thus, it evaluates the existence of small scale structure on the strings. For string networks with small-scale structure, k is a dynamical variable that depends on the RMS velocity of the network. In Ref. [118], the following ansatz for k was proposed

$$k(v) = \frac{2\sqrt{2}}{\pi}(1-\bar{v}^2)(1+2\sqrt{2}\bar{v}^3)\frac{1-8\bar{v}^6}{1-8\bar{v}^6}\,. \tag{3.12}$$

Therefore, although this model uses an unique scale to describe the network evolution, the effects of small-scale structure on the dynamics may be included in the evolution equation for the RMS velocity, by considering a velocity-dependent curvature parameter.

3.1.3 Loop Production and Energy Loss

Eqs. (3.6) and (3.7) do not take into account string interactions. When two cosmic strings meet they exchange partners and reconnect (see Fig 3.1), leading to the creation of two kinky cosmic strings. This particular type of interaction does not lead to any energy loss by the network, however the same process can lead to the formation of cosmic string loops in two ways: if a cosmic string self-intersects or when two kinky cosmic strings intersect at more than one point. Most of these cosmic string loops are very small, and consequently they begin to oscillate quasi-periodically and decay radiatively (in general via the emission of gravitational radiation). The production and decay of cosmic string loops leads, then, to energy losses, and it must be taken into consideration in Eq. (3.3).

The rate of loop production, as a result of string collision, has been estimated by Kibble in Ref. [106]. Let us regard the string configurations as a collection of independent segments of length L, each in a volume L^3. The probability of another segment of length ℓ (moving with velocity $\bar{v}$) encountering one of the other segments within a time δt is, approximatively,

$$\ell\bar{v}\frac{\delta t}{L^2}\,. \tag{3.13}$$

The probability of creation of a loop with a length within ℓ to $\ell + d\ell$ may, if we maintain the one scale assumption, be described by a scale-invariant function of the ratio ℓ/L. The rate of energy loss caused by loop production is, then, given by

$$\left.\frac{d\rho}{dt}\right|_{\text{loops}} \equiv \rho\frac{\bar{v}}{L}\int w(\ell/L)\frac{\ell}{L}\frac{d\ell}{L} \equiv \tilde{c}\bar{v}\frac{\rho}{L}\,, \tag{3.14}$$

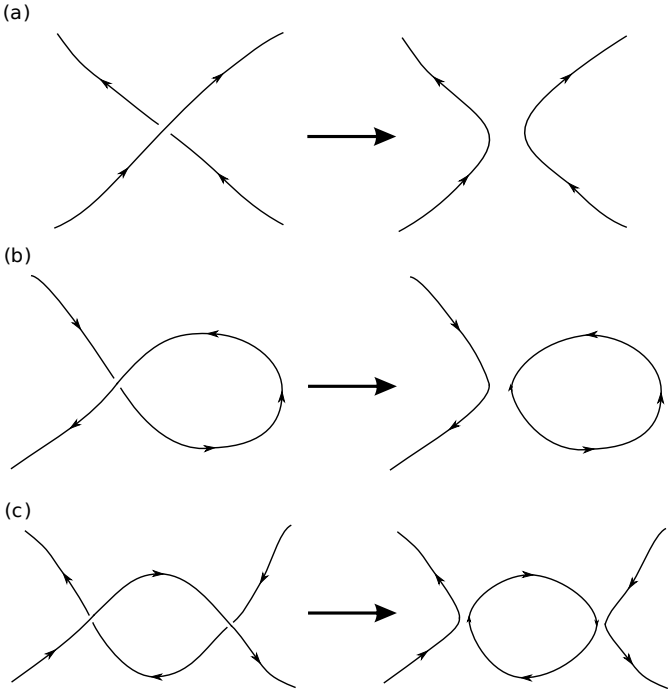

Figure 3.1: Possible outcomes of String Interaction: (a) The interaction of two cosmic strings leads to reconnection and the formation of two kinky cosmic strings;

(b) Cosmic String Self-interaction leads to the production of cosmic string loops;

(c) The formation of cosmic string loops can also occur when two kinky cosmic strings intersect at more than one point.

where the energy-loss parameter, $\tilde{c}$, was introduced. According to [4], the energy loss parameter is expected to be constant throughout the nertwork's evolution. Using Eq (3.5), we find that

$$\left.\frac{dL}{dt}\right|_{\text{loops}} = -\tilde{c}\bar{v}\,. \tag{3.15}$$

3.1.4 Frictional Forces

Throughout their evolution, cosmic strings scatter off the relativistic particles of the background plasma. This particle scattering results in a frictional force per unit length that might be described by [119]:

$$\mathbf{F} = -\frac{1}{\ell_f}\frac{\mathbf{v}}{\sqrt{1-\bar{v}^2}}\,, \tag{3.16}$$

where $\mathbf{v}$ is the string velocity vector and ℓ_f is the friction lengthscale, defined as

$$\ell_f = \frac{\mu}{\beta T^3}\,, \tag{3.17}$$

where T is the background temperature and β is a numerical factor related to the number of particle species interacting with the strings.

This frictional force can be included in Eqs. (2.66) and (2.67), by adding an

extra-term of the form

$$\left(U^{\alpha} - x^{\alpha}{}_{,\tilde{\mu}} x^{\lambda,\tilde{\mu}} U_{\lambda}\right) \frac{1}{\ell_f}\,, \tag{3.18}$$

where U^{α} is the four-velocity of the background fluid. In the case of a FRW universe, the four-velocity of radiation is given by

$$U^{\alpha} = \left(a^{-1}, 0, 0, 0\right)\,. \tag{3.19}$$

This extra effect may be included in Eqs (2.66) and (2.67) by replacing the Hubble Damping term by [119]:

$$2\frac{\dot{a}}{a} + \frac{a}{\ell_f}\,. \tag{3.20}$$

If we proceed as in Sec. 3.1.1 and 3.1.2, we find that

$$\frac{d\rho}{dt} + \left(2H + \frac{\bar{v}^2}{\ell_d}\right)\rho = -\tilde{c}\frac{\bar{v}}{L}\rho\,, \tag{3.21}$$

$$2\frac{dL}{dt} = \left(2H + \frac{\bar{v}^2}{\ell_d}\right)L + \tilde{c}\bar{v}\,, \tag{3.22}$$

$$\frac{d\bar{v}}{dt} = (1-\bar{v}^2)\left[\frac{k}{L} - \frac{\bar{v}}{\ell_d}\right]\,, \tag{3.23}$$

where the damping lengthscale, that includes damping caused both by Hubble expansion and by the frictional forces,

$$\frac{1}{\ell_d} = 2H + \frac{1}{\ell_f}\,, \tag{3.24}$$

was introduced. Eqs. (3.22) and (3.23) allow us to describe the cosmological evolution of a cosmic string networks, and they form the basis of the VOS model for cosmic strings.

3.2 VELOCITY-DEPENDENT ONE SCALE MODEL FOR P-BRANE NETWORKS

In Ref. [120], the VOS model for cosmic strings was generalized to isotropic and anisotropic $N+1$-dimensional backgrounds. Furthermore, a phenomenological VOS model [121, 122] for domain wall networks in isotropic backgrounds was shown to successfully describe the results of high-resolution field theory numerical simulations [8]. In this section, we develop a more general VOS model

that describes the dynamics of p-brane networks of arbitrary dimensionality in $N+1$-dimensional homogeneous and isotropic universes in a single framework. The work presented in this section was published in [14, 15].

3.2.1 Equation-of-State Parameter of a p-brane Network

In order to derive the equation of state for a p-brane network, let us start by computing the energy-momentum tensor of a p-brane. Consider a local inertial frame in which a p-brane segment is instantaneously at rest. For a locally flat p-brane, we may choose a local set of planar orthogonal coordinates $\left(t, x^1, \cdots, x^N\right)$, such that $x^1, \cdots, x^p$ parameterize the brane and $x^{p+1}, \cdots, x^N$ are perpendicular to it. The properties of a featureless p-brane do not change along the parallel directions, and, for that reason, the physical velocity is purely perpendicular to the brane. Therefore, the energy-momentum tensor, $T^{\mu\nu}$, must be invariant under Lorentz boosts along the tangential directions of the brane.

Consider a boost along one of the parallel directions $x^{\tilde{i}}$, with $\tilde{i} = 1, \cdots, p$. The energy-momentum tensor, transforms as

$$T^{\mu'\nu'} = \Lambda^{\mu'}_{\alpha}\Lambda^{\nu'}_{\beta}T^{\alpha\beta}\,, \tag{3.25}$$

where

$$\Lambda^{0'}_{0} = \Lambda^{\tilde{i}'}_{\tilde{i}} = \gamma\,, \qquad \Lambda^{0'}_{\tilde{i}} = \Lambda^{\tilde{i}'}_{0} = \gamma v\ , \qquad \Lambda^{l'}_{l} = 1\,, \tag{3.26}$$

and all other components vanish. Here $\tilde{i}' = 1, \cdots, p$, $l = 1, \cdots, N$ and $l \neq \tilde{i}$.

Hence

$$T^{0'l'} = \gamma T^{0l} + \gamma v T^{\tilde{i}l} = T^{0l}\,, \tag{3.27}$$

$$T^{\tilde{i}'l'} = \gamma T^{\tilde{i}} + \gamma v T^{0l} = T^{\tilde{i}l}\,, \tag{3.28}$$

$$\tag{3.29}$$

which leads to

$$T^{0l} = T^{\tilde{i}l} = 0\,. \tag{3.30}$$

Moreover,

$$T^{0'\tilde{i}'} = \gamma^2 v\left(T^{00} + T^{\tilde{i}\tilde{i}}\right) + \gamma^2\left(1+v^2\right)T^{0\tilde{i}} = T^{0\tilde{i}}\,, \tag{3.31}$$

from which we obtain

$$T^{0\tilde{i}} = 0\,. \tag{3.32}$$

Finally, we have that

$$T^{0'0'} = \gamma^2 T^{00} + \gamma^2 v^2 T^{\tilde{i}\tilde{i}} = T^{00}\,, \tag{3.33}$$

which yields

$$T^{\tilde{i}\tilde{i}} = -T^{00}\,. \tag{3.34}$$

If the p-brane is maximally symmetric with respect to the $N-p$ perpendicular directions and its energy is localized, then Derrick's theorem [54] implies that a necessary condition for stability is that [123]

$$\int d^D x T^{mm} = 0\,, \tag{3.35}$$

for $m \geqslant p+1$ (with $D = N-p$ and $d^D x = dx^{p+1} \times ... \times dx^N$). Furthermore, spherical symmetry with respect to the D perpendicular directions implies that, at the core, we should have that $T^{nm} = 0$, for $n \geqslant p+1$, $m \geqslant p+1$ and $n \neq m$. In most situations of interest in cosmology, the thickness of the p-brane is very small when compared to its curvature radii and may therefore be neglected. If the p-brane is infinitely thin, the non-vanishing components of the energy-momentum tensor are

$$T^{00} = \sigma_p \int d^p x \delta^N(\mathbf{x} - \mathbf{x}_p)\,, \quad \text{and} \qquad T^{\tilde{i}\tilde{i}} = -\sigma_p \int d^p x \delta^N(\mathbf{x} - \mathbf{x}_p)\,, \tag{3.36}$$

where σ_p is the (constant) p-brane mass per unit p-dimensional area, $\mathbf{x}$ is a N-vector whose components are cartesian coordinates, $\mathbf{x}_p$ represents the p-brane spatial profile, and $\delta^N(\mathbf{x})$ is the N-dimensional Dirac delta function.

Consider a perfect gas of planar p-branes, moving with an average velocity $\bar{v}$[1] inside a large volume, and let us assume, for simplicity, that they are aligned with the $(x_1, \cdots . x_p)$ coordinates. Although this is a simplistic construct, we shall see that it will allow us to derive an expression for the equation-of-state parameter of a p-brane network. Following the approach in Ref. [17], in the limit of many p-branes, the average energy-momentum tensor of the brane gas will be

$$\langle T_{\mu\nu} \rangle \simeq \frac{\tilde{T}_{\mu\nu}}{L^D}\,, \tag{3.37}$$

where we defined

[1] $\bar{v}$ will be properly defined in the next section.

$$\tilde{T}_{\mu\nu} = \int d^D x T_{\mu\nu} \,, \tag{3.38}$$

whose non-vanishing components are $\tilde{T}^0_0 = \sigma_p$, and $\tilde{T}^{\tilde{i}}_{\tilde{i}} = -\sigma_p$, for $\tilde{i} = 1, \cdots, p$. Furthermore, we made the assumption that, on average, there is approximately a p-brane segment of p-dimensional area L^p in each volume L^N. Under this assumption, the average number of p-branes per D-dimensional (perpendicular) area is given by L^{-D}. As in the case of the VOS model for Cosmic strings discussed in Sec. 3.1, this characteristic length, L, will be the unique scale used to describe the network.

Let us now assume that the p-branes are moving with an average velocity $\bar{v}$ in the positive x_l direction, with $l \geqslant p+1$. By performing a Lorentz boost of $\tilde{T}_{\mu\nu}$ along this direction, characterized by

$$\Lambda^{0'}_0 = \Lambda^{l'}_l = \gamma \,, \qquad \Lambda^{l'}_0 = \Lambda^{0'}_l = \gamma v \,, \quad \text{and} \qquad \Lambda^{i'}_i = 1 \,, \quad \text{for} \quad i \neq l \,, \tag{3.39}$$

it is straightforward to show that

$$\tilde{T}^{0'}_{0'} = \gamma^2 \sigma_p \,, \qquad \tilde{T}^{l'}_{l'} = \gamma^2 \bar{v} \sigma_p \,, \qquad \tilde{T}^{0'}_{l'} = \tilde{T}^{l'}_{0'} = \gamma^2 \bar{v} \sigma_p \,, \qquad \tilde{T}^{\tilde{i}'}_{\tilde{i}'} = -\sigma_p \,, \tag{3.40}$$

and that the remaining components vanish. The average energy-momentum tensor for the p-brane gas may, then, be obtained by averaging over all possible orientations and boost directions. We then find that

$$\langle T^\mu_\nu \rangle = \frac{\sigma_p}{N} \mathrm{diag}\left(N\gamma^2, v^2\gamma^2 - p, \cdots, v^2\gamma^2 - p \right) \,, \tag{3.41}$$

and, consequently,

$$w_p = \frac{\bar{\mathcal{P}}}{\bar{\rho}} = \frac{1}{N}\left[(p+1)\, \bar{v}^2 - p \right] . \tag{3.42}$$

Here, $\bar{\mathcal{P}}$ is the average brane pressure, defined as

$$\bar{\mathcal{P}} \equiv -\frac{1}{N} \left\langle T^i_i \right\rangle \,, \tag{3.43}$$

and $\bar{\rho}$ is the average p-brane energy density

$$\bar{\rho} \equiv \left\langle T^0_0 \right\rangle \,. \tag{3.44}$$

Note that Eq. (3.42) has two important limits. In the relativistic limit, with

$\bar{v} \to 1$, one has that $w \to 1/N$ independently of the dimensionality of p-branes. On the other hand, in the non-relativistic limit ($\bar{v} \to 0$), one has $w = -p/N$. Note also that Eq. (3.42) is identical to that obtained in Ref. [124] directly from the Dirac-born-Infeld action.

3.2.2 Lengthscale Evolution

Let $\bar{\rho}$ be the average p-brane density of the universe, defined as

$$\bar{\rho} = V^{-1} \int \rho dV \,, \tag{3.45}$$

where ρ is the p-brane energy density and V is the physical volume. Let us assume that the p-brane network is statistically homogeneous and isotropic on large enough scales, so that it behaves effectively as a brane gas. Energy-momentum conservation in a FRW universe implies that

$$\frac{d\bar{\rho}}{dt} + NH\left(\bar{\rho} + \bar{\mathcal{P}}\right) = 0 \,, \tag{3.46}$$

where

$$\bar{\mathcal{P}} = V^{-1} \int \mathcal{P} dV \tag{3.47}$$

is the average brane pressure.

It is straightforward to show that, in the case of a p-brane network, the energy-loss due to interface collapse may be described by a term of the same form as in Eq. (3.14). However, some remarks are necessary. For simplicity, we shall consider the most trivial case of flat p-branes. A moving p-brane sweeps a q-dimensional surface (with $q = p + 1$), with $N - q$ degrees of freedom. If $N \leqslant 2(N - q)$, two flat q-dimensional surfaces intersect in general. However, that is no longer true if $N > 2(N - q)$ (or equivalently $p < (N - 1)/2$), and a p-brane cannot be expected to necessarily encounter another one after travelling a distance L. In fact, due to the higher dimensionality of the background space, p-branes can miss each other. Therefore, in this case, any energy-loss mechanisms are expected to be less efficient. Moreover, in expanding backgrounds, the probability of interaction, for $p < (N - 1)/2$, is expected to decrease over time, insomuch that — even if $\tilde{c}$ is initially considerable — it is expected to decrease to very small values throughout the evolution. Nonetheless, we shall include a term of the form of Eq. (3.14) in the evolution equation for the energy density of p-branes, bearing in mind these differences for $p < (N - 1)/2$.

By introducing Eqs. (3.42) and (3.14) into Eq. (3.46), one finds that:

$$\frac{d\bar{\rho}}{dt} + \left(DH + \frac{\bar{v}^2}{\ell_d} \right) \bar{\rho} = -\frac{\tilde{c}\bar{v}}{L} \,, \tag{3.48}$$

where the effects of friction were included in the damping length,

$$\frac{1}{\ell_d} = (p+1)H + \frac{1}{\ell_f} \,, \tag{3.49}$$

and $D = N - p$. The scaling behaviour of ℓ_f will be discussed in Sec. 3.4. Here, we have also introduced the RMS velocity of the network that, in this case, is defined by

$$\bar{v}^2 \equiv \left\langle v^2 \right\rangle = \frac{\int v^2 \rho dV}{\int \rho dV} \,. \tag{3.50}$$

In this section, $\langle \cdots \rangle$ denotes the volume weighted average. An equivalent definition for 1-branes would be

$$\bar{v}^2 = \frac{\int v^2 \gamma dl}{\int \gamma dl} \,. \tag{3.51}$$

As in the case of cosmic strings, we assume that the p-brane network may be characterized by a single lengthscale, the characteristic length L. This scale may be defined as

$$\bar{\rho} \equiv \frac{\sigma_p L^p}{L^N} = \frac{\sigma_p}{L^{N-p}} \,. \tag{3.52}$$

Alternatively, one may use the physical length, defined as

$$\langle \rho/\gamma \rangle = \frac{\sigma_p}{L_{\rm ph}^{N-p}} \,. \tag{3.53}$$

This definition is not as useful as that in Eq. (3.52), since a direct relation between $L_{\rm ph}$, $\bar{\rho}$ and $\bar{v}$ does not exist. Albeit, $L_{\rm ph}$ has the advantage that it is only sensitive to the spatial profile of the network, and that it measures the physical distance between nearby branes. In any case, L and $L_{\rm ph}$ are, in general, very similar, except if the p-branes are ultra-relativistic, as we will discuss in Sec. 3.82.

Using (3.52), we then find that

$$\frac{dL}{dt} = HL + \frac{L}{D\ell_d}\bar{v}^2 + \frac{\tilde{c}}{D}\bar{v} \tag{3.54}$$

describes the evolution of L during the evolution of the p-brane network.

3.2.3 Velocity Evolution

In order to obtain the evolution equation for the RMS velocity, we average the equation of motion for the velocity of the p-branes, obtained in Sec 2.2.3. Multiplying Eq. (2.90) by v, making the weighted volume average, and then dividing by $\bar{v}$, one obtains

$$\frac{d\bar{v}}{dt} + \frac{1}{\bar{v}} \left\langle v(1-v^2) \left[(p+1)Hv - \kappa_{\parallel} \right] \right\rangle = 0 \,. \tag{3.55}$$

If we assume that

$$\left\langle v^4 \right\rangle = (\bar{v}^2)^2 \,, \tag{3.56}$$

this further simplifies to

$$\frac{d\bar{v}}{dt} + (1-\bar{v}^2) \left[\frac{\bar{v}}{\ell_d} - \frac{k}{L} \right] = 0 \,, \tag{3.57}$$

where $k = \bar{\kappa} L$, and

$$\bar{\kappa} = \frac{\left\langle v \left(1-v^2\right) \kappa_{\parallel} \right\rangle}{\bar{v} \left(1-\bar{v}^2\right)} = \frac{\int v \left(1-v^2\right) \kappa_{\parallel} \rho dV}{\bar{v} \left(1-\bar{v}^2\right) \int \rho dV} \,. \tag{3.58}$$

The assumption in Eq. (3.56) is valid in the relativistic limit up to first order in $(1-v)$, and it has negligible impact in the non-relativistic limit. This assumption is equivalent to that of the original VOS model for cosmic strings, in Eq. (3.8). Note that k is a dimensionless curvature, and it is also related to the existence of small scale structure: it measures the deviation of velocity direction from the curvature vectors, and, thus it is a measure of brane's smoothness (recall Eqs. (2.89) and (2.91)). It can, therefore, be easily identified with the momentum parameter in Eq. (3.11). Note also that although it is possible to construct network configurations with the same $\bar{v}$ but different $\bar{k}$, in most realistic situations it is sufficient to consider that $\bar{\kappa} = \bar{\kappa}(\bar{v})$.

Eqs. (3.54) and (3.57) constitute a unified VOS model for the dynamics of p-brane networks in $N+1$- dimensional FRW universes. Notice that this equations reduce, for $p = 1$, to the VOS equations of motion for cosmic strings in FRW universes of arbitrary dimensionality [4, 120], and that they were derived under the same assumptions. Note also that, for $p = N-1$ and $N = 3$, these equations reduce to the VOS equations of motion for domain wall networks in $3+1$-dimensional FRW universes derived using phenomenological arguments in Ref. [121]. As a matter of fact, the VOS equations for cosmic strings and domain wall differ mainly on the coefficient of the cosmological damping term,

that assumes the value 2 for cosmic strings, and N for domain walls. Therefore, the differences between the macroscopic evolution of cosmic string and domain wall networks are expected to increase as the dimensionality of space increases.

3.3 FRICTIONLESS SCALING REGIMES

In this section, we will use the generalized VOS model to study the scaling laws of p-brane networks in expanding and collapsing homogeneous and isotropic backgrounds, during the frictionless epoch. For simplicity, we shall assume that the dynamics of the universe is driven by a fluid with w = constant $\neq -1$, so that

$$a \propto t_*^{\beta}, \qquad \text{with} \quad \beta = \frac{2}{N(w+1)}\,. \tag{3.59}$$

Here $t_* \geqslant 0$ represents the time elapsed since the initial singularity (if $dt_* = dt$) or the time remaining up to the final singularity (if $dt_* = -dt$) at $t_* = 0$. We shall consider six different models labelled by M_i^s, where $s = \pm$ depending on whether $dt = \pm dt_*$ and $i = 1, 2$ or 3 for $\beta < 0$, $0 < \beta < 1$ or $\beta > 1$, respectively. The models M_2^+, M_3^+ and M_1^- represent expanding solutions with $t_* = 0$ either at the the big-bang (M_2^+ and M_3^+) or at the big rip (for M_1^-). The models M_1^+, M_2^- and M_3^- represent collapsing universes with $t_* = 0$ either at the the big-crunch (M_2^- and M_3^-) or at the initial infinite density singularity with $a_* = \infty$ (for M_1^+). The Hubble radius, $\left|H^{-1}\right|$, increases with time if $w > -1$. On the other hand, if $-1 < w < w_c$, with $w_c = (2-N)/N$ (so that $\beta > 1$) the comoving Hubble radius, $\left|H^{-1}\right|/a$, decreases with time. Note that the comoving Hubble radius will monotonously increase or decrease with time depending on whether $\ddot{a}$ is negative or positive, respectively. In this section, we shall assume that $\tilde{c} \geqslant 0$.

3.3.1 Linear Scaling Regime

If the friction lengthscale becomes negligible when compared to the Hubble radius, p-brane evolution is mainly determined by the competition between the Hubble expansion (or collapse) — which tends to stretch (or contract) the branes — and the energy loss due to brane interactions. As a result of both effects, the network evolves towards a linear scaling regime, which is a general attractor solution of the VOS equation (in models that admit this solution). During this regime the characteristic length L remains constant relative to the horizon $d_H \sim t$.

If we write

	$\dot{a}$	$\ddot{a}$	$\dot{H}$	C/E	Main Characteristic
M_1^+	$-$	$+$	$+$	C	Linear Scaling
M_2^+	$+$	$-$	$-$	E	Linear Scaling
M_3^+	$+$	$+$	$-$	E	Inflation
M_1^-	$+$	$-$	$+$	E	SuperInflation
M_2^-	$-$	$+$	$-$	C	Ultrarelativistic
M_3^-	$-$	$-$	$-$	C	Linear Scaling

Table 3.1: Summary of the main properties of the different M_i^s models. The label i takes the value $i = 1, 2$ or 3 for $\beta < 0$, $0 < \beta < 1$ or $\beta > 1$, respectively. On the other hand, $s = \pm$ depending on whether $dt = \pm dt_*$ and t_* is the time elapsed since the initial singularity ($s = +$) or the time remaining until the final singularity ($s = -$). The remaining $+$ and $-$ indicate the sign of the cosmological parameters represented in the table and the letters C and E indicate whether the model corresponds to a collapsing or to an expanding universe, respectively.

$$L = \xi(t_*)t_* \,, \tag{3.60}$$

Eq. (3.54) then yields:

$$\frac{\dot{\xi}}{\xi} = \frac{1}{t_*}\left[\beta\left(1 + \frac{p+1}{D}\bar{v}^2\right) - 1 \pm \frac{\tilde{c}}{D}\frac{\bar{v}}{\xi}\right] . \tag{3.61}$$

So, the linear scaling regime should be characterized by

$$\dot{\xi} = 0 \quad \text{and} \quad v = \text{constant} \,, \tag{3.62}$$

with

$$\xi = \sqrt{\left|\frac{k(k+\tilde{c})}{\beta(1-\beta)D(p+1)}\right|} \quad \text{and} \quad \bar{v} = \sqrt{\frac{(1-\beta)kD}{\beta(k+\tilde{c})(p+1)}} \,. \tag{3.63}$$

Note that we should have that

$$0 < \bar{v} < 1 \quad \text{and} \quad \xi > 0 \tag{3.64}$$

in order for $\bar{v}$ and ξ to have physical significance. These conditions are sufficient

to show that models M_3^+ and M_1^- do not admit linear scaling solutions (for $\tilde{c} \geqslant 0$). In the case of the M_2^- model, this scale-invariant regime would not persist, and for that reason we will not consider this model in this section: it will be treated in Sec. 3.82.

There are several complementary constraints which reduce significantly the possible range of parameters consistent with a linear scaling solution. The RMS velocity, $\bar{v}$, of maximally symmetric p-branes with a $S_{p-i} \otimes \mathbb{R}^i$ topology oscillating periodically in a Minkowski spacetime is given by Eq. (2.121). The minimum velocity of these branes, $v_{\rm min}^2 = 1/2$, corresponds to the case when one of the principal curvatures is non-zero ($i = p - 1$). The maximum velocity, $v_{\rm max}^2 = p/(p+1)$, corresponds to the case of fully spherically symmetric p-branes, for which all the principal curvatures of the surface are equal and non-zero ($i = 0$). Note that causality constraints do not allow for flat p-branes and, consequently, we do not consider the case of branes for whose principal curvatures are vanishing. For $\beta = 0$, the curvature parameter k must be equal to zero in order for a linear scaling solution with $\bar{v} \leqslant 1$ to be possible. In an expanding universe, the expansion of the universe hinders the velocity of the branes, leading to a smaller RMS velocity and a positive curvature parameter, k. Therefore, one expects that

$$0 < \bar{v} < v_{\rm max}, \qquad \text{for} \quad M_2^+ \,. \tag{3.65}$$

On the other hand, if the universe is collapsing, the resulting brane acceleration leads to larger $\bar{v}$ and a to negative curvature parameter. In this case,

$$v_{\rm min} < \bar{v} < 1, \quad \text{for} \quad M_1^+ \quad \text{and} \quad M_3^- \,. \tag{3.66}$$

Moreover, the characteristic lengthscale of the network is necessarily constrained by causality and, as a consequence, L is required to be smaller than the particle horizon at any given time[2]. In the case of models M_1^+, M_2^+ and M_3^-, this implies that

$$L < d_H = \int_{t_i}^{t} \frac{dt'}{a(t')} = \frac{t_*}{|1-\beta|} \,, \tag{3.67}$$

with $t_i = 0$ or $t_i = -\infty$, depending on whether $s = +$ or $-$, respectively. This constraint results in another restriction to the RMS velocity:

[2]This constraint is only relevant in the case of models that admit linear scaling solutions: in the case of the M_3^+ and M_1^-, the particle horizon is infinite.

$$\bar{v}^2 < (k + \tilde{c})^{-2} \,. \tag{3.68}$$

The constraints on the RMS velocity of p-brane networks for the M_1^+, M_2^+ and M_3^- models determine the range of values of the curvature parameter, k, for which linear scaling solutions are allowed, for any given β and N. Figs. 3.2 and 3.3 illustrate this range in the case of contracting (M_1^+ and M_3^-) and expanding (M_2^+) models, respectively, for $N-1$-branes (domain walls). The first thing to notice is that, in contracting models, linear scaling regimes are strictly forbidden if $\tilde{c} = 0$ (since $\bar{v}^2 < 0$ is not allowed). On the other hand, if $\tilde{c} \neq 0$, the consequent energy loss decelerates the branes, and the network may attain the linear scaling regime with a RMS velocity within the physically significant range in Eq. (3.66), for negative curvature parameters. The left and right panels of Fig. 3.2 show the range of the curvature parameter for which the linear scaling solutions are permitted, as a function of the expansion exponent, in the case of the models M_3^- and M_1^+, respectively (for $\tilde{c} = 0.5$). In both cases, scaling solutions are allowed for every value of β but the allowed range of k is strongly restricted. Also, in both models, for $\tilde{c} = 0.5$, the causality constraint, given by Eq. (3.68), does not introduce further restrictions on the $(k^2/N, \beta/(1-\beta))$ plane. However, as $\tilde{c}$ increases so does the scaling value of ξ and, therefore, the region for which causality is violated widens and inhibiting the attainment of this scale-invariant solution for some values of β. As a matter of fact, if the value $\tilde{c}$ is big enough, all linear scaling solutions may be forbidden.

In the case of model M_2^+, the network is able to reach a linear scaling regime for $\beta \leqslant 1 - p/N$ (or equivalently $v < v_{\max}$), even if $\tilde{c} = 0$, as the left panel of Fig. 3.3 illustrates. For larger values of β, the allowed range of the curvature parameter is only limited by causality. The presence of energy-loss mechanisms is also advantageous for the attainment of the linear scaling solutions in expanding universes: they decelerate the branes in such a way that it is possible to attain these solutions with $\bar{v} < v_{\max}$, for $0 \leqslant \beta < 1 - p/N$ and $\tilde{c} \neq 0$ (as shown in the right panel of Fig. 3.3).

Note, however, that the linear scaling solution in Eq. (3.63) is attainable for $\beta \geqslant 1 - p/N$ in M_2^+ models, even for non-interacting ($\tilde{c} = 0$) p-brane networks. In this case, the linear scaling solution would be characterized by

$$\xi = \sqrt{\left| \frac{k^2}{\beta(1-\beta)D(p+1)} \right|} \quad \text{and} \quad \bar{v} = \sqrt{\frac{(1-\beta)D}{\beta(p+1)}} \,. \tag{3.69}$$

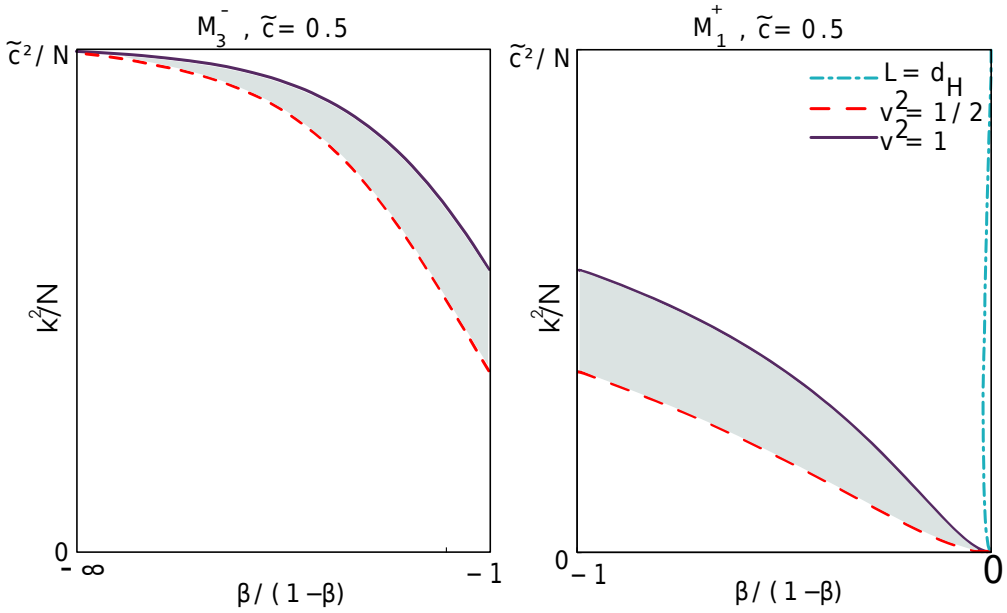

Figure 3.2: Range of values of the curvature parameter, k, for which domain wall networks are able to attain the linear scaling regime (grey area), as a function of $\frac{\beta}{1-\beta}$, for the M_3^- (right panel) and M_1^+ (left panel), for $\tilde{c} = 0.5$. The dash-dotted (blue) line represents the values of k^2/N for which $L = d_H$. The dashed (red) and solid (purple) lines correspond to points for which $v^2 = \frac{1}{2}$, and $v^2 = 1$, respectively. Note that, in this case, $k < 0$.

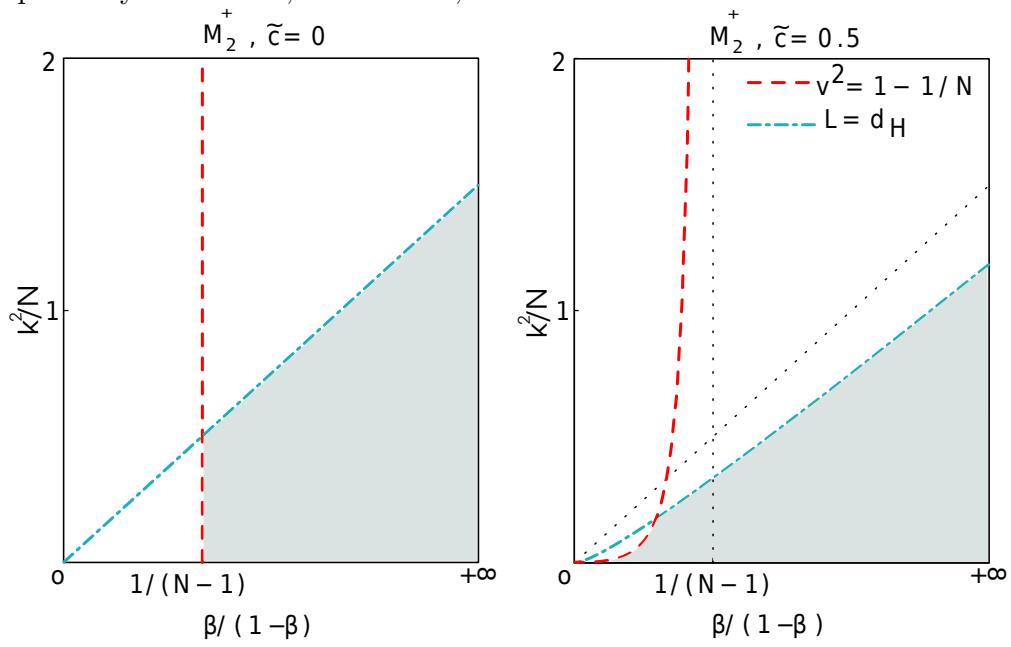

Figure 3.3: Range of values of the curvature parameter, k, for which domain wall networks are able to attain the linear scaling solution, as a function of $\frac{\beta}{1-\beta}$, for the M_2^+ model (grey area). The left and right panels represent the possible values of k^2/N, for $\tilde{c} = 0$ and $\tilde{c} = 0.5$, respectively. The dash-dotted (blue) lines correspond to $L = d_H$ and the dashed (red) lines correspond to $v^2 = 1 - \frac{1}{N}$.

In the case of cosmic string networks (with $p = 1$) in $N + 1$-dimensional backgrounds, linear scaling regimes are attainable in the absence of an energy-loss mechanism if

$$\beta \geqslant 1 - \frac{1}{N} \,. \tag{3.70}$$

This indicates that, if $N > 3$, these solutions are not attainable in radiation or matter-dominated eras. Despite the fact that, for $N > 3$, the probability of string interactions is expected to decrease over time (since, in this case, $p < (N-1)/2$), it is not clear that this process would lead to a vanishing energy-loss parameter: although the formation of cosmic string loops as a result of the collision of two strings is expected to be suppressed, it is not clear that the same would occur to loop formation due to string self-intersection. Note however that, if $\tilde{c} \neq 0$, even if it is very small, linear scaling solutions may be attainable for small values of the curvature parameter k (which correspond to networks with small-scale structure). These remarks are also valid to any branes with $p < (N-1)/2$: even though in this case $\tilde{c}$ is expected to be quite small, scale-invariant solutions might be possible for all values of β in the M_2^+ model ($0 < \beta < 1$).

3.3.2 Inflation and Superinflation

In the M_3^+ and M_1^- models, the expansion of the universe is accelerated with $\ddot{a} > 0$. The acceleration of the expansion hampers the velocity of the branes, and it is efficient enough to make these velocities arbitrarily small. In this case, Eq. (3.54) yields

$$\frac{dL}{dt} = HL \,, \qquad \text{so that} \qquad L \propto a \,. \tag{3.71}$$

Therefore, in these models, the network is conformally stretched. As a matter of fact, during this regime one has that

$$v \propto \frac{1}{Ha} \propto a^{-1-1/\beta} \to 0 \,. \tag{3.72}$$

The velocity then remains arbitrarily small, and consequently the stretching regime is able to persist in inflationary and superinflationary models.

Other question one might pose is whether or not a p-brane network is able to drive the acceleration of the universe. The Einstein equations for a $N + 1$-

dimensional FRW, in which the branes are the dominant component of the energy density, yield

$$\frac{\ddot{a}}{a} = -\frac{8\pi G_{N+1}}{N(N-1)}\left[(N-2)\bar{\rho} + N\bar{\mathcal{P}}\right], \tag{3.73}$$

$$\left(\frac{\dot{a}}{a}\right)^2 = \frac{16\pi G_{N+1}}{N(N-1)}\bar{\rho}, \tag{3.74}$$

where G_{N+1} is the $N+1$ dimensional Newton constant. These equations are a generalization of Eqs (1.10) and (1.12) for $N+1$-dimensional universes. Using this equations and Eqs. (3.46) and (3.42) one obtains

$$\beta = \frac{2}{N(1+w_p)} = \frac{2}{D+(p+1)\bar{v}^2}. \tag{3.75}$$

In order to accelerate the universe one needs $\beta > 1$ (or equivalently $w_p < w_c$) and, consequently

$$\bar{v}^2 < \frac{2-D}{p+1}. \tag{3.76}$$

We may then conclude that only domain walls ($D = N - p = 1$) are able to drive an inflationary phase. In the case of the domain wall dominated universe, the RMS velocity should then be such that

$$\bar{v}^2 < \frac{1}{N}, \tag{3.77}$$

if the universe is to accelerate.

3.3.3 Ultra-Relativistic Collapsing Solution

Consider the case of the M_2^- model which represents a collapsing universe with $0 < \beta < 1$. This model would admit linear scaling solutions, for $k < -\tilde{c}$. However, in this model, the comoving Hubble radius decreases with time. As a consequence, the curvature scale of the p-branes will necessarily become smaller than $\left|H^{-1}\right|$, and they will eventually freeze in comoving coordinates whilst travelling at the speed of light. The linear scaling regime would therefore never persist in the M_2^- model.

Though, in general, in the context of VOS models, the correlation length, L, may be identified with the physical distance travelled by a brane segment before encountering another segment of the same size, this identification breaks down in the ultrarelativistic limit [104, 105]. It follows from Eq. (3.53), that

$$L_{\rm ph} \sim \bar{\gamma}^{1/D}\, L\,, \tag{3.78}$$

where $\bar{\gamma} = (1-\bar{v}^2)^{-1/2}$. The fraction of the energy lost by the network due to interface collapse in a timescale dt may be estimated as

$$-\frac{d\bar{\rho}}{\bar{\rho}} = \frac{dL}{L} \sim \frac{v}{L_{\rm ph}}dt \sim \frac{v}{\bar{\gamma}^{1/D}L}dt\,. \tag{3.79}$$

In the ultrarelativistic limit, as $v \to 1$, we have that

$$\bar{\gamma} \propto a^{-(p+1)}\,. \tag{3.80}$$

Therefore, the efficiency of the energy-loss parameter is quickly driven towards zero, as the universe collapses:

$$\tilde{c} \propto \bar{\gamma}^{-1/D} \propto a^{(p+1)/D} \to 0\,. \tag{3.81}$$

Eq. (3.54) then yields

$$\dot{L} = \left(\frac{N+1}{N-p}\right) HL\,, \tag{3.82}$$

and, consequently,

$$L \propto a^{(N+1)/D}\,, \tag{3.83}$$

so that the physical lengthscale of the network freezes in comoving coordinates

$$L_{\rm ph} \propto a\,. \tag{3.84}$$

The network will then be conformally contracted, while moving at ultrarelativistic speeds. Notice that, since $\rho \propto L^{-D}$, we find that during this regime the brane density scales as

$$\rho \propto a^{-(N+1)}\,, \tag{3.85}$$

and thus, in this model, the p-brane network will asymptotically behave as a radiation component.

3.4 FRICTION DOMINATED REGIMES

The frictional force per unit of p-dimensional area exerted on a p-brane as a result particle scattering can be estimated as [98]:

$$\mathbf{F} \sim n\sigma_t v_T \Delta\mathbf{p} \tag{3.86}$$

where $n \propto a^{-N}$ is the particle density, $v_T \sim 1$ is the thermal velocity of the interacting particles, σ_t is the transport cross-section for the particle scattering and $\Delta\mathbf{p} \propto a^{-1}\mathbf{v}$ is the average momentum transferred per collision. Note that, we have assumed that the interacting particles are massless, and that brane motion is non-relativistic. As in the case of cosmic strings [125], the scattering cross-section of p-branes should depend only on the typical wavelength of the scattered particles, λ. On dimensional grounds, we may write:

$$\sigma_t \propto \lambda^{D-1}, \tag{3.87}$$

and, given the fact that $\lambda \propto a$, we have that

$$\mathbf{F} \propto a^{-(p+2)}\mathbf{v}\,. \tag{3.88}$$

Using Eq. (3.16), we find that the friction lengthscale scales as

$$\ell_f \propto a^{p+2}\,, \tag{3.89}$$

throughout the evolution of the network.

In Secs. 3.4.1 and 3.4.2, we will discuss the scaling regimes that arise during the friction dominated phase of the evolution of an expanding universe. The existence of the stretching and Kibble regimes for cosmic string networks was established in Ref. [4], using the VOS model for cosmic strings — although the existence of the latter was previously suggested by Kibble in Ref. [126]. The scaling laws for these regimes were derived for the case of domain walls in 3 spatial dimensions in Ref. [121], using a VOS model for domain walls derived using phenomenological arguments. In Sec. 3.4.3, we will then briefly discuss these regimes in the collapsing models.

3.4.1 Stretching Regime

If the density of p-branes is initially low, the characteristic lengthscale of the network will be close to the horizon, and, consequently, it will be much larger than the friction lengthscale. In this limit,

$$\frac{d\bar{v}}{dt} \ll \frac{\bar{v}}{\ell_f}\,, \quad \text{so that} \quad v \simeq k\frac{\ell_f}{L}\,. \tag{3.90}$$

Given the fact that $\ell_f \ll L$, we expect the p-branes to have very small velocities. In this limit,

$$\frac{dL}{dt} \simeq HL\,, \quad \text{so that} \quad L \propto a\,, \tag{3.91}$$

and the p-branes are conformally stretched.

Note, however, that, during this regime, the velocity scales as

$$\bar{v} \sim \frac{\ell_f}{L} \propto a^{p+1}\,. \tag{3.92}$$

Therefore, during thus regime, the velocity increases quickly, and consequently this regime is necessarily transient.

3.4.2 Kibble Regime

The Kibble regime emerges as the friction lengthscale approaches the characteristic lengthscale of the network ($\ell_f/L \sim HL$). Given the fact that, during this regime, the RMS velocity is higher than it has hitherto been, a considerable amount of energy will be lost due to brane interaction (in this case $HL \sim \tilde{c}\bar{v}$). As a result, even though the dynamics is still dominated by friction, the scaling laws are different from those of the stretching regimes:

$$L \propto \sqrt{\frac{\ell_f}{|H|}} \propto a^{\frac{1}{2\beta}[\beta(p+2)-1]} \tag{3.93}$$

$$\bar{v} \propto \sqrt{\ell_f\,|H|} \propto a^{\frac{1}{2\beta}[\beta(p+2)+1]} \tag{3.94}$$

This regime is also transient: as the universe expands, the friction lengthscale grows faster then L, and it will eventually overcome it (as a matter of fact, for $\beta < 1/(p+2)$, L decreases with time). At this point, friction becomes subdominant, thus bringing the Kibble regime to an end.

This regime is unavoidable. If the initial density of the network is high enough, the Kibble regime will occur right after the formation of the p-branes, and the network will not experience the stretching regime. If, on the other hand, the initial brane density is sufficiently low for the network to experience the stretching regime, the Kibble regime will follow it.

3.4.3 Friction-Dominated Regimes in Collapsing Universes

The scaling solutions given by Eqs. (3.91-3.94) also account for the dynamics of a p-brane network in collapsing universes during the friction dominated era. Note however that, in this case, the friction lengthscale decreases with time, and friction domination is the endpoint of the network's evolution: as ℓ_f decreases, the network comes to a standstill in comoving coordinates and, then, it is conformally contracted. In this regime, the average density of the network is given by $\rho \propto a^{-1}$.

As the universe contracts, the background temperature and density increase and approach those of the original brane-forming phase transition. At that point, the branes dissolve back into the high radiation background.

3.5 CONCLUSIONS

In this chapter, we have studied the evolution of p-brane networks, in flat expanding and collapsing homogeneous and isotropic backgrounds with an arbitrary number of spatial dimensions, using a Velocity-Dependent One-Scale Model. This model allows us to characterize the evolution of the network by following the cosmological evolution of its characteristic lengthscale and average root-mean-square velocity. We used this model to study the different scaling regimes that arise in collapsing and expanding universes, both on friction dominated and frictionless epochs. We particularly focused on the conditions that a p-brane network must satisfy in order for linear scaling regimes to be attainable.

This work is a significant improvement over previous analytical studies of domain wall dynamics (with $p = N-1$), unifying in a common framework the dynamics of domain wall networks in expanding/collapsing and frictionless/friction-dominated regimes. Notice also that, for $N = 3$ and $p = N - 1$, this model reproduces the VOS model for domain walls derived phenomenologically in Ref. [121], and thus confirms its validity. Moreover, this analytically-derived generalization provides an important tool to describe the evolution of domain wall networks in more than 3 spatial dimensions which, up to now, was restricted to very special configurations.

Our model provides a unified semi-analytic description of p-brane network dynamics, highlighting the common and distinctive features characterizing the evolution of p-brane networks of different dimensionality. In particular, it highlights the similarities between cosmic string and domain wall network evolution in $3+1$ dimensions, which may be of particular relevance for the study of cosmic superstrings.

4

Domain Walls and Dark Energy

Domain walls are often regarded as malignant objects in cosmology. As the universe expands, the background energy density decreases faster than the domain wall energy density, and consequently domain walls will eventually become the dominant energy component. In the case of cosmic strings, domination may be avoided due to the attainment of the linear scaling regime, which has the fortunate property that the string density remains constant relative to the background density. Domain wall networks also appear to evolve towards a scale-invariant solution, however, in this case

$$\frac{\bar{\rho}_\sigma}{\rho_b} \propto t\,, \tag{4.1}$$

where $\bar{\rho}_\sigma$ is the domain wall energy density. Therefore, domain wall domination seems unavoidable, even in the linear scaling regime.

Moreover, it has been pointed out in Ref. [127] that the gravitational effects of domain walls would introduce excessively large anisotropies in the cosmic microwave background, if they are originated at high-energy scales. However, if the walls are light enough (i.e., if they have a small surface tension), they may not dominate the energy density until the present time. In this case, the wall-forming phase transition should occur at an energy scale smaller than about $1\,\mathrm{MeV}$ ($\sigma \sim \eta^3 \lesssim (1\mathrm{MeV})^3$) — This is known as the Zel'dovich bound[1].

[1]Note however, the classical derivation of this bound involves the assumption that there is, roughly, one defect per Hubble volume. In many scenarios of interest, the number of defects per Hubble volume might be significantly larger and, in that case, domain wall tension should

Although domain walls are subject to this tight constraint, they may still play interesting cosmological roles. In particular, it has been suggested in Ref. [5] that a domain wall network could be a candidate for dark energy, provided that it is frozen by cosmological expansion. In this case the observed acceleration of the expansion of the universe would be a consequence of domain wall domination of the energy density of the universe. The conditions under which these frozen, or frustrated, networks might arise have been studied in detail in [6, 7, 128], and the results seem to rule out that scenario. Moreover, it has been argued in [129, 130] that if a bias is introduced — for example, if there exists a slight asymmetry between the minima of the potential of the model or if one of the vacua is, for some reason, favoured over the others — the domain wall network may be destabilized, and they may eventually decay. Biased domain wall networks may not only provide a way to evade the Zel'dovich bound, but are also behind the devaluation scenario [131], proposed as a possible solution to the Cosmological Constant Problem.

In this chapter, we will explore these possible connections between domain wall networks and dark energy. In order to analyse these paradigms, one needs to understand the dynamics of domain wall networks. We will, therefore, start by using the results of the previous chapters to outline the main features of their dynamics, in Sec. 4.1. We will then adapt the equations of motion for domain walls to these dark energy scenarios. In the case of frustrated networks, we will incorporate the dynamical effect of massive junctions in the Velocity-dependent One-scale model to study their potential role in frustration. Moreover, we will develop an analytical model for biased domain walls, in order to analyse the devaluation scenario.

4.1 DOMAIN WALL DYNAMICS

In this section, we will briefly discuss domain wall dynamics, using the results of the previous chapters. Let us start by considering the case of a thin domain wall in a $3+1$ dimensional FRW universe. Using Eq. (2.107), we find that the evolution equation for its velocityis given by

$$\frac{dv}{dt} = (1-v^2)\left[\frac{f(v)}{R_i} - 3Hv\right], \tag{4.2}$$

where $f(v) = 2\gamma^{1/2}s$, for spherically symmetric domain walls ($p = 2$ and $i = 0$), or $f(v) = \gamma s$, for a domain wall with cylindrical symmetry ($p = 2$ and $i = 1$). For a spherically symmetric domain wall, the invariant radius is defined as

be subjected to even more stringent bounds.

$R_0 = |q|\,\gamma^{1/2}a$, and its evolution is described by an evolution equation of the form (see Eq. (2.108))

$$\frac{dR_0}{dt} = \left(1 - \frac{3}{2}v^2\right) HR_0\,. \tag{4.3}$$

As to the case of domain walls with cylindrical symmetry, the invariant radius is defined as $R_1 = |q|\,\gamma a$, and satisfies the following equation of motion:

$$\frac{dR_1}{dt} = \left(1 - 3v^2\right) HR_1\,. \tag{4.4}$$

Let us now move to the case of the (averaged) evolution equation for a domain wall network in a $3+1$ dimensional FRW universe. These equations are written in terms of the characteristic length, which in this case is defined as

$$\bar{\rho}_\sigma \equiv \frac{\sigma}{L}\,, \tag{4.5}$$

and in terms of the RMS velocity of the network, $\bar{v}$. In this case, Eqs. (3.54) and (3.57) yield, respectively

$$\frac{dL}{dt} = HL(1 + 3\bar{v}^2) + \frac{L}{\ell_f}\bar{v}^2 + \tilde{c}\bar{v}\,, \tag{4.6}$$

$$\frac{d\bar{v}}{dt} = (1 - \bar{v}^2)\left(\frac{k}{L} - 3H\bar{v} - \frac{\bar{v}}{\ell_f}\right)\,. \tag{4.7}$$

These equations are in agreement with the phenomenological VOS model for domain wall networks developed in Ref. [121].

Let us ignore the both network's energy losses and the frictional forces due to particle scattering. When comparing Eqs. (4.2) and (4.7), we find that, even though v and $\bar{v}$, are defined differently, the matching between their evolution equation is closer than one might naively expect. As a matter of fact, they differ only in the form of the phenomenological curvature term. However, when contrasting Eqs. (4.3) and (4.4) with Eq. (4.7), the discrepancies appear significant. Note, however, that these differences arise from the fact that R_0 (or R_1) and L are defined very differently.

Consider the case of a spherically symmetric domain wall. Its physical radius is defined in such a way that the energy of the defect is proportional to R_0^2.

When considering a network, however, the characteristic length is such that $L = \sigma V/E$, and thus the evolution equations for these two variables are not even comparable. Instead, in order to compare these two equations, we can define an effective characteristic lengthscale proportional to the squared root of the network's energy:

$$E = \bar{\rho} V = \sigma L_{\rm eff}^2 \,, \tag{4.8}$$

so that

$$L_{\rm eff} \propto \frac{a^{3/2}}{L^{1/2}} \,. \tag{4.9}$$

Introducing Eq. (4.9) into Eq. (4.6), we find a sugestive

$$\frac{dL_{\rm eff}}{dt} = \left(1 - \frac{3}{2}\bar{v}^2\right) H L_{\rm eff} \,, \tag{4.10}$$

which scales precisely as R_1. This expression highlights the fact that the differences between Eqs. (4.3) and (4.7) are mainly apparent

Bearing in mind that, in the case of a domain wall with cylindrical symmetry, R_1 is proportional to the energy per unit length of the defect, an equivalent definition would be

$$L \propto \frac{a^2}{L_{\rm eff}} \,. \tag{4.11}$$

We then have that, in this case,

$$\frac{dL_{\rm eff}}{dt} = (1 - 3\bar{v}^2) H L_{\rm eff} \,, \tag{4.12}$$

which is in agreement with Eq. (4.4), indeed.

4.2 DOMAIN WALL NETWORKS WITH MASSIVE JUNCTIONS AND DARK ENERGY

As discussed in the previous chapter, a domain wall dominated universe could undergo accelerated expansion, provided that the RMS velocity of the network is small enough. It is then natural to enquire if domain wall networks could play the role of dark energy. Recall that the equation-of-state parameter of a domain wall network is, on average, given by:

$$w^2 = \bar{v}^2 - \frac{2}{3} \,. \tag{4.13}$$

It is evident, given the observational constraints in Eq. (1.52), that domain wall networks cannot be the unique contributor to the dark energy budget. However, if the RMS velocity is very small — so that the network is frozen in comoving coordinates — it is able to provide a negative pressure: at most $w = -2/3$ In this case, the domain wall network is said to be frustrated and it may, in principle, give a significant contribution to dark energy. These frustrated domain wall networks were suggested as a candidate for dark energy in Refs. [5, 49].

The conditions under which a domain wall network is able to frustrate were extensively studied in Refs. [6, 132, 7, 8]. If frustrated domain wall networks are to provide a significant contribution to the dark energy budget, they have to satisfy two main requirements:

1. The energy density must be of the same order as the critical density in the present:
$$\bar{\rho}_\sigma = \frac{\sigma}{L} \sim \rho_c \,. \tag{4.14}$$

2. Fluctuations generated by domain walls have to be smaller than 10^{-5} on scales of the order of the Hubble radius, H_0^{-1}, or otherwise they would generate strong (unobserved) signatures on the cosmic microwave background[2].

These two conditions are sufficient to exclude standard domain wall networks as a potential dark energy source. It has been shown in Ref. [6], using a VOS model for domain walls, that these conditions can only be satisfied by frustrated domain wall networks if the curvature parameter is very small ($k \ll 1$). Standard domain wall networks without junctions have a curvature parameter that is, in general, close to unity, $k \sim 1$, and therefore they can ruled out as a dark energy candidates.

The inclusion of junctions in domain wall networks severely increases the complexity of the problem. In this case, the possible lattice configurations depend on energetic, geometrical and topological considerations, and their stability depends both on local and global considerations. The conditions under which 2-dimensional domain wall networks with junctions are able to frustrate have been studied in detail in Ref. [6], and several stability factors have been identified. First of all, it has been shown that domain with less than 6 edges are unstable if only Y-type junctions — where 3 domain walls meet — exist. The authors have

[2]This is a conservative estimate: according to [8], the CMB observational data limits these fluctuations to 10^{-5} down to smaller scales of approximately $H_0^{-1}/100$.

further shown that if the average dimensionality of the junctions is increased, the average number of edges per domain decreases, also leading to the formation of unstable domains. Another factor of instability would be the presence of an hierarchy of tensions: domain walls with higher tension tend to collapse, leading to the increase of the dimensionality of the junctions. On the other hand, the authors found that the probability of annihilation of two nearby triple junctions decreases as the number of vacua increases. In fact, in models with more than two vacua connected by domain walls of the same tension, only stable Y-type junctions would form. Note that the only possible equilibrium configuration with triple wall junctions is an hexagonal "honeycomb" lattice. Although this lattice configuration seems to be stable, it is not expected to arise in realistic wall-forming phase transitions nor to be the result of the evolution of a realistic network. As matter of fact, very small curvature parameters ($k \ll 1$) are only expected in very special configurations — such as the hexagonal lattice, square lattices with X-type junctions and triangular lattices with *-type junctions — corresponding to very specific initial conditions which would violate causality if they were to extend over scales larger than the particle horizon. This realization lead the authors to conjecture that frustrated domain walls networks are not expected to arise naturally from realistic phase transitions.

These results were tested numerically, using 2 and 3-dimensional high-resolution field theory simulations [7, 132, 8]. In order to do so, the authors not only used some pre-existing domain wall models, but have also developed an "ideal model", which has maximal probability of evolving towards frustration. This ideal model has a large number of vacua connected by domain walls of equal tension, so that the major sources of instability are removed (for a specific realization see [7]). The use of this model then allowed the authors to avoid testing the large variety of domain walls field-theory models existent in the literature. The results of these simulation seem to confirm the *no-frustration conjecture*, even in the case of the ideal model: the dynamical behaviour of the networks did not show any evidence of evolving towards frustration, but instead it was consistent with the attainment of a scaling solution. These results seem then to conclusively rule out frustrated domain wall networks as dark energy candidates.

In these studies, the contributions of the domain wall junctions to the energy density were assumed to be very small. However, massive monopole-type junctions can effectively freeze a domain wall network, provided that they are heavy enough. In that case, their contribution to the energy budget could not be neglected, and it has been argued in Refs. [6, 8] that it would lead to an

equation-of-state parameter even greater than $-2/3$, which is incompatible with the observational bounds. In this section, we investigate the impact of string and monopole-type junctions on the dynamics of domain wall networks. However, accounting for the detailed contribution of the junctions on domain wall networks is not a trivial task. The VOS model for domain wall networks does not take into account the dynamical contributions of junctions. Moreover, the standard PRS algorithm — implemented in all field theory numerical simulations in order to ensure fixed comoving resolution — increases artificially the impact of junctions on the overall dynamics during the course of the simulations. This effect is not very important for the light junctions which are usually considered in such simulations, but it could be relevant in the case of heavy junctions. In order to overcome these problems, we develop a semi-analytical non-relativistic VOS model for the evolution of the characteristic length and velocity of domain wall networks that incorporates the contribution of string and monopole-type junctions in the overall dynamics. We, then, analyse the conditions under which massive monopole-type junctions are able to frustrate the domain wall network and determine whether or not such a frustrated network could account for a significant fraction of the Dark Energy of the Universe. In order to do so, we will consider the best possible scenario as far as frustration is concerned, assuming that the junctions are massive enough to render the network non-relativistic. This work was published in [12].

4.2.1 Non-relativistic VOS model with massive junctions

Consider the configuration represented in figure 4.1 where four junctions of energy per unit length μ are connected by four planar domain walls of energy per unit length σ, defining a square domain of characteristic size l. Three domain walls meet at each (Y-type) string junction. Here we assume that nothing varies along the direction perpendicular to the square domain, so that the infinite string junctions have no curvature. In this case, the domain wall dynamics is effectively two-dimensional. The energy per unit length of this configuration is given by the sum of the contributions from the four domain walls, moving with velocity v, the four cosmic string, moving with velocity $v_\mu = \sqrt{2}v$, and from the four static domain walls:

$$E = 4\sigma\gamma l + 4\mu\gamma_\mu + 2\sigma\sqrt{2}(l_0 - l)\,, \tag{4.15}$$

where we defined $\gamma = (1 - v^2)^{-1/2}$, $\gamma_\mu = (1 - v_\mu^2)^{-1/2}$, and $v = -(dl/dt)/2$.

For simplicity, we shall make the approximation that the shape is maintained

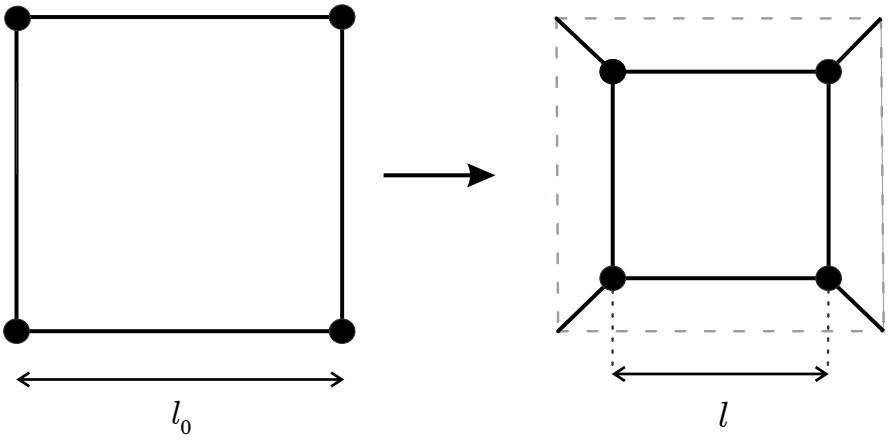

Figure 4.1: The left panel represents the 2-dimensional domain wall configuration prior to collapse. Solid lines represent domain walls of superficial tension σ and the dots represent string junctions of tension μ. The right panel represents the configuration after some time has elapsed.

during the collapse of the square domain. In this case, the domain walls do not acquire curvature, and it remains concentrated in the vertices. Although we expect the domain walls to acquire curvature in the course of collapse, this approximation will capture the relevant physics, and does not affect our main results. It then follows from energy conservation that, in Minkowski spacetime, the equation of motion for v is given by

$$\frac{dv}{dt} + (1-v^2)\frac{s(v)}{l}\left(\frac{1}{1+\frac{\mu}{\sigma l}g(v)}\right) = 0\,, \tag{4.16}$$

where

$$s(v) = 2 - \frac{\sqrt{2}}{\gamma}\,, \tag{4.17}$$

and

$$g(v) = \left(\frac{\gamma_\mu}{\gamma}\right)^3\,. \tag{4.18}$$

The physical meaning of Eq. (4.16), can be summarized very briefly:

1. Domain Walls are accelerated due to the curvature which, in this particular configuration, remains concentrated at the vertices;

2. The acceleration of the domain walls can be reduced due to the inertia of the cosmic string junctions, which are connected to the domain walls.

Note that Eq. (4.16) does not apply directly to the case of the domain wall network with string junctions, since it has been obtained for a very particular

configuration. Albeit, we shall use it as a guide into the fundamental aspects of the networks' dynamics.

The characteristic lengths of the two-dimensional domain wall network and of the string-type junctions, L_σ and L_μ, are defined as

$$\bar{\rho}_\sigma = \frac{\sigma}{L_\sigma} \quad \text{and} \quad \bar{\rho}_\mu = \frac{\mu}{L_\mu^2}\,, \tag{4.19}$$

where $\bar{\rho}_\sigma$ and $\bar{\rho}_\mu$ represent the average density of domain walls and the average density of cosmic string junctions, respectively. The relation between L_μ and L_σ depends on the geometrical properties of the domain wall network. For a regular hexagonal lattice with Y-type junctions, each string junction is shared by three hexagons, and thus $L_\mu/L_\sigma = 3^{1/4}/2^{1/2}$. Similar arguments can be used to show that, for a regular square lattice with X-type junctions, $L_\mu/L_\sigma = 2$, while $L_\mu/L_\sigma = 3^{3/4}$ for a regular triangular lattice with $*$-type junctions. We see that, in general the characteristic lengths are similar ($L_\mu/L_\sigma \sim 1$) and, consequently, we shall assume that $L_\mu = L_\sigma = L$.

Identifying l with $L/2$ in Eq. (4.16), we find that, in the non-relativistic limit,

$$\frac{d\bar{v}}{dt} + \frac{k}{L}\left(\frac{1}{1+\frac{\mu}{\sigma L}}\right) = 0. \tag{4.20}$$

with $k = 2s(0) = 1 - \sqrt{2}/2$. This equation preserves the generic form of the acceleration term contained in Eq. (4.16). If we include the accurate damping term caused by Hubble expansion, it should provide an approximate description (up to numerical factors of order unity) of the evolution of the characteristic velocity of a non-relativistic domain wall network with junctions in 2 spatial dimensions. Note, however, that in the case of the network, the curvature parameter represents an average over the whole network rather than the specific configuration represented in Figure 4.1, as in Eq. (3.58). Also, maintaining the notation of the previous chapter, we use bars to represent RMS averaged quantities, so that $\bar{v}$ represents the RMS velocity of the domain wall network, and so on.

Note that

$$\frac{1}{1+\frac{\mu}{\sigma L}} = \frac{\frac{\sigma}{L}}{\frac{\sigma}{L}+\frac{\mu}{L^2}} = \frac{\bar{\rho}_\sigma}{\bar{\rho}} = f_\sigma\,, \tag{4.21}$$

where $\bar{\rho} = \bar{\rho}_\sigma + \bar{\rho}_\mu$ is the total energy density and $f_\sigma = \frac{\bar{\rho}_\sigma}{\bar{\rho}}$ is the fraction of energy density which is due to domain walls. This allows us to rewrite eq (4.20)

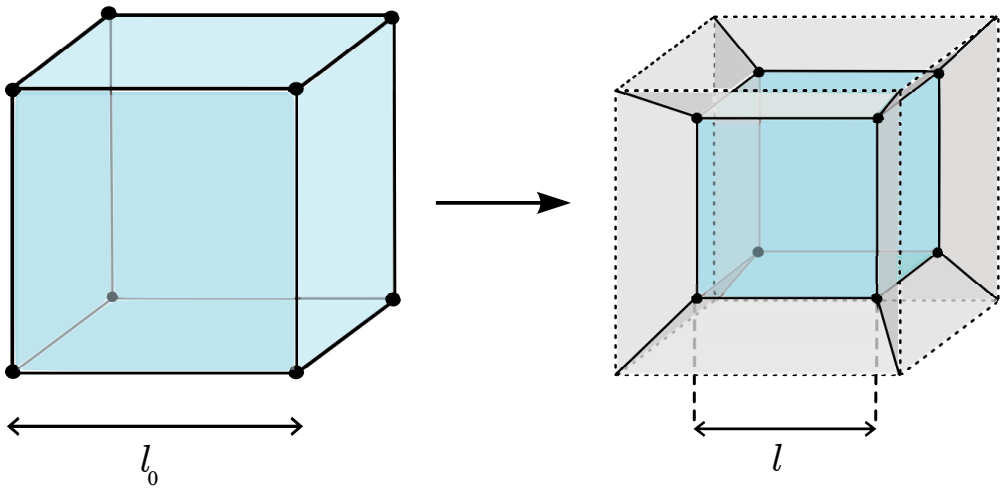

Figure 4.2: The left panel represents the 3-dimensional domain wall configuration prior to collapse. The planes represent domain walls with a superficial tension σ, solid lines represent string junction of tension μ, and the dots represent monopole-type junctions of mass m. The right panel represents the configuration after some time has elapsed.

as:

$$\frac{d\bar{v}}{dt} + \frac{k}{L} f_\sigma = 0\,. \tag{4.22}$$

Given this equation, the generalization to the 3 dimensional case is trivial. In three spatial dimensions, domain walls meet at string junctions, which may, in turn, intersect at monopole junction (see [8] and references therein for details on specific field theory models and network realizations). In this case, we need to consider the impact of monopole-type junctions, of mass m and energy density

$$\bar{\rho}_m = \frac{m}{L_m^3} \tag{4.23}$$

on the network dynamics. One may suspect that, in this case, both domain walls and cosmic strings contribute to the acceleration of the network, and that this acceleration is damped by the monopoles. So, we may infer that the evolution equation for the velocity should be of the same form as Eq. (4.22) but with $f_\sigma \leftrightarrow f_\sigma + f_\mu$. To verify that this is indeed the case, let us consider a cubic configuration as represented in Fig. 4.2, and assume that, as in the case of the 2-dimensional network, the curvature is concentrated at the vertices, so that the domain walls and string junctions do not acquire curvature during collapse.

The energy of this configuration is given by

$$E = 6\sigma l^2\gamma + 12\mu\gamma_\mu l + 8\gamma_m m + 3\sqrt{2}\sigma(l_0^2 - l^2) + 4\sqrt{3}(l_0 - l)\,, \tag{4.24}$$

where $v_\mu = \sqrt{2}v$ is the velocity of the cosmic string junctions, $v_m = \sqrt{3}v$ is the velocity of the monopole junctions, $\gamma_\mu = (1 - v_\mu^2)^{-1/2}$, $\gamma_m = (1 - v_m^2)^{-1/2}$ and $dl/dt = -2v_\mu = -2\sqrt{2}v$.

Energy conservation, in this case, yields

$$\frac{dv}{dt}\left[\sigma l^2 + 4\mu l\left(\frac{\gamma_\mu}{\gamma}\right)^3 + 4m\left(\frac{\gamma_m}{\gamma}\right)^3\right] + (1 - v^2)\left[4s_\sigma(v)\sigma l + 8s_\mu(v)\mu\right] = 0\,. \tag{4.25}$$

As in the case of the 2-dimensional network, we will use this equation to infer the general form of the curvature term. In the non-relativistic limit, we may identify l with $L/4$ to obtain

$$\frac{d\bar{v}}{dt} + \frac{k}{L}\frac{1}{1 + \frac{m}{\sigma L + \mu L^2}}\,, \tag{4.26}$$

up to coefficients of order unity. It is straightforward to show that this equation is equivalent to:

$$\frac{d\bar{v}}{dt} + \frac{k}{L}\left(f_\sigma + f_\mu\right) = 0\,, \tag{4.27}$$

with $L = L_m = L_\mu = L_\sigma$. Here we introduced the energy density fractions of the various components, defined as

$$f_\sigma = \frac{\bar{\rho}_\sigma}{\bar{\rho}} = \frac{1}{1 + \frac{m}{\sigma L^2} + \frac{\mu}{\sigma L}}\,, \tag{4.28}$$

$$f_\mu = \frac{\bar{\rho}_\mu}{\bar{\rho}} = \frac{1}{1 + \frac{m}{\mu L} + \frac{\sigma L}{\mu}}\,, \tag{4.29}$$

$$f_m = \frac{\bar{\rho}_m}{\bar{\rho}} = \frac{1}{1 + \frac{\mu L}{m} + \frac{\sigma L^2}{m}}\,, \tag{4.30}$$

where $\bar{\rho} = \bar{\rho}_\sigma + \bar{\rho}_\mu + \bar{\rho}_m$.

We have implicitly assumed that the energy of the domain walls, as well as that of string and monopole junctions, is localized. This is not always a good approximation. For example, in the case of global monopoles, there is a nearly constant long-range force between monopoles and anti-monopoles, which is rele-

vant to the dynamics[3]. In Ref. [134], local and global hybrid networks of cosmic strings and monopoles were studied. The author has shown that the forces between monopoles and anti-monopoles lead to the annihilation of the network shortly after creation (though in some particular cases the network can, in fact, be relatively long-lived). It is reasonable to expect that, in the case of a domain wall network with string-type and monopole-type junctions, the long-range forces between monopole and anti-monopole would also lead to the annihilation of the network. Note, however, that this particular model is developed with the specific purpose of investigating whether the inertia caused by the presence of massive junctions is sufficient to frustrate a domain wall network, and if such a network could contribute to the acceleration of the universe. Since such long-range forces would constitute an additional obstacle to the frustration of the domain wall network, and maintaining the best case scenario premise, we will not consider them. Nevertheless, by considering non-standard kinetic terms, it is possible to localize the energy of the monopoles inside their core [123]. These localized k-monopoles interact very little, if they are sufficiently distant from one another, and hence they are not expected to lead to the rapid annihilation of the network.

Given the fact that we intend to describe these networks in a cosmological context, we also need to account for the deceleration caused by the Hubble expansion. Recall that (planar) domain walls, (planar) cosmic strings and monopoles behave differently under Hubble expansion:

$$\gamma\, v \propto a^{-3} \quad \Leftrightarrow \quad \frac{dv}{dt} + 3vH(1-v^2) = 0\,, \tag{4.31}$$

$$\gamma_\mu v_\mu \propto a^{-2} \quad \Leftrightarrow \quad \frac{dv_\mu}{dt} + 2v_\mu H(1-v_\mu^2) = 0\,, \tag{4.32}$$

$$\gamma_m v_m \propto a^{-1} \quad \Leftrightarrow \quad \frac{dv_m}{dt} + v_m H(1-v_m^2) = 0\,, \tag{4.33}$$

for domain walls, cosmic strings and point masses respectively. The behaviour of the domain wall network with massive junctions under expansion will be determined at any time by the current dominant component of the energy density. Therefore, we use the energy density fractions as weight factors in the estimate of the Hubble damping term to be added to Eq. (4.27). The equation describing the evolution of the characteristic velocity of the network then becomes, in the non-relativistic limit,

[3]See, for example, [133] and references therein

$$\frac{d\bar{v}}{dt} + H\bar{v}(1 + f_\mu + 2f_\sigma) + \frac{k}{L}\left(\frac{1}{1 + \frac{m}{\mu L + \sigma L^2}}\right) = 0\,, \tag{4.34}$$

where $1 + f_\mu + 2f_\sigma = f_m + 2f_\mu + 3f_\sigma$, and we have assumed that $\bar{v} = \bar{v}_\mu = \bar{v}_m$ (we will justify this assumption later in this section).

Let us now derive a evolution equation for the characteristic lengthscale, L. Cosmological expansion also has different impacts on the energy density of domain walls, string and monopole-type junctions. In the absence of energy-loss mechanisms,

$$\bar{\rho}_\sigma \propto \bar{\gamma} a^{-1} \quad \Leftrightarrow \quad \frac{d\bar{\rho}_\sigma}{dt} + H(1 + 3\bar{v}^2)\bar{\rho}_\sigma = 0\,, \tag{4.35}$$

$$\bar{\rho}_\mu \propto \bar{\gamma}_\mu a^{-2} \quad \Leftrightarrow \quad \frac{d\bar{\rho}_\mu}{dt} + 2(1 + \bar{v}_\mu^2)H\bar{\rho}_\mu = 0\,, \tag{4.36}$$

$$\bar{\rho}_m \propto \bar{\gamma}_m a^{-3} \quad \Leftrightarrow \quad \frac{d\bar{\rho}_m}{dt} + 3\left(1 + \frac{\bar{v}_m^2}{3}\right)H\bar{\rho}_m = 0\,, \tag{4.37}$$

for domain walls, cosmic strings and point masses, respectively. In the course of network evolution, energy will be exchanged between the different components, leading to similar characteristic velocities: $\bar{v}_m \sim \bar{v}_\mu \sim \bar{v}$. Let Q_X be the energy transferred per unit of time and volume from the component X to the other two components. To account for the energy transfer between the different components, one needs to include extra terms Q_σ, Q_μ and Q_m on the right-hand side of Eqs. (4.35-4.37), respectively.

Taking into account that

$$Q_\sigma + Q_\mu + Q_m = 0\,, \tag{4.38}$$

and that

$$\frac{d\bar{\rho}}{dt} = \frac{d\bar{\rho}_\sigma}{dt} + \frac{d\bar{\rho}_\mu}{dt} + \frac{d\bar{\rho}_m}{dt}\,, \tag{4.39}$$

the energy transfer terms cancel out when considering the evolution of the total energy density:

$$\frac{d\bar{\rho}}{dt} + \left[(3 - f_\mu - 2f_\sigma) + \bar{v}^2\,(1 + f_\mu + 2f_\sigma)\right] H\bar{\rho} = 0\,. \tag{4.40}$$

We could add a term proportional to $v\bar{\rho}/L$ to right-hand side of Eq. (4.40), in order to account for any energy losses by the network. Note, however, that in

the non-relativistic limit, this term can be neglected. In any case, it is easy to verify that this term leads to a larger L and, consequently, it is prejudicial to frustration. Again, we will be considering the best case scenario for frustration: the absence of any energy loss mechanisms.

Using Eqs (4.19) and (4.23), we then obtain the evolution equation for the lengthscale of the network

$$\frac{dL}{dt} = \left[1 + \bar{v}^2 \frac{2f_\sigma + f_\mu + 1}{3 - f_\mu - 2f_\sigma}\right] HL\,. \tag{4.41}$$

In the non-relativistic regime, with $\bar{v} \ll 1$, one has that

$$\frac{dL}{dt} = HL\,, \quad \text{so that} \quad L \propto a\,, \tag{4.42}$$

and

$$\bar{\rho}_m \propto a^{-3}\,, \quad \bar{\rho}_\mu \propto a^{-2} \quad \text{and} \quad \bar{\rho}_\sigma \propto a^{-1}\,. \tag{4.43}$$

Note that the energy density of domain walls decays more slowly than that of cosmic strings and of monopoles. Therefore, even if at early times the energy density of monopoles is dominant, the domain walls will eventually overcome their domination and become the most significant part of the energy density. They will, then, necessarily determine the late time evolution of the network.

Note that Eqs (4.34) and (4.41) reduce to the standard non-relativistic VOS equations of motion (Eqs. (3.6) and (3.7)), if we set $\bar{\rho}_\sigma = \bar{\rho}_m = 0$, assuming there are no energy losses. On the other hand, if we set $\bar{\rho}_\mu = \bar{\rho}_m = 0$, we also recover the standard non-relativistic VOS equations form domain wall networks.

4.2.2 Implications for dark energy

The main aim of this subsection is to investigate the conditions under which massive monopole-type junctions are able to frustrate a domain wall network and to determine whether or not such a frustrated domain network could account for a significant fraction of the energy density of the universe. We shall work with the best possible scenario and assume that the domain wall network is effectively frustrated ($v \ll 1$) and, consequently, it will be sufficient to consider the non-relativistic regime. We shall also assume that $\bar{\rho}_m$ is always much greater than either $\bar{\rho}_\sigma$ or $\bar{\rho}_\mu$ up to the present day, in order to maximize the impact of the massive junctions on the dynamics of the domain wall network. Relaxing these assumptions, would make this mechanism less efficient from the point of view of frustration.

Solving Eq. (4.34) in the matter dominated era, assuming that $\bar{\rho}_\mu = 0$ and $\bar{\rho}_m \gg \bar{\rho}_\sigma$ and neglecting the decaying mode, one obtains

$$H\bar{v} \sim \frac{2}{5}\frac{d\bar{v}}{dt} = \frac{2}{7}\frac{k_0}{L}\frac{\bar{\rho}_\sigma}{\bar{\rho}_m}\,. \tag{4.44}$$

A similar analysis for $\bar{\rho}_\sigma = 0$ and $\bar{\rho}_m \gg \bar{\rho}_\mu$ would give

$$H\bar{v} \sim \frac{2}{3}\frac{d\bar{v}}{dt} = \frac{2}{5}\frac{k_0}{L}\frac{\bar{\rho}_\mu}{\bar{\rho}_m}\,. \tag{4.45}$$

In both limits one has

$$\bar{v}^2 \lesssim HL\bar{v} \sim k_0\frac{\bar{\rho}_\sigma + \bar{\rho}_\mu}{\bar{\rho}_m}\,, \tag{4.46}$$

where we have taken into account that $\bar{v} \lesssim LH$ due to the fact that the characteristic velocity, $\bar{v}$, does not change abruptly. The result given in Eq. (4.46) is rather robust and has a simple physical interpretation. For non-relativistic domain wall or string networks with junctions one has $\bar{v}^2 \lesssim k$. In the case of a network with a dominant component of monopole-type junctions, only a fraction of the kinetic energy (approximately $(\bar{\rho}_\sigma + \bar{\rho}_\mu)/\bar{\rho}_m$) generated due to the curvature is transferred to the domain walls and strings, due to the large inertia of the monopole-type junctions.

The amplitude of the fractional energy density fluctuations, δ, associated with domain walls on a physical scale, L_V, much larger than the characteristic scale, L, of a domain wall network is given approximately by

$$\delta \equiv \frac{\delta\bar{\rho}_\sigma}{\rho_c} \sim \frac{\Omega_\sigma}{\sqrt{N}}\,, \tag{4.47}$$

where $N \sim (L_V/L)^3$ is the number of domain walls on a volume $V = L_V^3$, $\Omega_\sigma = \bar{\rho}_\sigma/\rho_c$, and $\delta\bar{\rho}_\sigma$ is the root mean square fluctuation in the domain wall energy density on a given scale L_V. Recall that the amplitude of CMB temperature fluctuations generated by domain walls, around the present time is contrained to be smaller than 10^{-5} down to scales of the order of $L_V = H_0^{-1}$. This implies that

$$\delta \sim \Omega_{\sigma 0}(H_0 L_0)^{3/2} \lesssim 10^{-5}\,. \tag{4.48}$$

Consequently, we should have that

$$H_0 L_0 \lesssim 10^{-3}\Omega_{\sigma 0}^{-2/3}\,, \tag{4.49}$$

which results in the constraint $L_0 \lesssim \Omega_{\sigma 0}^{-2/3}$Mpc. If there are no abrupt changes on the domain wall velocity, this also translates into a stringent limit on the

characteristic velocity of the domain walls at the present time:

$$\bar{v}_0 \lesssim H_0 L_0 \lesssim \Omega_{\sigma 0}^{-2/3} 10^{-3} \,. \tag{4.50}$$

Hence, using Eq. (4.46) with $k_0 \sim 1$ one obtains

$$k \frac{\bar{\rho}_{\sigma 0} + \bar{\rho}_{\mu 0}}{\bar{\rho}_{m0}} \sim (H_0 L_0)^2 \lesssim \Omega_{\sigma 0}^{-4/3} 10^{-6} \,. \tag{4.51}$$

The value of the curvature parameter has been estimated using high-resolution numerical simulations of domain wall evolution [8]. As previously pointed out, these simulations indicate that standard domain wall networks without junctions $k \sim 1$, while for networks with junctions smaller values have been observed, but still of order unity. A value of $k \ll 1$ is only expected in the case of unnatural configurations which cannot be expected from realistic phase transition (e.g. the previously discussed 2-dimensional "honeycomb" lattice). Consequently, we shall assume that $k \sim 1$.

Note that domain walls would need to have an average energy density of the order of the critical density to provide a significant contribution to the dark energy, so we shall assume that $\Omega_{\sigma 0} \sim 1$. Therefore, a sucessful domain wall scenario for dark energy would require that

$$L_0 \lesssim 1\,\mathrm{Mpc} \,, \qquad \text{and} \qquad \bar{v}_0 \lesssim 10^{-3} \,. \tag{4.52}$$

Using Eq. (4.51), we see that these values can only be achieved if

$$\frac{\bar{\rho}_{\sigma 0}}{\bar{\rho}_{m0}} \lesssim 10^{-6} \,, \tag{4.53}$$

and, therefore, the energy density of the junctions would have to be 6 orders of magnitude larger than the critical density[4]. Such high value is clearly in complete disagreement with all cosmological evidence. Clearly, if $\Omega_{\sigma 0}$ is very small, frustration may effectively occur but in that case domain walls would not play a relevant role as a dark energy component.

4.2.3 General Considerations on the Frustration of p-Brane Networks

In this section, we will consider the effect of a generic interaction mechanism between p-branes and other cosmological component on the dynamics of p-brane networks, in order to study their potential role in frustration. This work was published in [16].

[4] If one was to limit the CMB fluctuations generated by domain walls to be smaller than 10^{-5} down to smaller scales of $H_0^{-1}/100$, a stronger result would be obtained.

As discussed previously, analytical and numerical studies indicate that domain wall evolution does not result naturally in the frustration of the network. Frustration would, then, require the presence of an additional mechanism to decelerate the domain walls. Note however that the relevant question is not whether or not there are mechanisms that can frustrate the network — for instance, massive junctions or the mechanism described in [135, 136] clearly do the job — but whether or not this frustrated network could contribute to the dark energy budget. In order to address this question, let us consider the case of a p-brane network and let us assume an interaction mechanism between the p-branes and a component average density $\rho_{\rm int}$ exists. A very conservative upper limit to the total momentum per unit volume transferred from that component to the p-branes in one Hubble time,

$$\left|\frac{d\mathbf{p}}{dV}\right| \sim \frac{\bar{\rho}}{H}\left|\frac{d\bar{v}}{dt}\right|_{\rm int}\,, \tag{4.54}$$

would be $\rho_{\rm int}$. In this case, we should have that

$$\left|\frac{d\bar{v}}{dt}\right|_{\rm int} \lesssim \chi H\,, \tag{4.55}$$

with $\chi = \rho_{\rm int}/\rho$. The effects of this interaction mechanism on the network dynamics may then be included in Eqs. (3.57) and (3.54) by redefining the damping length:

$$\frac{1}{\ell_d} = (p+\chi+1)\,H + \frac{1}{\ell_f}\,, \tag{4.56}$$

where we have assume that the efficiency of interaction mechanism is the maximum possible: $|d\bar{v}/dt|_{\rm int} = \chi H$.

In homogeneous and isotropic universes with a decelerating power-law expansion, in the frictionless regime ($\ell_f \ll H^{-1}$), a p-brane network may admit linear scaling solution of the form of Eq. (3.62) if χ is constant. In this case,

$$\xi = \sqrt{\left|\frac{k(k+\tilde{c})}{\beta(1-\beta)D(p+\chi+1)}\right|} \qquad \text{and} \qquad \bar{v} = \sqrt{\frac{(1-\beta)kD}{\beta(k+\tilde{c})(p+\chi+1)}}\,. \tag{4.57}$$

Therefore, this interaction mechanism may decelerate the branes slightly. However, if the interacting component of the energy density is subdominant (that is, if $\chi \lesssim 1$), its potential role on the frustration of the networks — characterized by $L \ll H^{-1}$ and $v \ll 1$ — is very limited. Relaxing the assumption

that the p-brane network is the dominant energy component may clearly help frustration: if $\rho_{\rm int} \gg \rho$ ($\chi \gg 1$), the interaction mechanism may decelerate the branes effectively, and freeze the network in comoving coordinates. However, in this case, $\rho_{\rm int}$ would be the main contributor to the energy budget.

Clearly, assuming that χ is time independent is unrealistic: one would expect the expansion of the background to affect the efficiency of any realistic interaction mechanism (for instance, the ratio $\chi = \rho_{\rm int}/\rho$ is expected to be a function of the scale factor). Nonetheless, Eqs. (3.57) and (3.54) (with a damping length as in Eq. (4.56)) show that considering a time varying χ does not help much if its present value is $\chi_0 \lesssim 1$. As matter of fact, frustration might only occur, under these circumstances, for networks which have $k \ll 1$ for $v \ll 1$. This generalizes the previously mentioned result that the frustration of domain wall networks can only occur for $k \ll 1$ to p-branes of arbitrary dimensionality. In the particular case of domain walls, there is very strong analytical and numerical evidence that networks (with or without junctions) are unlikely to attain $k \ll 1$ in the non-relativistic limit, if they are the dominant energy component [6]. This result effectively rules out domain wall networks as a cosmologically relevant dark energy candidate: frustration can either occur if the network is design to have $k \ll 1$ in the non-relativistic limit — which appears to be unrealistic — or if χ is much larger than unity — in which case the domain wall energy density would be subdominant and would not contribute significantly to the dark energy budget.

For $p < N - 1$, the Hubble damping is less efficient and, thus, frustration is even less likely to result from the natural evolution of the network. Therefore, unless there is a natural mechanism that drives k towards zero in the non relativistic limit — which seems unlikely — the *no frustration conjecture* is also expected to apply to any realistic and cosmologically relevant p-brane network.

The mechanism for the frustration of domain wall network in Refs. [135, 136] is expected to face similar problems. The authors perform field theory simulations of a model with $\mathbb{Z}_2 \times U(1)$ symmetry in (2+1)-dimensions. Their model has two discrete vacua, allowing for domain walls and a conserved Noether charge. The authors argue that the Noether charge and currents become localized on the walls, forming kinky vortons, providing a possible mechanism for the frustration of domain wall networks. However, the authors do not calculate the overall equation of state of the network. Had they done that, they would have found significant deviations with respect to that of a frustrated featureless domain wall gas ($w = -2/3$).

4.3 BIASED DOMAIN WALLS AND THE DEVALUATION MECHANISM

The cosmological constant is the simplest explanation for the current acceleration of the universe. It fits remarkably well the observational constraints from several cosmological probes and it has a natural physical interpretation as the vacuum energy density. However, the observed value of the cosmological constant is extraordinarily low, more than 120 order of magnitude smaller than the particle physics predictions. The theoretical value for vacuum density is sometimes humorously dubbed "the worst theoretical prediction in the history of physics", but this discrepancy is indeed a fundamental problem in modern physics.

In Ref. [9], the authors proposed a dynamical solution to the cosmological constant problem, involving the evolution of a biased domain wall network. In the simplest model of biased domain walls, the vacuum states separated by a wall have a slight energy difference, so that one of these vacua has a smaller energy density [137, 129, 130]. As a result of this energy difference, the domain wall feels a dynamically relevant pressure that pushes it towards the domain with the highest energy density [130, 138]. Depending on its importance relative to other processes— most notably the surface tension— the walls may be long-lived (as in the standard case) or disappear almost immediately. Biased domain walls were originally envisioned as a way to evade the Zel'dovich bound, however they are also behind the devaluation scenario proposed in [9].

This scenario requires a model with a potential which has a large number of nearly degenerate minima, spanning a large number of values of vacuum energy. After inflation, different patches of the universe are expected to fall into different minima, leading to the formation of a biased domain wall network. The domain walls would then feel a pressure that would drive them towards the regions of higher energy density. As a result, these regions would be suppressed and the universe would be driven towards lower and lower values of the cosmological constant.

In this section, we will make a detailed analysis of the Devaluation scenario. We will start by analyzing the dynamics of biased domain walls, both by studying a simple field theory realization and by developing an analytical model that incorporates the effect of bias on the evolution equations for domain walls. We will then use the results to carry out a thorough analysis of the devaluation scenario. This work was published in [10].

4.3.1 Qualitative analysis of Biased Domain Walls

Let us then consider the simplest field theory model

$$\mathcal{L} = \frac{1}{2}\phi_{,\mu}\phi^{,\mu} - V(\phi)\,, \tag{4.58}$$

with a tilted potential

$$V(\phi) = \frac{\lambda}{4}\eta^4\left[\left(\frac{\phi^2}{\eta^2} - 1\right)^2 + \kappa\frac{\phi}{\eta}\right]. \tag{4.59}$$

It then follows [98] that the height of the potential barrier and surface tension are respectively

$$V_0 = \frac{\lambda}{4}\eta^4\,, \tag{4.60}$$

$$\sigma \sim \sqrt{\lambda}\eta^3\,, \tag{4.61}$$

while the wall thickness and the asymmetry parameter (energy difference between the two vacua) are respectively

$$\delta \sim \frac{\eta}{\sqrt{V_0}} \sim (\sqrt{\lambda}\eta)^{-1} \tag{4.62}$$

$$\varepsilon = 2\kappa V_0\,. \tag{4.63}$$

The dynamics of biased domain walls are determined by the competition between the surface pressure,

$$p_T = \frac{\sigma}{R}\,, \tag{4.64}$$

(caused by the superficial tension), and the volume pressure,

$$p_V = \varepsilon\,, \tag{4.65}$$

originated by the energy difference between vacua. At early times, the dynamics of the domain walls is dominated by the surface tension, which acts to increase the radius of curvature of the wall. However, when the domains become large enough, the volume pressure becomes comparable to the surface pressure, leading to the decay of the domain walls [130, 139]. In flat space-time this happens when

$$R \sim \frac{\sigma}{\varepsilon}\,. \tag{4.66}$$

For instance, we phenomenologically expect that at the Ginzburg temperature (when the network first becomes well-defined) the correlation length should approximately be given by $L \sim (\lambda\eta)^{-1}$ and, in this case, we have that

$$\left(\frac{p_V}{p_T}\right)_{T_G} \sim \frac{\kappa}{2\sqrt{\lambda}}\,. \tag{4.67}$$

Typically one might expect this to be smaller than unity but not much less. However, there is, in principle, enough parameter freedom to make it much larger or much smaller than that. When the volume pressure dominates, one expects that the walls will move with an acceleration

$$\frac{\varepsilon}{\sigma} \sim \lambda^{1/2}\kappa\eta\,. \tag{4.68}$$

On the other hand, if the surface pressure dominates initially the walls may survive long enough to reach a linear scaling regime, $L \sim t$. Understanding, how fast the volume pressure becomes important — or equivalently how long the walls will survive and how fast they will decay — is a key issue in several cosmological scenarios, including devaluation. Moreover, the Zel'dovich bound [127] provides an additional and often limiting observational constraint.

4.3.2 Analytic Model for Biased Domain Walls

Modelling the effect of this bias is fairly straightforward in the context of the microscopic model we introduced in Sec 4.1. Suppose that the two vacua on either side of a domain wall have different energy densities $V_{\rm in}$ and $V_{\rm out}$ and let $\varepsilon = V_{\rm in} - V_{\rm out}$ be their energy difference. The resulting effect on domain wall dynamics is very easy to understand if we consider a planar domain wall in Minkowski space. In this case the inner and outer regions of the domain wall are not well defined but we shall assume that the domain wall is moving in the direction out $\rightarrow$ in. Energy conservation implies that

$$d(\sigma\gamma) = v dt \varepsilon\,, \tag{4.69}$$

from which we get

$$\frac{dv}{dt} = \frac{\varepsilon}{\sigma\gamma^3}\,; \tag{4.70}$$

we can immediately note that this is coincides with Eq. (4.68) apart from the relativistic gamma factors. With our conventions, if the wall is moving towards the region with higher energy density ($\varepsilon > 0$), this region becomes smaller, and, consequently, the wall gains momentum to compensate the energy loss. This confirms the expectation that the domain wall will feel a pressure which will tend to drive it into the region of higher energy density. We can alternatively write this as

$$\frac{dv}{dt} = (1-v^2)^{3/2}\frac{\kappa\lambda^{1/2}}{2}\eta \equiv \frac{(1-v^2)^{3/2}}{R_v}\,, \tag{4.71}$$

which highlights the fact that ε acts like an effective curvature, and therefore accelerates the wall. Its distinguishing feature is that the scale is set by the micro-physics of the model in question (ultimately by the form of the potential), rather than the macroscopic dynamics (as is the case for the usual curvature radius of the walls). Moreover, this lengthscale is constant, whereas the usual curvature radius increases as the walls evolve. This implies that the volume pressure term will gradually become more dynamically relevant. Having said that, note that the extra γ factor can switch this term off if the walls become ultra-relativistic ($v \to 1$). It is then clear that we can now add this volume pressure correction to our domain wall evolution equation (4.2), yielding

$$\frac{dv}{dt} = (1-v^2)\left(\frac{f(v)}{R_i} + \frac{\varepsilon}{\sigma\gamma} - 3Hv\right)\,, \tag{4.72}$$

or equivalently

$$\frac{dv}{dt} = (1-v^2)\left(\frac{f(v)}{R_i} + \frac{\gamma^{-1}}{R_v} - 3Hv\right)\,. \tag{4.73}$$

The effect of the bias can also be added to Eqs. (4.3) and (4.4), in order to incorporate in the evolution of the wall invariant radius, R. In the case of spherically symmetric domain wall, the equation of motion takes the form

$$\frac{dR_0}{dt} = \left(1 - \frac{3}{2}v^2\right)HR_0 + \frac{\varepsilon v R_0}{2\sigma\gamma}\,, \tag{4.74}$$

or, using the definition of R_v in Eq. (4.71), it can be written in the more suggestive form

$$\frac{dR_0}{dt} = \left(1 - \frac{3}{2}v^2\right)HR_0 + (1-v^2)^{1/2}\frac{v}{2}\frac{R_0}{R_v}\,. \tag{4.75}$$

Similarly, for domain walls with cylindrical symmetric, we find that:

$$\frac{dR_1}{dt} = \left(1 - 3v^2\right)HR_1 + \frac{\varepsilon v R_1}{\sigma\gamma}\,, \tag{4.76}$$

or equivalently

$$\frac{dR_1}{dt} = \left(1 - 3v^2\right) HR_1 + (1 - v^2)^{1/2} v \frac{R_1}{R_v} \,. \tag{4.77}$$

Recall that, when extrapolating to a biased domain wall network, Eqs. (4.74) and (4.76) should be compared to Eqs. (4.10) and (4.12). Notice that this additional term due to the bias may be regarded as an additional energy loss by the network. As discussed previously, the importance of this term is expected to grow as the walls evolve, although it switches off in the ultra-relativistic limit.

It obviously follows from the above discussion that this model reproduces the result [130] that domains with a larger energy density will decay when their typical size $R \gtrsim \sigma/\varepsilon$, and indeed it provides a more quantitative estimate—since the relativistic gamma factor may be significant. We may also compare the importance of the pressure term with that of the Hubble damping term in Eq. (4.2). For non-relativistic domain walls the pressure term dominates over the Hubble damping term slightly earlier than over the curvature term (assuming that $R \lesssim H^{-1}$). However, for $R \sim H^{-1}$ and v not too small, the two criteria are very similar. If $R \lesssim H^{-1}$ and the above criteria are satisfied, then the domains with a larger energy density disappear exponentially fast. This result is the basis of the devaluation mechanism.

As an illustrative example of the effect of bias on the dynamics of biased domain walls, we have solved Eqs (4.72) and (4.74) numerically for a spherical domain wall, initially at rest, with a higher vacuum energy in its inner domain. This allowed us to determine the evolution of the domain wall's physical radius, $q_0 = R_0 \gamma^{-1/2}$, until collapse (which was defined as the moment when q_0 vanishes).

Fig. 4.3 shows the time of collapse of a spherical domain wall, with or without bias, and the relative difference between these collapse times as a function of the ratio between its initial wall invariant radius, R_0, and the initial Hubble radius. The bias term acts as a further mechanism to accelerate the domain walls, allowing them to overcome the Hubble damping term faster and thus making them collapse in a shorter period of time. The relative importance of this effect grows as the initial radius increases. However, the curvature term becomes negligible for large R and, therefore, in this limit, the dynamics of the wall is essentially determined by the bias term. As a result, the relative difference tends to a constant, in this limit.

Fig. 4.4 shows the relative difference between the collapse time, with and

without an energy difference between minima, for ε/σ ranging from 0 to 100 (for a spherical domain wall with $R(t_i) = H_i^{-1}$). Notice that as the bias term's importance grows, this relative difference tends to a constant. Given the bias term makes the velocity become ultra-relativistic faster, the time of collapse with bias has an obvious lower bound, given by the time a photon takes to travel a distance equal to the initial physical radius of the domain wall, in a flat FRW universe. This minimum collapse time is given by:

$$t_c^{min} \sim \left(\frac{a(t_i)(1-\beta)q_i + t_i}{t_i^{\beta}} \right)^{1/(1-\beta)} , \tag{4.78}$$

where β is the expansion exponent and q_i is the initial physical radius. In this particular case of the collapse of a spherical domain wall with $q_i = 1$ during the radiation dominated era, this lower bound yields $t_c^{min} \sim 4$, and the relative difference tends to $\Delta \sim 0.33$ as ε/σ increases[5]. This simple example clearly shows that the effect of bias, as a source of instability, is limited.

4.3.3 The devaluation mechanism

The devaluation mechanism [9] aims to explain the observed small non-vanishing value of the cosmological constant using the dynamics of biased domain walls. The key physical idea is that, under plausible circumstances, a network of unstable domain walls might form at a certain critical temperature, dividing the universe in many different regions with different values of the vacuum energy density. Domain walls separating different vacuum domains will then feel a pressure which will tend to suppress those with higher energy thus driving the universe towards lower and lower values of the cosmological constant.

A simple potential that has the relevant features is

$$V(\phi) = V_0 \cos(\pi\phi) - \varepsilon\frac{\phi}{2} + C , \tag{4.79}$$

where V_0 is effectively the barrier height and ε is the energy difference between minima. From the original paper [9], the expectation is that

$$\eta \sim V_0^{1/4} > 10\text{MeV} , \tag{4.80}$$

and obviously

[5] We took $t_i = 1$ and $a(t_i) = 1$.

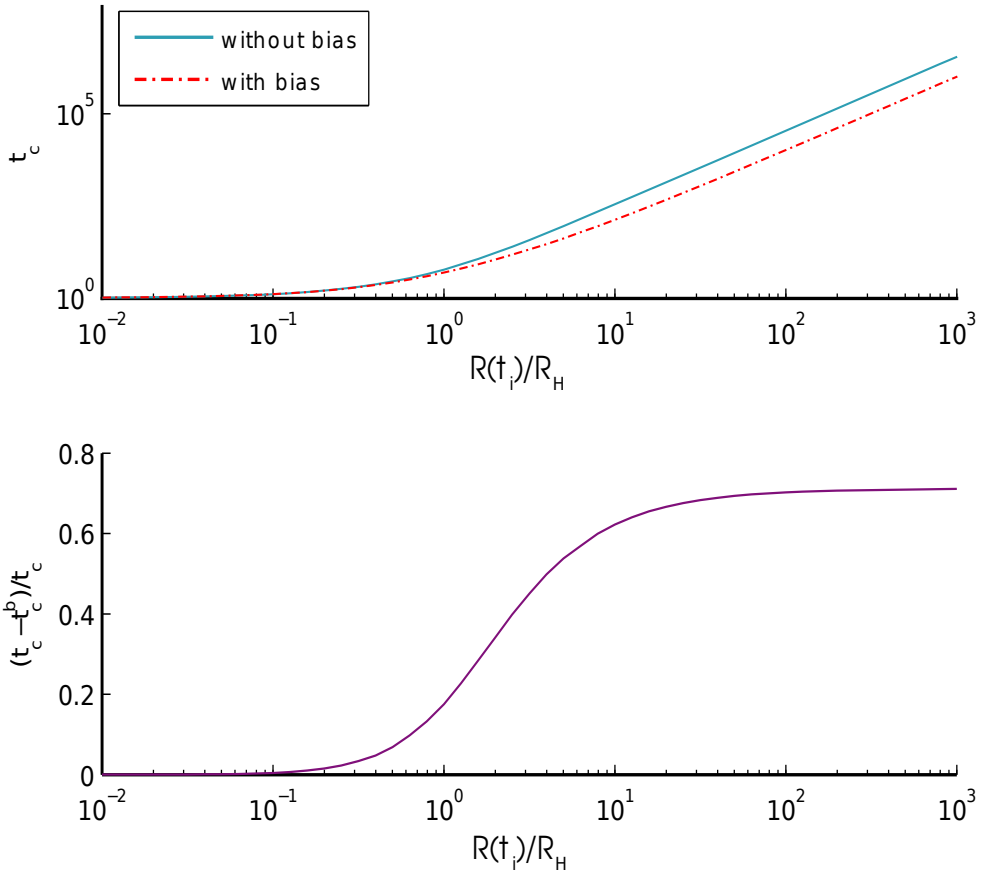

Figure 4.3: In the top panel it is represented the collapse time of a spherical domain wall (in units of initial time), with (t_c^b) and without (t_c) an energy difference between domains, as function of the ratio between the initial wall invariant radius and the initial Hubble radius. On the lower panel, it is represented the relative difference between the time of collapse with and without bias. We took $\varepsilon/\sigma = 1$.

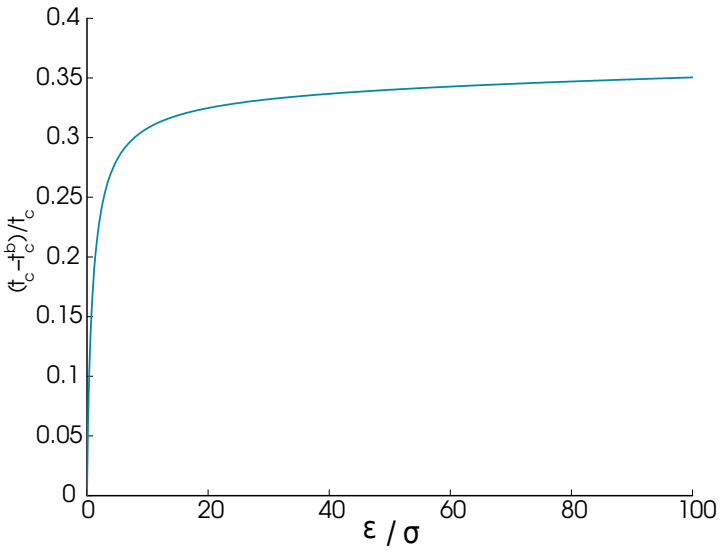

Figure 4.4: The relative difference between time of collapse with and without bias for ε/σ ranging from 0 to 100 and for a spherical domain wall with $R(t_i) = H_i^{-1}$

$$\varepsilon^{1/4} \sim \rho_c^{1/4} \sim 10^{-3}\text{eV}\,. \tag{4.81}$$

It is important to realize that, in this particular model, all the domain walls interpolating between successive pairs of minima in the above potential have similar tensions. The model also requires a large number of minima, but the exact number is actually not relevant for the analysis that follows. Moreover, it was argued that domains with negative energy vacua would be suppressed so that the domain wall dynamics would lower the cosmological constant to the lowest non-negative value possible ($\rho_{vac} \sim \varepsilon \sim \rho_c$). We will question the validity of this assumption later on.

The initial conditions are expected to be such that $L_i \sim T_G^{-1} \sim V_0^{-1/4} \sim \eta^{-1}$, which is significantly smaller than the Hubble radius:

$$\frac{R_H}{L_i} \sim \frac{m_{Pl}}{V_0^{1/4}} \lesssim 10^{20}\,. \tag{4.82}$$

Clearly, with $L_i \sim \eta^{-1}$, the surface pressure $p_T \sim \eta^4 \sim V_0$ will initially dominate the volume pressure $p_V \sim \varepsilon$ and the walls will initially be very stable. So for this choice of parameters, devaluation is not very efficient.

On the other hand, the largest correlation length we can have (which corresponds to the largest instability) is $L \sim t$. Recalling that

$$t \sim \frac{m_{Pl}}{T^2} \tag{4.83}$$

in the radiation era, and

$$t \sim \frac{m_{Pl}}{T^{3/2} T_{eq}^{1/2}} \tag{4.84}$$

in the matter era, we find that, in this maximal instability case, the domain walls become unstable and disappear for

$$\left(\frac{T}{m_{Pl}}\right)^2 \sim \frac{\varepsilon}{V_0} \frac{\eta}{m_{Pl}} , \tag{4.85}$$

$$\left(\frac{T}{m_{Pl}}\right)^{3/2} \sim \frac{\varepsilon}{V_0} \frac{\eta}{m_{Pl}} \left(\frac{m_{Pl}}{T_{eq}}\right)^{1/2} , \tag{4.86}$$

respectively. In order for the decay to happen in the radiation era we need $T > T_{eq} \sim 1\text{eV}$, and using Eq. (4.81) we find

$$\eta_{rad} \lesssim 100\,\text{keV} , \tag{4.87}$$

which is clearly incompatible with the assumed bound in Eq. (4.80). It then follows that if this mechanism (at least as originally envisioned) is to explain the observed value of the cosmological constant, the domain walls must survive through the radiation era, and decay only in the matter era. In other words, in the original scenario, devaluation must occur late in the history of the universe, and not early. This is due to the energy scale required to match the observed value of the cosmological constant, and is another manifestation of the underlying fine-tuning. Repeating the calculation for a decay during the matter era (and ignoring the effect of the recent acceleration phase on the expansion rate, which is negligible in this context), we now find

$$\eta_{mat} \lesssim 10\,\text{MeV} , \tag{4.88}$$

which saturates the bound given by Eq. (4.80).

Therefore the best we can do is to have a network that disappears around today. If so, and again neglecting the effect of the recent dark energy domination, we would expect the cosmological constant to be

$$\frac{\rho_{vac}^{1/4}}{m_{Pl}} \sim \left(\frac{\eta}{m_{Pl}}\right)^{3/4} \left(\frac{T_0}{m_{Pl}}\right)^{3/8} \left(\frac{T_{eq}}{m_{Pl}}\right)^{1/8} , \tag{4.89}$$

and since $T_{eq} \sim 1\text{eV}$ and $T_0 \sim 2 \times 10^{-4}\text{eV}$ we get

$$\rho_{vac}^{1/4} \sim \left(\frac{\eta}{m_{Pl}}\right)^{3/4} 10^{13}\text{eV} \tag{4.90}$$

from which we would get $\rho_{vac}^{1/4} = 10^{-3}\,\text{eV}$ for $\eta \sim 10\,\text{MeV}$ as previously stated.

There is, however, an obvious problem with such a scenario: 10MeV domain walls decaying today are observationally ruled out. For the rather classic Zel'dovich bound [127], $\eta \sim 1\,\text{MeV}$, we only get $\rho_{vac}^{1/4} \sim 10^{-4}\text{eV}$. This is optimistic not only because the observational bound is somewhat lower, but also because we really want the network to decay a bit before today to be clear of observational problems.

Indeed, for late devaluation there are several extra requirements (absent in the case of early devaluation) which need to be satisfied. If devaluation is not complete and there are some walls still around, their average contribution to the energy density of the universe needs to be $\rho_\sigma \lesssim 10^{-5}\rho_c$. Otherwise, assuming that the characteristic size of the domains is $\gtrsim H^{-1}$, there would be a detectable contribution of domain walls to the cosmic microwave background anisotropies. This means that the wall tensions are strongly constrained. We know from Eq. (4.66) that if we have two contiguous domains with a vacuum energy difference of ε then the domain with larger vacuum density will be exponentially suppressed when $\varepsilon \gtrsim \sigma/L$. Recall that σ/L is the average energy density of the domain wall network and that, as we saw, ρ_σ must be at least five orders of magnitude smaller than the critical density. So in this case,

$$\rho_{vac}^{1/4} \lesssim 10^{-4}\,\text{eV}\,, \tag{4.91}$$

and devaluation would lead to a vacuum energy density significantly smaller than the critical density at the present time. In fact this number might even be smaller than that, depending on the domain wall tensions.

Beyond particular realizations of the devaluation mechanism, several general comments can be made about the underlying physical scenario. Before touching upon some of these, let us note that this simple model may allow for positive and negative values of the vacuum energy density. It is argued [9] that gravitation itself may prevent the vacuum energy density from attaining negative values. However, here we will be mainly concerned with the evolution of domain wall networks during the matter and radiation eras in which the contribution of the domain wall and the vacuum energy densities can be neglected. In this context, there is no cut-off that prevents the vacuum energy densities from attaining

negative values. Such a mechanism can only operate when the vacuum energy densities are the dominant contribution for the dynamics of the universe. Hence, a low-energy cut-off of the order of the critical density at the present time needs to be introduced by hand in the devaluation model, which is clearly not an attractive feature of the model.

In this scenario a domain wall network forms at a critical temperature $T_c \sim V_0^{1/4}$. It is straightforward to put a lower bound on the number, N, of domains that are initially present in a region with a comoving size of the order of the Hubble radius at the present day,

$$N \gtrsim \left(\frac{T_{\rm eq}}{T_0}\right)^{3/2} \left(\frac{T_{\rm c}}{T_{\rm eq}}\right)^{3} . \tag{4.92}$$

Assuming a fixed energy difference beween successive minima and that the barrier height and tuning of the potential are roughly comparable (as in the simple devaluation toy model introduced above), we see that the difference in energy densities between successive minima is bounded from below,

$$\varepsilon \lesssim \frac{T_c^4}{N} \sim T_c (T_0\, T_{\rm eq})^{3/2} , \tag{4.93}$$

if all the minima are populated at the time when the network forms. In fact, if we assume that close to T_c the domains rapidly attain a typical size of the order of the Hubble radius then

$$\varepsilon \sim T_c (T_0\, T_{\rm eq})^{3/2} , \tag{4.94}$$

which is much larger that the energy density at the present time. Of course, not all the minima need to be populated and, in this case, ε can be smaller. However,the domain wall tension would no longer be the same for all domain walls, since domain walls would in general interpolate between distant minima. We also note that a single domain with the lowest possible energy density does not necessarily survive domain wall evolution since, even in the absence of the devaluation mechanism (which will only operate for $\varepsilon \gtrsim \sigma/L$), domain wall dynamics in the scaling regime naturally leads to the suppression of most of the available domains during each Hubble time.

The above analysis also confirms the naive expectation that the devaluation mechanism can only be effective if $L \lesssim H^{-1}$. If this is not the case (either because the walls are somehow pushed outside the horizon, or in the opposite limit, $L \ll H^{-1}$), the dynamics of the domain walls is even less efficient in suppressing domains with larger values of the vacuum density. In the absence of friction, and assuming that $L \lesssim H^{-1}$, a domain wall network will in fact approach the

scaling regime, with $L \propto H^{-1}$, which is quite generically an attractor solution. Friction may slow down the domain walls, and if they are sufficiently light, the evolution may be friction dominated up to the present time, but this will not help.

Therefore the devaluation scenario does not naturally lead to the required value of the vacuum energy density. A simple and physically intuitive way of expressing this is in terms of fine-tuning. A cosmological constant is considered unappealing because its observational value is many orders of magnitude below what one would naturally expect from particle physics considerations. From this perspective, the motivation of the devaluation scenario is that it would lead to a small value in a natural way. However, this is not so because the same fine-tuning problem is still there, since we still need a low energy cut-off.

Many of the features of this simplest implementation of devaluation can be relaxed. We may have complex domain wall networks with junction, domain walls with tensions that may be correlated with the differences between the vacuum energy densities. In fact the domain walls may not all be formed at the same time, with additional domains with smaller energy densities separated by low tension domain walls being formed only at smaller critical temperatures. Still, it is clear that the devaluation mechanism is too efficient and consequently it will always be necessary to introduce by a hand a low energy cut-off of the order of the critical density at the present day.

In more realistic particle physics scenarios there will typically be many coupled scalar fields that can lead to domain walls. From a phenomenological point of view, there are several reasons why this more general case may differ from the simplest implementation of the devaluation mechanism. The potential may be significantly more complicated, as in landscape-type scenarios. This by itself need not be a great advantage, since in any case energy minimization criteria will always favour evolution down the potential, regardless of the number of fields. In particular, any number of uncoupled fields will lead to a scenario very similar to the single-field case. More important, though, is the existence of coupled fields, since this generically leads to domain wall networks with junctions, and also to more complicated spectra of wall tensions, which need not necessarily be of comparable magnitude.

The presence of walls with significantly different tensions may be important to the network dynamics. Recall that biased walls will decay when their characteristic size grows to $L \gtrsim \sigma/\varepsilon$. Since in this model ε is effectively fixed to the observed vacuum energy density, we see that higher-tension walls are actually

more stable than lower-tension walls (since a larger characteristic size is needed to make them decay). Notice that this is contrary to standard energy minimization arguments, whereby higher-tension walls tend to decay into lower-tension walls. If we now consider a network of walls with junctions and a non-trivial hierarchy of tensions, and temporarily assume that the various types of walls with different tensions have comparable characteristic sizes (which may be too naive an assumption), then one may reach a threshold where the lowest-tension walls present become unstable and decay. This may render the whole network unstable and make it disappear well below what one would expect from a stability analysis for the higher-tension walls. Therefore this mechanism may increase the efficiency of devaluation. However, given that the devaluation mechanism is already too efficient in its simplest implementation this extra efficiency will not help. Hence, it seems that a low energy cut-off of the order of the critical density at the present day would still be necessary in order for devaluation to stop at the observed value of the dark energy density.

4.4 CONCLUSIONS

In this chapter, we have discussed the potential role of frustrated domain wall networks as a dark energy component. We have imposed strong constraints on the characteristic length and velocity of domain wall networks with string and monopole-type junctions using a semi-analytical VOS model. We have shown that a successful domain wall scenario for dark energy would require that $L_0 \lesssim 1\,\mathrm{Mpc}$ and $v_0 \lesssim 10^{-3}$. We have demonstrated that such small values of L_0 and v_0 could only be achieved if the contribution of the monopole-type junctions to the total density of the universe was several orders of magnitude larger than that of domain walls and strings (assuming $\Omega_{\sigma 0} \sim 1$), in complete disagreement with observations. These results highlight the main difficulty with alternative mechanisms for the frustration of domain wall networks. The inclusion of additional degrees of freedom such as heavy junctions and friction may slightly reduce the characteristic length and velocity of domain walls; however it is insufficient to lead to frustration, due to the limited amount of matter with which domain walls can interact while conserving energy and momentum at present time.

Moreover, we studied the effect that a generic interaction mechanism between p-branes and another cosmological component may have on the dynamics of p-brane networks. We demonstrated that, if p-branes are the dominant

component of the universe, then frustration is not possible unless the curvature parameter is driven towards very small values for non-relativistic networks or if the expansion is accelerated. In the case of domain walls there is very strong analytical and numerical evidence (both in two ($N = 2$, $p = 1$) and 3 ($N = 3$, $p = 2$) spatial dimensions) that k never becomes much smaller than unity (except deep into inflationary or friction dominated regimes), thus preventing frustration from being attained for realistic domain wall networks playing a dark energy role. We conjectured that this may be a general result, valid for any realistic p-brane network independently of the values of N and p with $1 \leqslant p \leqslant N - 1$.

We have also studied the evolution of biased domain walls in the early universe by including the dynamical effects of bias in the microscopic equations of motion for domain walls. We discussed the roles played by the superficial tension and the volume pressure (caused by the energy difference between nearby vacua) in the evolution of the domain walls, and quantified their effects by looking at the collapse of spherical domain walls. These results were then applied to the devaluation scenario, suggested as a possible solution to the cosmological constant problem. Our results indicate that devaluation will, in general, lead to values of the cosmological constant that differ by several orders of magnitude from the observationally inferred value. We also argued that, beyond any particular realizations, this scenario is expected to be too efficient and, therefore, it does not naturally lead to the required energy density. In order to do so, the devaluation scenario requires a low-energy cut-off of the order of the critical density at the present on the spectra of the vacuum energy density. As a consequence, the devaluation scenario cannot be regarded as a satisfactory solution to the cosmological constant problem.

5

Conclusions

This thesis focused mainly on the dynamics of p-brane networks in higher dimensional Friedmann-Robertson-Walker universes, and their cosmological consequences. In order to study the cosmological consequences of p-brane networks, it is necessary to understand the dynamics of p-branes. For that reason, we started by studying the dynamics of $N-1$-branes, or domain walls, and computed analytically the equation of motion for the velocity of a curved thin domain wall — whose curvature radii are much larger than its thickness — in $N+1$-dimensional homogeneous and isotropic backgrounds. We demonstrated specifically that the dynamics of domain walls is independent of the form of the potential — which is only required to support stable domain wall solution — and it does not depend on the form of the kinetic term of the lagrangian density. We have also demonstrated that the modification to the scalar field equation of motion, implemented in many cosmological field theory simulation of domain wall networks in order to ensure fixed comoving thickness (known as PRS algorithm), does not affect the dynamics of thin domain walls.

Furthermore, we derived the equation of motion for the velocity of a infinitely thin and featureless p-brane of arbitrary dimensionality, and obtained its normal acceleration. We have also studied in detail the dynamics of closed p-brane solutions with a $S_{p-i} \otimes \mathbb{R}^i$ topology, and obtained equations of motion for their velocity and invariant radius, in FRW universes. The dynamics of these p-brane loops were studied in several cosmological backgrounds, with constant and time-dependent expansion rates, experiencing expansion and collapse. This study

allowed us to obtain constraints on the root-mean-square velocity of p-brane loops in expanding and collapsing universes, and to understand the evolution of p-brane loops under expansion.

We moved on to consider the case of p-brane networks in higher dimensional FRW background. By averaging the equation of motion for a p-brane, we were able to obtain a evolution equation for the RMS velocity of a p-brane network. We also assumed that the p-brane network is statistically homogeneous and isotropic at large scales, so that it can be treated as brane gas. This allowed us to obtain an evolution equation for the p-brane energy density and for the characteristic length of the network. The equations of motion for RMS velocity and for characteristic length of the network constitute a generalization of the Velocity-Dependent One-Scale Network for cosmic strings, to the case of p-brane networks in FRW universes with an arbitrary number of spatial dimensions.

This generalized VOS model allowed us to study the scaling regimes that arise in different expanding and collapsing cosmological models, both in the friction-dominated and frictionless epochs. We studied, in particular, the conditions under which p-brane networks are able to reach linear scaling solutions. We used the previously derived constraints on the RMS velocity to determine the allowed range of the curvature parameter, for which these solution are attainable. We have also discussed the particular case of cosmic string networks in $N+1$-dimensions, and constrained the values of the expansion exponent, β, for which these linear scaling solutions might arise in the absence of the energy-loss mechanism. We have shown that, for non-vanishing energy-loss parameter, these linear scaling solutions are attainable for all $0 < \beta < 1$, provided that the curvature parameter has an adequate value.

We gave special attention to the cosmological consequences of domain wall networks and their relations to dark energy. We adapted the VOS model for domain walls to account for the dynamical effects of string and monopole-type junctions on the evolution of domain wall networks. We found that the presence of massive junctions is able to effectively "freeze", or frustrate, the domain wall networks, provided that their energy density is several orders of magnitude larger than that of the domain walls. Domain wall networks are able to provide a phase of accelerated expansion, provided that their velocity is small enough. For this reason, frustrated domain wall networks have been suggested as dark energy candidates. However, frustration does not seem to arise naturally as a result of the evolution of domain wall networks without the existence of an alternative mechanism to decelerate the walls. Our results indicate that, although the presence of heavy junctions can effectively frustrate the network, this would require a very large junction energy density, that is not in agreement with

observational results. Therefore, our results seem to rule out frustrated domain wall networks with massive junctions as dark energy candidates. Moreover, we demonstrated that considering alternative frictional mechanisms does not help much: in order to decelerate the branes, we should either have that $k \ll 1$ in the non-relativistic limit, or the contribution of the branes to the energy density should be subdominant. Therefore, any frustrated domain wall network would be unable to contribute significantly to the dark energy density.

We have also studied the dynamics of biased domain walls, that (in the simplest realization) arise when the minima of the potential of the model are nearly-degenerate. In this case, there is another dynamical effect to take into consideration in the motion of the domain walls: the pressure that results from the energy difference between minima. This pressure drives the domain walls towards the region of higher vacuum energy density. We have adapted the equation of motion for domain walls to account for this dynamical effect, and found that it may be interpreted as an effective curvature term, that aids domain collapse. We used these results to study the devaluation scenario, that was proposed as a dynamical solution to the cosmological constant problem. According to this scenario, after inflation, different patches of the universe fall into different minima of a potential with a large number of nearly degenerate minima, spanning a wide range of vacuum density values, and, therefore, a biased domain wall network permeates the universe. These domain walls would, then, feel a volume pressure towards the regions of higher energy density, that would lead to the suppression of these regions. As a consequence, the natural evolution of the biased domain wall network would lead to the disappearance of regions with higher values of the cosmological constant, and the universe would natural evolve towards small values of the vacuum energy density. However, our results show that, beyond of specific realization of this scenario, devaluation would require a low-energy cut-of in order to reproduce the observed value of the cosmological constant. In other words, this scenario also suffers from fine-tuning problems.

List of Publications

- *The cosmological evolution of p-brane networks*, L. Sousa and P. P. Avelino, Phys. Rev, D84 063502 (2011)
- *p-brane dynamics in $N+1$-dimensional FRW universes: a unified framework*, L. Sousa and P. P. Avelino, Phys. Rev. D83 103507 (2011)
- *Domain wall network evolution in $(N+1)$-dimensional FRW universes*, P. P. Avelino and L. Sousa, Phys. Rev. D83 043530 (2011)
- *Evolution of Domain Wall Netoworks: the PRS algorithm*, L. Sousa and P. P. Avelino, Phys. Rev. D81 087305 (2010)
- *Impact of string and monopole-type junctions on domain wall dynamics: implications for dark energy*, L. Sousa and P. P. Avelino, Phys. Lett. B689 145-148 (2010)
- *p-Brane dynamics in $(N+1)$-dimensional FRW universes*, P. P. Avelino, R. Menezes and L. Sousa, Phys. Rev. D79 043519 (2009)
- *Dynamics of Biases Domain walls and the Devaluation mechanism*, P. P. Avelino, C. J. A. P. Martins and L. Sousa, Phys. Rev. D78 043521 (2008)

Bibliography

[1] G. R. Dvali, Q. Shafi, and S. Solganik. D-brane inflation. 2001.

[2] Saswat Sarangi and S. H. Henry Tye. Cosmic string production towards the end of brane inflation. *Phys. Lett.*, B536:185–192, 2002.

[3] Mahbub Majumdar and Anne-Christine Davis. D-brane anti-brane annihilation in an expanding universe. *JHEP*, 0312:012, 2003.

[4] C.J.A.P. Martins and E.P.S. Shellard. Quantitative string evolution. *Phys.Rev.*, D54:2535–2556, 1996.

[5] Martin Bucher and David N. Spergel. Is the dark matter a solid? *Phys.Rev.*, D60:043505, 1999.

[6] Pedro Pina Avelino, C. J. A. P. Martins, J. Menezes, R. Menezes, and J. C. R. E. Oliveira. Frustrated expectations: Defect networks and dark energy. *Phys. Rev.*, D73:123519, 2006.

[7] P.P. Avelino, C.J.A.P. Martins, J. Menezes, R. Menezes, and J.C.R.E. Oliveira. Defect junctions and domain wall dynamics. *Phys.Rev.*, D73:123520, 2006.

[8] P. P. Avelino, C. J. A. P. Martins, J. Menezes, R. Menezes, and J. C. R. E. Oliveira. Dynamics of domain wall networks with junctions. *Phys. Rev.*, D78:103508, 2008.

[9] Katherine Freese, James T. Liu, and Douglas Spolyar. Devaluation: A dynamical mechanism for a naturally small cosmological constant. *Phys. Lett.*, B634:119–124, 2006.

[10] P. P. Avelino, C. J. A. P. Martins, and L. Sousa. Dynamics of Biased Domain Walls and the Devaluation Mechanism. *Phys. Rev.*, D78:043521, 2008.

[11] P. P. Avelino, R. Menezes, and L. Sousa. p-brane dynamics in N+1-dimensional FRW universes. *Phys. Rev.*, D79:043519, 2009.

[12] L. Sousa and P.P. Avelino. Impact of string and monopole-type junctions on domain wall dynamics: implications for dark energy. *Phys.Lett.*, B689:145–148, 2010. * Brief entry *.

[13] L. Sousa and P. P. Avelino. Evolution of domain wall networks: The Press-Ryden-Spergel algorithm. *Phys. Rev.*, D81:087305, 2010.

[14] P. P. Avelino and L. Sousa. Domain wall network evolution in (N+1)-dimensional FRW universes. *Phys. Rev.*, D83:043530, 2011.

[15] L. Sousa and P. P. Avelino. p-brane dynamics in (N+1)-dimensional FRW universes: a unified framework. *Phys. Rev.*, D83:087305, 2011.

[16] L. Sousa and P. P. Avelino. Cosmological evolution of p-brane networks. *Phys. Rev. D*, 84:063502, Sep 2011.

[17] E.W. Kolb and M.S. Turner. *The early universe*. Frontiers in physics. Westview Press, 1994.

[18] E. Papantonopoulos. *The physics of the Early Universe*. Lecture notes in physics. Springer, 2005.

[19] G. Gamow. Expanding universe and the origin of elements. *Phys.Rev.*, 70:572–573, 1946.

[20] Arno A. Penzias and Robert Woodrow Wilson. A Measurement of excess antenna temperature at 4080-Mc/s. *Astrophys.J.*, 142:419–421, 1965.

[21] R.H. Dicke, P.J.E. Peebles, P.G. Roll, and D.T. Wilkinson. Cosmic Black-Body Radiation. *Astrophys.J.*, 142:414–419, 1965.

[22] John C. Mather, D.J. Fixsen, R.A. Shafer, C. Mosier, and D.T. Wilkinson. Calibrator design for the COBE far infrared absolute spectrophotometer (FIRAS). *Astrophys.J.*, 512:511–520, 1999.

[23] P. Molaro, S. A. Levshakov, M. Dessauges-Zavadsky, and S. D'Odorico. The cosmic microwave background radiation temperature at z = 3.025 toward QSO 0347-3819. *Astronomy and Astrophysics*, 381:L64–L67, January 2002.

[24] G. Steigman. Big Bang Nucleosynthesis: Probing the First 20 Minutes. *Carnegie Observatories Astrophysics Series Vol. 2: Measuring and Modeling the Universe*, pages 169–195, 2004.

[25] Richard H. Cyburt, Brian D. Fields, and Keith A. Olive. An Update on the big bang nucleosynthesis prediction for Li-7: The problem worsens. *JCAP*, 0811:012, 2008.

[26] E. Komatsu et al. Seven-Year Wilkinson Microwave Anisotropy Probe (WMAP) Observations: Cosmological Interpretation. *Astrophys.J.Suppl.*, 192:18, 2011.

[27] Reid B. A. Eisenstein D. J. Percival, W. J. et al. Baryon acoustic oscillations in the Sloan Digital Sky Survey Data Release 7 galaxy sample. *Monthly Notices of the Royal Astronomical Society*, 401:2148–2168, 2010.

[28] Adam G. Riess, Lucas Macri, Stefano Casertano, Megan Sosey, Hubert Lampeitl, et al. A Redetermination of the Hubble Constant with the Hubble Space Telescope from a Differential Distance Ladder. *Astrophys.J.*, 699:539–563, 2009. * Brief entry *.

[29] R. Amanullah et al. Spectra and Light Curves of Six Type Ia Supernovae at 0.511 ¡ z ¡ 1.12 and the Union2 Compilation. *Astrophys. J.*, 716:712–738, 2010.

[30] N. Suzuki et al. The Hubble Space Telescope Cluster Supernova Survey: V. Improving the Dark Energy Constraints Above z¿1 and Building an Early-Type-Hosted Supernova Sample. 2011.

[31] Adam G. Riess et al. A 3Space Telescope and Wide Field Camera 3. *Astrophys. J.*, 730:119, 2011.

[32] Bruno Leibundgut. Cosmological Implications from observations of Type Ia supernovae. *Ann.Rev.Astron.Astrophys.*, 39:67–98, 2001.

[33] Adam G. Riess et al. Observational evidence from supernovae for an accelerating universe and a cosmological constant. *Astron.J.*, 116:1009–1038, 1998.

[34] S. Perlmutter et al. Measurements of Omega and Lambda from 42 high redshift supernovae. *Astrophys.J.*, 517:565–586, 1999. The Supernova Cosmology Project.

[35] Adam G. Riess, Robert P. Kirshner, Brian P. Schmidt, Saurabh Jha, Peter Challis, et al. BV RI light curves for 22 type Ia supernovae. *Astron.J.*, 117:707–724, 1999.

[36] Ya.B. Zel'dovich. The Cosmological constant and the theory of elementary particles. *Sov.Phys.Usp.*, 11:381–393, 1968.

[37] Edmund J. Copeland, M. Sami, and Shinji Tsujikawa. Dynamics of dark energy. *Int.J.Mod.Phys.*, D15:1753–1936, 2006.

[38] Adam G. Riess et al. Type Ia supernova discoveries at z ¿ 1 from the Hubble Space Telescope: Evidence for past deceleration and constraints on dark energy evolution. *Astrophys.J.*, 607:665–687, 2004.

[39] C. Wetterich. Cosmology and the Fate of Dilatation Symmetry. *Nucl.Phys.*, B302:668, 1988.

[40] Bharat Ratra and P.J.E. Peebles. Cosmological Consequences of a Rolling Homogeneous Scalar Field. *Phys.Rev.*, D37:3406, 1988.

[41] Joshua A. Frieman, Christopher T. Hill, Albert Stebbins, and Ioav Waga. Cosmology with ultralight pseudo Nambu-Goldstone bosons. *Phys.Rev.Lett.*, 75:2077–2080, 1995.

[42] Edmund J. Copeland, Andrew R Liddle, and David Wands. Exponential potentials and cosmological scaling solutions. *Phys.Rev.*, D57:4686–4690, 1998.

[43] Paul J. Steinhardt, Li-Min Wang, and Ivaylo Zlatev. Cosmological tracking solutions. *Phys.Rev.*, D59:123504, 1999.

[44] C. Armendariz-Picon, Viatcheslav F. Mukhanov, and Paul J. Steinhardt. Essentials of k essence. *Phys.Rev.*, D63:103510, 2001.

[45] Neven Bilic, Gary B. Tupper, and Raoul D. Viollier. Unification of dark matter and dark energy: The Inhomogeneous Chaplygin gas. *Phys.Lett.*, B535:17–21, 2002.

[46] P.P. Avelino, L.M.G. Beca, J.P.M. de Carvalho, and C.J.A.P. Martins. The lambda-CDM limit of the generalized Chaplygin gas scenario. *JCAP*, 0309:002, 2003.

[47] R.R. Caldwell. A Phantom menace? *Phys.Lett.*, B545:23–29, 2002.

[48] Shinji Tsujikawa. Modified gravity models of dark energy. *Lect. Notes Phys.*, 800:99–145, 2010.

[49] Richard A. Battye, Martin Bucher, and David Spergel. Domain wall dominated universes. 1999.

[50] T. W. B. Kibble. Topology of Cosmic Domains and Strings. *J. Phys.*, A9:1387–1398, 1976.

[51] T. W. B. Kibble. Some Implications of a Cosmological Phase Transition. *Phys. Rept.*, 67:183, 1980.

[52] J. Goldstone. Field Theories with Superconductor Solutions. *Nuovo Cim.*, 19:154–164, 1961.

[53] T. Vachaspati. *Kinks and domain walls: an introduction to classical and quantum solitons*. Cambridge University Press, 2006.

[54] G. H. Derrick. Comments on nonlinear wave equations as models for elementary particles. *J. Math. Phys.*, 5:1252–1254, 1964.

[55] Alan H. Guth. The Inflationary Universe: A Possible Solution to the Horizon and Flatness Problems. *Phys.Rev.*, D23:347–356, 1981.

[56] Andrei D. Linde. A New Inflationary Universe Scenario: A Possible Solution of the Horizon, Flatness, Homogeneity, Isotropy and Primordial Monopole Problems. *Phys.Lett.*, B108:389–393, 1982.

[57] Andreas Albrecht and Paul J. Steinhardt. Cosmology for Grand Unified Theories with Radiatively Induced Symmetry Breaking. *Phys.Rev.Lett.*, 48:1220–1223, 1982.

[58] Edward Witten. Cosmic Superstrings. *Phys. Lett.*, B153:243, 1985.

[59] Levon Pogosian, S. H. Henry Tye, Ira Wasserman, and Mark Wyman. Observational constraints on cosmic string production during brane inflation. *Phys. Rev.*, D68:023506, 2003.

[60] Eunhwa Jeong and George F. Smoot. Search for cosmic strings in CMB anisotropies. *Astrophys. J.*, 624:21–27, 2005.

[61] Juan Garcia-Bellido, Raul Rabadan, and Frederic Zamora. Inflationary scenarios from branes at angles. *JHEP*, 01:036, 2002.

[62] Keshav Dasgupta, Carlos Herdeiro, Shinji Hirano, and Renata Kallosh. D3/D7 inflationary model and M-theory. *Phys. Rev.*, D65:126002, 2002.

[63] Edi Halyo. Inflation from rotation. 2001.

[64] C. P. Burgess et al. The Inflationary Brane-Antibrane Universe. *JHEP*, 07:047, 2001.

[65] Stephon H. S. Alexander. Inflation from D - anti-D brane annihilation. *Phys. Rev.*, D65:023507, 2002.

[66] Ashoke Sen. Stable non-BPS bound states of BPS D-branes. *JHEP*, 08:010, 1998.

[67] Ashoke Sen. SO(32) spinors of type I and other solitons on brane- antibrane pair. *JHEP*, 09:023, 1998.

[68] Nicholas T. Jones, Horace Stoica, and S. H. Henry Tye. The production, spectrum and evolution of cosmic strings in brane inflation. *Phys. Lett.*, B563:6–14, 2003.

[69] Mahbub Majumdar and Anne Christine-Davis. Cosmological creation of D-branes and anti-D-branes. *JHEP*, 0203:056, 2002.

[70] Edmund J. Copeland, Robert C. Myers, and Joseph Polchinski. Cosmic F- and D-strings. *JHEP*, 06:013, 2004.

[71] Shamit Kachru et al. Towards inflation in string theory. *JCAP*, 0310:013, 2003.

[72] Joseph Polchinski. Introduction to cosmic F- and D-strings. 2004.

[73] Nicholas T. Jones, Horace Stoica, and S. H. Henry Tye. Brane interaction as the origin of inflation. *JHEP*, 07:051, 2002.

[74] Joseph Polchinski. Collision of Macroscopic Fundamental Strings. *Phys.Lett.*, B209:252, 1988.

[75] Mark G. Jackson, Nicholas T. Jones, and Joseph Polchinski. Collisions of cosmic F and D-strings. *JHEP*, 0510:013, 2005.

[76] Anastasios Avgoustidis and E.P.S. Shellard. Effect of reconnection probability on cosmic (super)string network density. *Phys.Rev.*, D73:041301, 2006.

[77] S.-H.Henry Tye, Ira Wasserman, and Mark Wyman. Scaling of multitension cosmic superstring networks. *Phys.Rev.*, D71:103508, 2005.

[78] A. Avgoustidis and E.P.S. Shellard. Velocity-Dependent Models for Non-Abelian/Entangled String Networks. *Phys.Rev.*, D78:103510, 2008.

[79] A. Pourtsidou, A. Avgoustidis, E.J. Copeland, L. Pogosian, and D.A. Steer. Scaling configurations of cosmic superstring networks and their cosmological implications. *Phys.Rev.*, D83:063525, 2011.

[80] P. M. Saffin. A practical model for cosmic (p,q) superstrings. *JHEP*, 09:011, 2005.

[81] Edmund J. Copeland and P. M. Saffin. On the evolution of cosmic-superstring networks. *JHEP*, 11:023, 2005.

[82] Mark Hindmarsh and P. M. Saffin. Scaling in a SU(2)/Z(3) model of cosmic superstring networks. *JHEP*, 08:066, 2006.

[83] Jon Urrestilla and Alexander Vilenkin. Evolution of cosmic superstring networks: a numerical simulation. *JHEP*, 02:037, 2008.

[84] Levon Pogosian and Mark Wyman. B-modes from cosmic strings. *Phys.Rev.*, D77:083509, 2008. * Brief entry *.

[85] Neil Bevis, Mark Hindmarsh, Martin Kunz, and Jon Urrestilla. CMB polarization power spectra contributions from a network of cosmic strings. *Phys.Rev.*, D76:043005, 2007.

[86] Levon Pogosian, S.-H.Henry Tye, Ira Wasserman, and Mark Wyman. Cosmic Strings as the Source of Small-Scale Microwave Background Anisotropy. *JCAP*, 0902:013, 2009. * Brief entry *.

[87] Neil Bevis, Mark Hindmarsh, Martin Kunz, and Jon Urrestilla. CMB power spectra from cosmic strings: predictions for the Planck satellite and beyond. *Phys.Rev.*, D82:065004, 2010.

[88] Robert Brandenberger, Hassan Firouzjahi, and Johanna Karouby. Lensing and CMB Anisotropies by Cosmic Strings at a Junction. *Phys.Rev.*, D77:083502, 2008.

[89] Joseph Polchinski and Jorge V. Rocha. Cosmic string structure at the gravitational radiation scale. *Phys.Rev.*, D75:123503, 2007.

[90] David Garfinkle and Ruth Gregory. Corrections to the Thin Wall Approximation in General Relativity. *Phys. Rev.*, D41:1889, 1990.

[91] V.A. Toponogov. *Differential geometry of curves and surfaces: a concise guide*. Birkhäuser, 2006.

[92] E. Kreyszig. *Differential geometry*. Dover books on advanced mathematics. Dover Publications, 1991.

[93] H. Arodz. Thick domain walls in a polynomial approximation. *Phys.Rev.*, D52:1082–1095, 1995.

[94] H. Arodz. On expansion in the width for domain walls. *Nucl.Phys.*, B450:174–188, 1995.

[95] Ruth Gregory, David Haws, and David Garfinkle. The Dynamics of Domain Walls and Strings. *Phys.Rev.*, D42:343–348, 1990.

[96] Brandon Carter and Ruth Gregory. Curvature corrections to dynamics of domain walls. *Phys.Rev.*, D51:5839–5846, 1995.

[97] B. S. Ryden W. H. Press and D. N. Spergel. Dynamical Evolution of Domain Walls in an Expanding Universe. *Astrophys. J. 347*, 590, 1989.

[98] A. Vilenkin and E.P.S. Shellard. *Cosmic strings and other topological defects*. Cambridge monographs on mathematical physics. Cambridge University Press, 2000.

[99] Neil Turok and Pijushpani Bhattacharjee. Stretching Cosmic Strings. *Phys.Rev.*, D29:1557, 1984.

[100] P. P. Avelino, C. J. A. P. Martins, and E. P. S. Shellard. Effects of Inflation on a Cosmic String Loop Population. *Phys. Rev.*, D76:083510, 2007.

[101] P. S. Letelier, P. R. Holvorcem, and G. Grebot. Cosmic loops and bubbles in expanding universes. *Class. Quant. Grav.*, 7:597–610, 1990.

[102] Rama Basu and Alexander Vilenkin. Evolution of topological defects during inflation. *Phys. Rev.*, D50:7150–7153, 1994.

[103] P. P. Avelino, R. R. Caldwell, and C. J. A. P. Martins. Cosmological consequences of string-forming open inflation models. *Phys. Rev.*, D59:123509, 1999.

[104] P. P. Avelino, C. J. A. P. Martins, C. Santos, and E. P. S. Shellard. Topological defects in contracting universes. *Phys. Rev. Lett.*, 89:271301, 2002.

[105] P. P. Avelino, C. J. A. P. Martins, C. Santos, and E. P. S. Shellard. Topological defects: A problem for cyclic universes? *Phys. Rev.*, D68:123502, 2003.

[106] T. W. B. Kibble. Evolution of a System of Cosmic Strings. *Nucl. Phys.*, B252:227, 1985.

[107] David P. Bennett. The Evolution of Cosmic Strings. *Phys.Rev.*, D33:872, 1986.

[108] David P. Bennett. Evolution of Cosmic Strings 2. *Phys.Rev.*, D34:3592, 1986.

[109] Andreas Albrecht and N. Turok. Evolution of Cosmic Strings. *Phys.Rev.Lett.*, 54:1868–1871, 1985.

[110] Andreas Albrecht and Neil Turok. Evolution of Cosmic String Networks. *Phys.Rev.*, D40:973–1001, 1989.

[111] David P. Bennett and Francois R. Bouchet. Evidence for a Scaling Solution in Cosmic String Evolution. *Phys.Rev.Lett.*, 60:257, 1988.

[112] David P. Bennett and Francois R. Bouchet. Cosmic String Evolution. *Phys.Rev.Lett.*, 63:2776, 1989.

[113] David P. Bennett and Francois R. Bouchet. High Resolution Simulations of Cosmic String Evolution. 1. Network Evolution. *Phys.Rev.*, D41:2408, 1990.

[114] Bruce Allen and E.P.S. Shellard. Cosmic String Evolution: a Numerical Simulation. *Phys.Rev.Lett.*, 64:119–122, 1990.

[115] T.W.B. Kibble and Edmund J. Copeland. Evolution of small scale structure on cosmic strings. *Phys.Scripta*, T36:153–166, 1991.

[116] Edmund J. Copeland, T.W.B. Kibble, and Daren Austin. Scaling solutions in cosmic string networks. *Phys.Rev.*, D45:1000–1004, 1992.

[117] Daren Austin, Edmund J. Copeland, and T.W.B. Kibble. Evolution of cosmic string configurations. *Phys.Rev.*, D48:5594–5627, 1993.

[118] C. J. A. P. Martins and E. P. S. Shellard. Extending the velocity-dependent one-scale string evolution model. *Phys. Rev.*, D65:043514, 2002.

[119] A. Vilenkin. Cosmic string dynamics with friction. *Phys. Rev.*, D43:1060–1062, 1991.

[120] A. Avgoustidis and E. P. S. Shellard. Cosmic string evolution in higher dimensions. *Phys. Rev.*, D71:123513, 2005.

[121] P. P. Avelino, C. J. A. P. Martins, and J. C. R. E. Oliveira. One-scale model for domain wall network evolution. *Phys. Rev.*, D72:083506, 2005.

[122] P. P. Avelino, R. Menezes, and J. C. R. E. Oliveira. Unified paradigm for interface dynamics. *Phys. Rev.*, E83:011602, 2011.

[123] P. P. Avelino, D. Bazeia, R. Menezes, and J. G. G. S. Ramos. Localized D-dimensional global k-defects. *European Physical Journal C*, 71:1683–+, June 2011.

[124] Timon Boehm and Robert Brandenberger. On T-duality in brane gas cosmology. *JCAP*, 0306:008, 2003.

[125] Allen E. Everett. Cosmic Strings in Unified Gauge Theories. *Phys. Rev.*, D24:858, 1981.

[126] T. W. B. Kibble. Phase Transitions in the Early Universe. *Acta Phys. Polon.*, B13:723, 1982.

[127] Ya. B. Zeldovich, I. Yu. Kobzarev, and L. B. Okun. Cosmological consequences of the spontaneous breakdown of discrete symmetry. *Zh. Eksp. Teor. Fiz.*, 67:3–11, 1974.

[128] P.P. Avelino, D. Bazeia, R. Menezes, and J. Oliveira. Bifurcation and pattern changing with two real scalar fields. *Phys.Rev.*, D79:085007, 2009.

[129] Graciela B. Gelmini, Marcelo Gleiser, and Edward W. Kolb. Cosmology of biased discrete symmetry breaking. *Phys. Rev.*, D39:1558, 1989.

[130] Sebastian E. Larsson, Subir Sarkar, and Peter L. White. Evading the cosmological domain wall problem. *Phys. Rev.*, D55:5129–5135, 1997.

[131] Katherine Freese, James T. Liu, and Douglas Spolyar. Devaluation: A dynamical mechanism for a naturally small cosmological constant. *Phys. Lett.*, B634:119–124, 2006.

[132] Pedro P. Avelino, C.J.A.P. Martins, J. Menezes, R. Menezes, and J.C.R.E. Oliveira. Scaling of cosmological domain wall networks with junctions. *Phys.Lett.*, B647:63–66, 2007.

[133] C.J.A.P. Martins and A. Achucarro. Evolution of local and global monopole networks. *Phys.Rev.*, D78:083541, 2008.

[134] C. J. A. P. Martins. Evolution of Hybrid Defect Networks. *Phys. Rev.*, D80:083527, 2009.

[135] Richard A. Battye, Jonathan A. Pearson, Simon Pike, and Paul M. Sutcliffe. Formation and evolution of kinky vortons. *JCAP*, 0909:039, 2009.

[136] Richard A. Battye and Jonathan A. Pearson. Charge, junctions and the scaling dynamics of domain wall networks. *Phys.Rev.*, D82:125001, 2010.

[137] A. Vilenkin. Gravitational Radiation from Cosmic Strings. *Phys.Lett.*, B107:47–50, 1981.

[138] P. Sikivie. Of Axions, Domain Walls and the Early Universe. *Phys. Rev. Lett.*, 48:1156–1159, 1982.

[139] Joshua A. Frieman, G. B. Gelmini, Marcelo Gleiser, and Edward W. Kolb. Solitogenesis: Primordial Origin of Nontopological Solitons. *Phys. Rev. Lett.*, 60:2101, 1988.